

STATISTICAL FREQUENCY-DISTANCE CURVES, INITIAL MODEL



OT

U.S. DEPARTMENT OF COMMERCE / Office of Telecommunications

STATISTICAL FREQUENCY-DISTANCE CURVES, INITIAL MODEL

R. D. JENNINGS
L. E. VOGLER
J. J. STEPHENSON



U.S. DEPARTMENT OF COMMERCE
Elliot L. Richardson, Secretary

Betsy Ancker-Johnson, Ph. D.
Assistant Secretary for Science and Technology

OFFICE OF TELECOMMUNICATIONS
John M. Richardson, Acting Director



April 1976

**UNITED STATES DEPARTMENT OF COMMERCE
OFFICE OF TELECOMMUNICATIONS
STATEMENT OF MISSION**

The mission of the Office of Telecommunications in the Department of Commerce is to assist the Department in fostering, serving, and promoting the nation's economic development and technological advancement by improving man's comprehension of telecommunication science and by assuring effective use and growth of the nation's telecommunication resources.

In carrying out this mission, the Office

- Conducts research needed in the evaluation and development of policy as required by the Department of Commerce
- Assists other government agencies in the use of telecommunications
- Conducts research, engineering, and analysis in the general field of telecommunication science to meet government needs
- Acquires, analyzes, synthesizes, and disseminates information for the efficient use of the nation's telecommunication resources.
- Performs analysis, engineering, and related administrative functions responsive to the needs of the Director of the Office of Telecommunications Policy, Executive Office of the President, in the performance of his responsibilities for the management of the radio spectrum
- Conducts research needed in the evaluation and development of telecommunication policy as required by the Office of Telecommunications Policy, pursuant to Executive Order 11556

PREFACE

The model development work reported herein was accomplished at the direction of the Office of Telecommunication Policy. This report documents the first phase in the development of a very general model for assessing the variability (probabilistic nature) of electromagnetic compatibility and its influence upon frequency management.

TABLE OF CONTENTS

	Page
PREFACE	iii
LIST OF FIGURES	vii
LIST OF TABLES	xiii
ABSTRACT	1
1. BACKGROUND	2
1.1 Applications	2
1.2 Concept and Utility of Frequency-Distance Curves	3
1.3 Statistical Frequency-Distance Curves	7
2. GENERAL DESIGN	15
2.1 Design Objectives	15
2.2 General Structure	15
2.3 Design of Statistical Frequency-Distance Model	20
3. TYPICAL APPLICATIONS	24
3.1 Frequency Management Problem	24
3.2 Engineering/System Design Problem	33
4. CONCLUSIONS	53
5. REFERENCES	56
APPENDIX A. USER'S GUIDE	59
A.1 Functional Nature of the Model	59
A.2 Input Data for the Model	63
A.2.1 General Data	69
A.2.2 Data for INSPECT	74
A.2.3 Data for NEWSPEC	77
A.2.4 Antenna Data	80
A.2.5 Propagation Data	88
APPENDIX B. SAMPLE MODEL APPLICATIONS	93
B.1 Sample Number 1. Example of the Statistical F-D Model Using the Ground-to-Air Propagation Loss Model and Point-Amplitude Spectrum and Receiver Response Data	94

TABLE OF CONTENTS (Continued)

	Page
B.2 Sample Number 2. Example of the Statistical F-D Model Using the Ground-to-Ground Propagation Loss Model and Point-Amplitude Spectrum and Receiver Response Data	105
B.3 Sample Number 3. Example of the Statistical F-D Model Using the Ground-to-Air Propagation Loss Model and Synthesized Spectrum and Receiver Response Characteristics	116
APPENDIX C. EMISSION SPECTRUM/RECEIVER SELECTIVITY MODELS	127
C.1 Subroutine INSPECT Theory and Application	127
C.2 Subroutine NEWSPEC Theory and Application	135
APPENDIX D. ANTENNA POWER GAIN STATISTICS	171
APPENDIX E. OFF-FREQUENCY REJECTION CALCULATION	179
APPENDIX F. PROPAGATION LOSS MODELS	183
F.1 Ground-to-Ground Propagation Model	183
F.2 Ground-to-Air Propagation Model	185
APPENDIX G. CONVOLUTION SUBROUTINE	187

LIST OF FIGURES

Figure		Page
1-1.	Pictorial representation of the basic factors considered in generating a frequency-distance curve	4
1-2.	Sample curve (as would result from using discrete data) illustrating the frequency-distance separation concept (1 n mi = 1.85 km)	6
1-3.	Sample frequency-distance separation curves generated from discrete data to illustrate parametric treatment of the I.F. I/N criterion (1 n mi = 1.85 km)	8
1-4.	Sample statistical frequency-distance separation curve illustrating application for a specified frequency separation (1 n mi = 1.85 km)	12
1-5.	Sample statistical frequency-distance separation curve illustrating application for a specified distance separation (1 n mi = 1.85 km)	13
2-1.	Functional block diagram of the statistical frequency-distance curves model	19
3-1.	Statistical frequency-distance curves for Land Mobile Radio systems operating in the 406-420 MHz band--fixed equipment transmitter with antenna 200 ft (60.96 m) above terrain vs mobile receiver for interference criterion I/N = 0 dB (1 mi = 1.6 km)	26
3-2.	Statistical frequency-distance curves for Land Mobile Radio systems operating in the 406-420 MHz band--fixed equipment transmitter with antenna 200 ft (60.96 m) above terrain vs fixed equipment receiver with antenna 100 ft (30.48 m) above terrain for interference criterion I/N = 0 dB (1 mi = 1.6 km)	27
3-3.	Statistical frequency-distance curves for MILSATCOM Airborne transmitter (60 dB/decade roll-off rate) vs RML-4 receiver (100 dB/decade fall-off rate; 1 mi = 1.6 km)	36

LIST OF FIGURES (Cont.)

Figure	Page
3-4. Statistical frequency-distance curves for MILSATCOM Airborne transmitter (60 dB/decade roll-off rate) vs RML-4 receiver (140 dB/decade fall-off rate; 1 mi = 1.6 km)	37
3-5. Statistical frequency-distance curves for MILSATCOM Airborne transmitter (ECAC emission envelope) vs RML-4 receiver (100 dB/decade fall-off rate; 1 mi = 1.6 km)	38
3-6. Statistical frequency-distance curves for MILSATCOM Airborne transmitter (ECAC emission envelope) vs RML-4 receiver (140 dB/decade fall-off rate; 1 mi = 1.6 km)	39
A-1. Functional block diagram of the statistical frequency-distance curves model	61
B-1. Completed general data sheet for Sample 1	95
B-2. Completed data sheet for subroutine INSPECT for Sample 1	96
B-3. Completed data sheet for subroutine ANTSTAT for Sample 1	97
B-4. Completed loss data sheet for Sample 1	98
B-5. Normalized spectral power density envelope for transmitter 1 used in Sample 1	99
B-6. Normalized receiver selectivity curve for receiver 1 used in Sample 1	100
B-7. Statistical frequency-distance curves for transmitter 1-receiver 1 pair for Sample 1 using the ground-to-air propagation loss model (1 n mi = 1.85 km)	104
B-8. Completed general data sheet for Sample 2	107
B-9. Completed data sheet for subroutine INSPECT for Sample 2	108
B-10. Completed data sheet for subroutine ANTSTAT for Sample 2	109
B-11. Completed loss data sheet for Sample 2	110

LIST OF FIGURES (Cont.)

Figure	Page
B-12. Normalized spectral power density envelope for transmitter 3A for Sample 2	111
B-13. Normalized selectivity curve for receiver 6A for Sample 2	112
B-14. Statistical frequency-distance curves for transmitter 3A-receiver 6A pair for Sample 2 using the ground-to-ground propagation loss model (1 n mi = 1.85 km)	115
B-15. Completed general data sheet for Sample 3	117
B-16. Completed data sheet for subroutine NEWSPEC for Sample 3	118
B-17. Completed data sheet for subroutine ANTSTAT for Sample 3	119
B-18. Synthesized pulse (time domain waveform) for transmitter NEWSPECT TEST for Sample 3	121
B-19. Synthesized spectral power density curve for transmitter NEWSPECT TEST for Sample 3	122
B-20. Synthesized receiver selectivity curve for receiver TEST (21 PTS) for Sample 3. This selectivity curve corresponds to a 5-pole Butterworth filter	124
B-21. Statistical frequency-distance curves for transmitter NEWSPECT TEST - receiver TEST (21 PTS) pair for Sample 3 using NEWSPEC subroutine and the ground-to-air propagation loss model (1 n mi = 1.85 km)	126
C.2-1. Synthesized pulse shape for the AN/APN-133 radar altimeter operating in the low altitude mode	138
C.2-2. Synthesized pulse shape for the AN/APN-133 radar altimeter operating in the high altitude mode	139
C.2-3. Synthesized pulse shape for the AN/APN-159 radar altimeter operating in the high altitude mode	140

LIST OF FIGURES (Cont.)

Figure	Page
C.2-4. Synthesized pulse shape for the AN/APN-159 radar altimeter operating in the low altitude mode . . .	141
C.2-5. Synthesized pulse shape for the In-Flight Devices ground avoidance radar	142
C.2-6. Synthesized pulse shape for the Bonzer TRN/70 radar altimeter	143
C.2-7. Synthesized power density spectrum for the AN/APN-133 radar altimeter operating in the low altitude mode	146
C.2-8. Synthesized power density spectrum for the AN/APN-133 radar altimeter operating in the high altitude mode	147
C.2-9. Synthesized power density spectrum for the AN/APN-159 radar altimeter operating in the high altitude mode	148
C.2-10. Synthesized power density spectrum for the AN/APN-159 radar altimeter operating in the low altitude mode	149
C.2-11. Synthesized power density spectrum for the In-Flight Devices ground avoidance radar	150
C.2-12. Synthesized power density spectrum for the Bonzer TRN-70 radar altimeter	151
C.2-13. Chebyshev filter with 1 dB ripple in the passband ($\epsilon^2 = 0.259$) and $N=3$ controlling the slope of the wings	153
C.2-14. Chebyshev filter with 1 dB ripple in the passband ($\epsilon^2 = 0.259$) and $N=5$ controlling the slope of the wings	154
C.2-15. Synthesized spectral power density for the AN/APN-133 radar altimeter in the low altitude mode after additional filtering using a 3-pole Chebyshev filter with 1 dB ripple in the passband.	157
C.2-16. Synthesized spectral power density for the AN/APN-133 radar altimeter in the high altitude mode after additional filtering using a 3-pole Chebyshev filter with 1 dB ripple in the passband.	158

LIST OF FIGURES (Cont.)

Figures	Page
C.2-17. Synthesized spectral power density for the AN/APN-159 radar altimeter in the high altitude mode after additional filtering using a 3-pole Chebyshev filter with 1 dB ripple in the passband	159
C.2-18. Synthesized spectral power density for the AN/APN-159 radar altimeter in the low altitude mode after additional filtering using a 3-pole Chebyshev filter with 1 dB ripple in the passband	160
C.2-19. Synthesized spectral power density for the In-Flight Devices' ground avoidance radar after additional filtering using a 3-pole Chebyshev filter with 1 dB ripple in the passband	161
C.2-20. Synthesized spectral power density for the Bonzer TRN-70 radar altimeter after additional filtering using a 3-pole Chebyshev filter with 1 dB ripple in the passband	162
C.2-21. Synthesized spectral power density for the AN/APN-133 radar altimeter in the low altitude mode after additional filtering using a 3-pole Butterworth filter	164
C.2-22. Synthesized spectral power density for the AN/APN-133 radar altimeter in the high altitude mode after additional filtering using a 3-pole Butterworth filter	165
C.2-23. Synthesized spectral power density for the AN/APN-159 radar altimeter in the high altitude mode after additional filtering using a 3-pole Butterworth filter	166
C.2-24. Synthesized spectral power density for the AN/APN-159 radar altimeter in the low altitude mode after additional filtering using a 3-pole Butterworth filter	167
C.2-25. Synthesized spectral power density for the In-Flight Devices ground avoidance radar after additional filtering using a 3-pole Butterworth filter	168

LIST OF FIGURES (Cont.)

Figure	Page
C.2-26. Synthesized spectral power density for the Bonzer TRN-70 radar altimeter after additional filtering using a 3-pole Butterworth filter	169

LIST OF TABLES

Table	Page
3-1. Tabular Data for Land Mobile Radio Systems Operating in the 406-420 MHz Band with Transmitting Antenna 200 ft (60.96 m) High and Mobile Unit Receiving Antenna	28
3-2. Tabular Data for Land Mobile Radio Systems Operating in the 406-420 MHz Band with Transmitting Antenna 200 ft (60.96 m) and Receiving Antenna 100 ft (30.48 m) High	29
3-3. Tabular Data for MILSATCOM Airborne Transmitter (60 dB/Decade Roll-Off) vs RML-4 Receiver (100 dB/Decade Fall-Off)	40
3-4. Tabular Data for MILSATCOM Airborne Transmitter (60 dB/Decade Roll-Off) vs RML-4 Receiver (140 dB/Decade Fall-Off)	42
3-5. Tabular Data for MILSATCOM Airborne Transmitter (ECAC Emission Envelope) vs RML-4 Receiver (100 dB/Decade Fall-Off)	44
3-6. Tabular Data for MILSATCOM Airborne Transmitter (ECAC Emission Envelope) vs RML-4 Receiver (140 dB/Decade Fall-Off)	46
A-1. Sample Forms to Provide Input Data for the Statistical Frequency-Distance Curves Model	64
A-2. Statistics for Typical High-Gain Antennas ($G > 25$ dBi).	83
A-3. Statistics for Typical Medium-Gain Antennas ($10 \text{ dBi} \leq G \leq 25 \text{ dBi}$)	84
A-4. Statistics for Typical Low-Gain Antennas ($G > 10$ dBi)	85
A-5. Estimates of Terrain Roughness	90
A-6. Surface Types and Constants	91
D-1. Statistics for Typical High-Gain Antennas ($G > 25$ dBi)	173
D-2. Statistics for Typical Medium-Gain Antennas ($10 \text{ dBi} \leq G \leq 25 \text{ dBi}$)	174
D-3. Statistics for Typical Low-Gain Antennas ($G < 10$ dBi)	175

STATISTICAL FREQUENCY-DISTANCE CURVES, INITIAL MODEL

R. D. Jennings*, L. E. Vogler*, and J. J. Stephenson**

This report describes an initial computer program that produces statistical frequency-distance curves. The computer program has been developed as a tool for use by the frequency managers' community of OTP/IRAC.

The statistical frequency-distance curves estimate the minimum distance separation that is required between a victim receiver and an interferer as a function of the frequency offset between them. The curves are parametric in the probability or percent of time that interference is permissible. The model uses statistical variations in antenna gain and propagation loss to compute the probability of interference. Appendices of the report describe the propagation loss and antenna gain models and the method used to combine them to produce the statistical frequency-distance curves. Operating instructions and several sample applications also are included as appendices.

Key words: Compatibility; computer model; distance separation; electromagnetic compatibility; emission spectrum; frequency-distance curve; frequency management; frequency separation; interference; off-frequency rejection; propagation loss; receiver selectivity; statistics.

* The authors are with the Institute for Telecommunication Sciences, Office of Telecommunications, U.S. Department of Commerce, Boulder, Colorado 80302.

** The author is with the Space Environment Laboratory, National Oceanic and Atmospheric Administration, U.S. Department of Commerce, Boulder, Colorado 80302.

1. BACKGROUND

1.1 Applications

The engineer or analyst faced with frequency management problems usually has a work load and schedule that restrict him to a brief engineering analysis. He is faced with continual demands for day-to-day decisions in the assignment of the available frequencies of the finite radio frequency resource. Further, he is called upon to solve or resolve reported, actual, and/or expected problems of unsatisfactory performances due to radio frequency interference (electromagnetic incompatibility) between existing, real-world systems or expected new systems.

Two of the basic variables available to the engineer or analyst for making trade-offs, or in solving his frequency assignment problems are the tuned frequency of a system and the physical distance that separates it from other systems. However, analysis other than the use of engineering judgment in consideration of these variables requires him to perform fairly detailed and lengthy calculations on a case-by-case transmitter-receiver pair basis. This places a severe limitation on the number of assignments and/or problems that he can consider.

The computer based model described in this report provides an easy-to-use engineering technique that will allow improved design and planning of frequency assignments.

Also, this model as it now exists, can be used at an early concept stage in system development to assist in examining the trade-offs in transmitter and receiver designs such as filtering, tuning, modulation type, data rates, etc.

1.2 Concept and Utility of Frequency-Distance Curves

The basic factors considered in generating a frequency-distance curve are shown in figure 1-1. The interfering transmitter is tuned to some frequency f_T and generates a power spectrum that is a function of modulation type and equipment. The signal then is fed to an antenna where it is radiated over the propagation path to the antenna of the victim receiver. The victim receiver has a bandpass characteristic again dependent on signal characteristics or modulation type and the filtering employed.

Given the characteristics of two systems as shown in figure 1-1, one then can compute the amount of power in the victim receiver output due to that interfering source. If we compare that output power to a maximum power level, defined by the user of the model, that the victim receiver can tolerate, a decision can be made concerning the transmitter's effects. Quite often, this maximum tolerable power level depends on the particular characteristics of the received interference, and is different for different classes of interference.

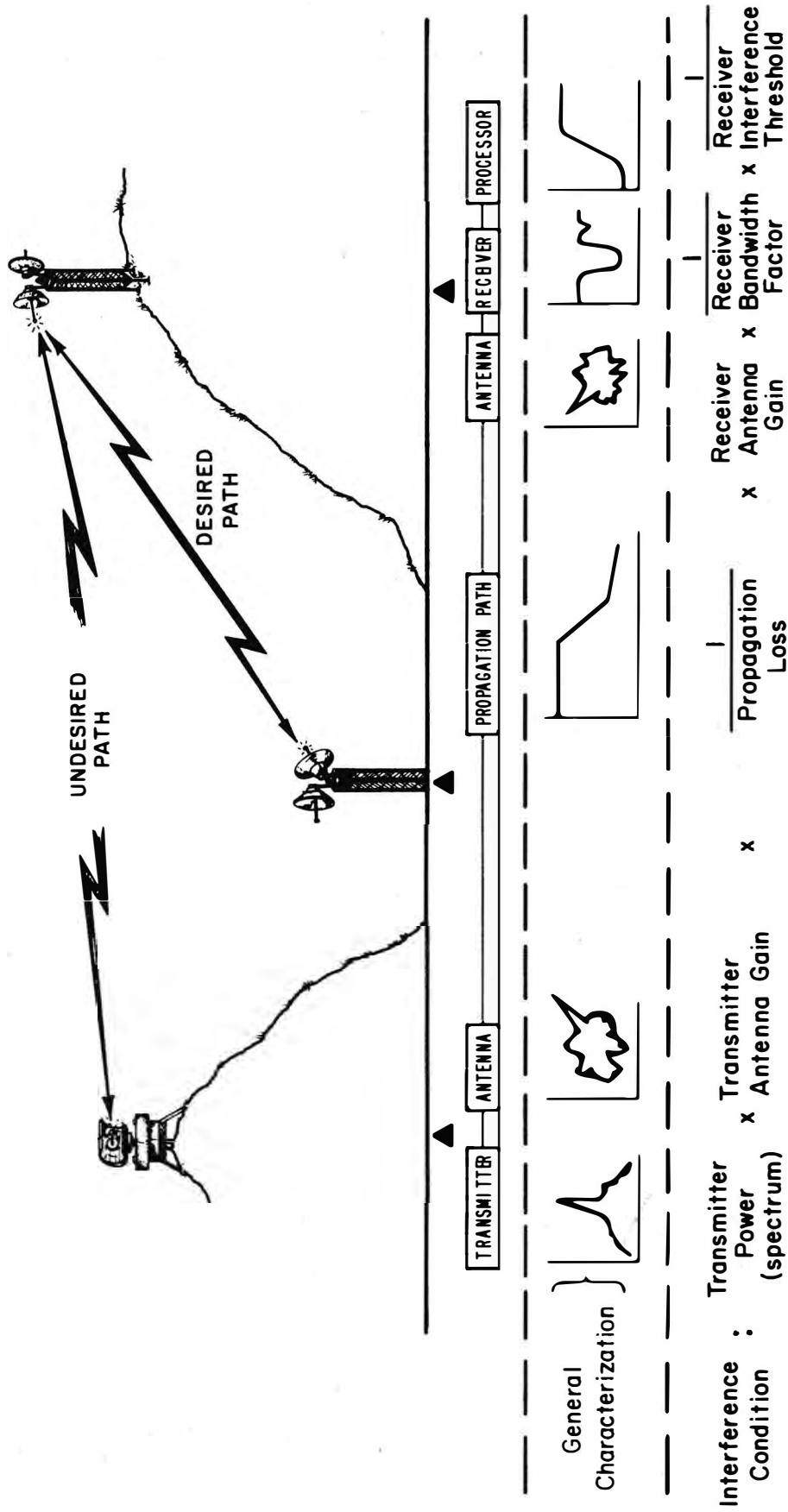


Figure 1-1. Pictorial representation of the basic factors considered in generating a frequency-distance curve.

In order to examine the trade-offs possible by varying the frequency separation between systems as well as their spatial separation, a parameter is needed to compare the results in system performance. The performance measure that is used in this model is the interference-to-noise power ratio (I/N) at the victim receiver detector. The noise power, N, is the internal noise power of the victim receiver. This I/N can be converted to a signal-to-interference ratio provided that the desired signal level and the level of interference or noise are known.

This frequency-distance separation concept is illustrated by the curve in figure 1-2. For example, in case #1 shown by dashed lines, the curve shows that if the interfering transmitter and the victim receiver antennas are physically separated by 9 n mi (16.7 km) and the tuned frequencies of the systems are separated by at least 12 MHz, the interference power from the transmitter will not exceed the noise power of the receiver (I/N=0 dB). In case #2, shown by dotted lines, the curve shows that if the interfering transmitter and the victim receiver have tuned frequencies which are separated by 30 MHz, the units must be physically separated by at least 3.9 n mi (7.2 km) for the interference power to be equal to or less than the receiver noise power.

The procedure is to determine the amount of interference protection required for a given frequency

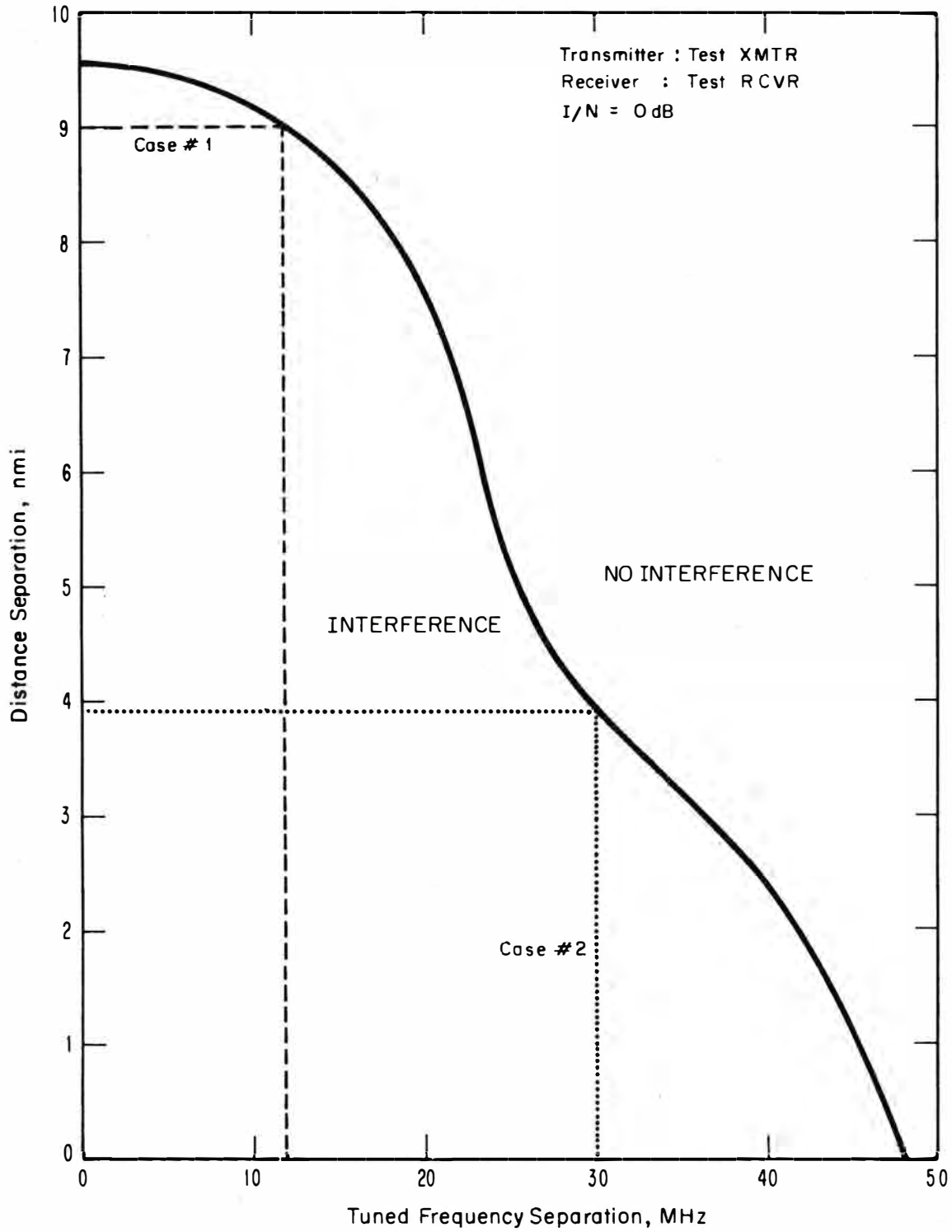


Figure 1-2. Sample curve (as would result from using discrete data) illustrating the frequency-distance separation concept (1 n mi = 1.85 km).

separation and interference signal level, and then solve the propagation calculation backwards (i.e., given loss, find distance) to determine the amount of distance separation required to give that protection. This represents one point on the curve as is shown by case #1 in figure 1-2. This procedure is repeated then for all frequency separations of interest to generate a complete F-D curve.

This idea can be extended to generate curves for different levels of I/N that will bound the problem of interest. An example is shown in figure 1-3 where the F-D curves are parameterized for four values of I/N. These values could represent four levels of transmitter power, or four levels of antenna gain, etc., where the four values might be known operating power ranges or, perhaps, the antenna gains that are not known precisely. In any case, the output represents another useful form that can display the trade-offs available.

1.3 Statistical Frequency-Distance Curves

Recall that the discussion of the frequency-distance separation concept thus far has considered only the discrete, single-valued specification of all parameters of interest. A more useful concept results when the parameters are statistically characterized.

The equipment characteristics and propagation factors

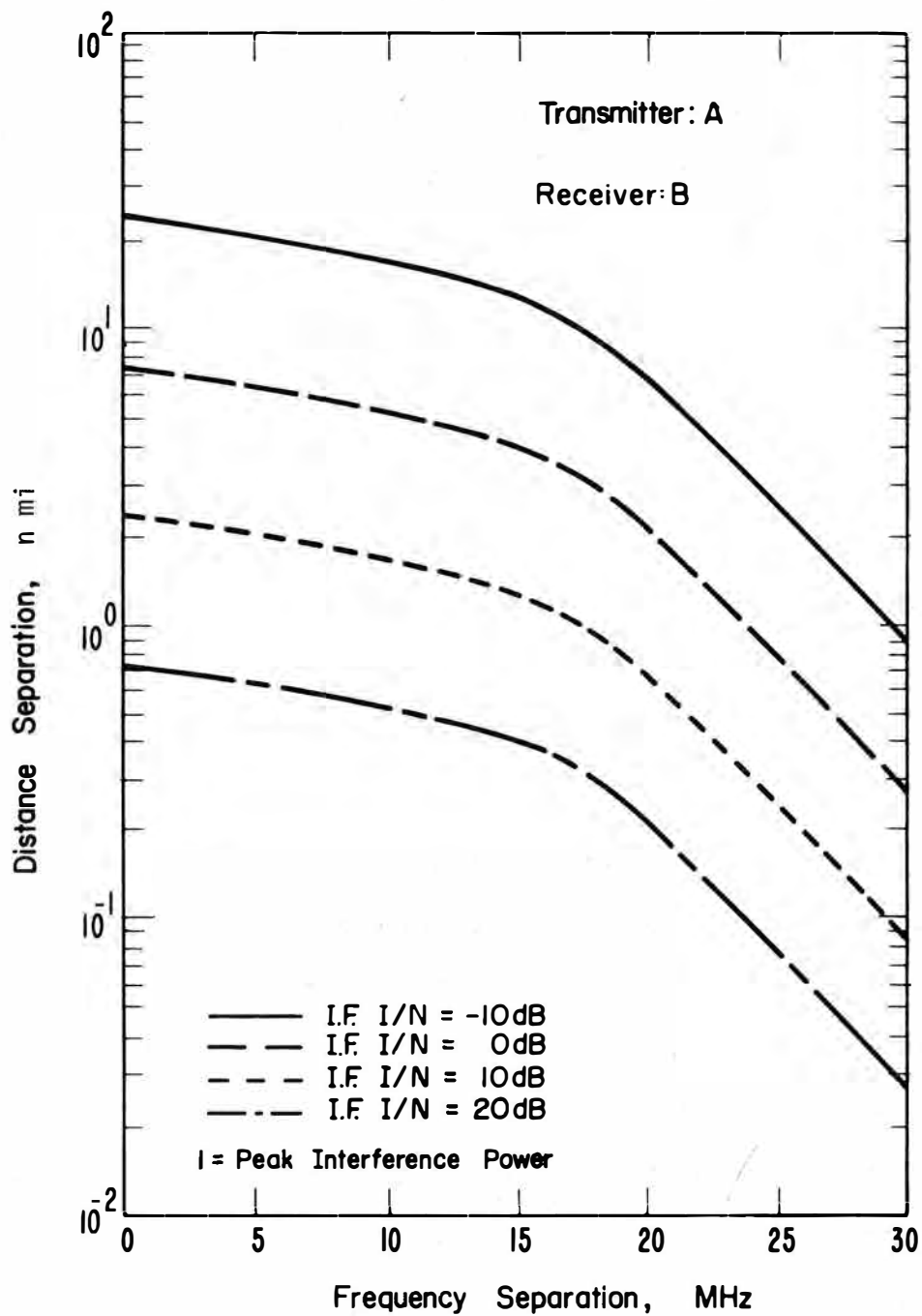


Figure 1-3. Sample frequency-distance separation curves generated from discrete data to illustrate parametric treatment of the I.F. I/N criterion (1 n mi = 1.85 km).

that one uses to compute a frequency-distance curve rarely will be the actual values found in the field. As an example, if a transmitter is designed to be a single frequency, fixed tuned device, there is some tolerance associated with the nominal specification of tuned frequency. Further, as that transmitter is used in the field it may be retuned and modified as a result of routine maintenance, resulting in a changed emission characteristic. These same phenomena of instability, modifications, and general in-situ performance apply to all of the components of the system. Therefore, to make the F-D concept generally applicable to the "typical" or field problems, the characteristics associated with each component of the system should be represented statistically.

The concept of a range of data describing a single factor, such as output power, is important to the probabilistic nature of frequency-distance trade-offs. In the past, a single value--usually a conservative or worst case estimate--has been used, when in fact the frequency manager has known that factors like output power have a range of values in practice.

When this range of values is known, usually as a result of measurements, it is described as a "distribution" for input to statistical models. These distributions can be variously described as probability density functions or cumulative distribution functions. For example, the power

output of the transmitter can be expressed as a distribution of powers.

Once a distribution is known (even if it is assumed) the user may select any probability of occurrence that is appropriate to the problem at hand. For example, one may use (1) a value for power that represents the average value for all of the transmitters sampled, (2) a value for power applicable to only 10% (or any other percentile) of the transmitters or (3) a value for power which represents 90% of the transmitters. This selection of appropriate probabilities of occurrence allows an improved consideration of actual field conditions.

One would like to have these distributions for all of the component elements, making it truly a statistical F-D model. However, our initial consideration is restricted to the statistics of the propagation loss and antenna power gain components.

Statistical frequency-distance curves provide trade-offs which apply for the full range of probabilities of occurrence. For example, the curves could portray interference expected with low probability of occurrence (i.e., 10% of the cases or time), with high probability of occurrence, (i.e., 99% of the cases or time) or on the average (i.e., 50% of the time). Thus, one has a tool with

great utility, since it can be applied to problems over a broad range of conditions.

Various interpretations of probabilistic F-D curves are possible. For example, figures 1-4 and 1-5 present the same curves but different interpretations are illustrated. The dashed lines in figure 1-4 illustrate an interpretation for a specified frequency separation. When the interfering transmitter (TEST XMTR) and the victim receiver (TEST RCVR) have tuned frequencies which are separated by 10 MHz and their antennas are physically separated by 18 n mi (33.3 km), the interference criterion of $I/N=10$ dB will be violated 10% of the time. If they are separated by 13 n mi (24.1 km), the I/N will be greater than 10 dB 50% of the time. If they are 7 n mi (13.0 km) I/N will be greater than 10 dB 90% of the time.

The dashed lines in figure 1-5 illustrate an interpretation for a specified distance separation. When antennas for the interfering transmitter (TEST XMTR) and the victim receiver (TEST RCVR) are physically separated by 15 n mi (27.8 km) and the systems have tuned frequencies which are separated by 8 MHz, the interference criterion of $I/N=10$ dB will be violated 90% of the time. If the tuned frequencies are separated by 9 MHz, the I/N of 10 dB will be exceeded 50% of the time. If they are 11 MHz apart, the I/N will be greater than 10 dB 10% of the time. The same curves also could be generated for other values of I/N resulting in families of statistical F-D curves.

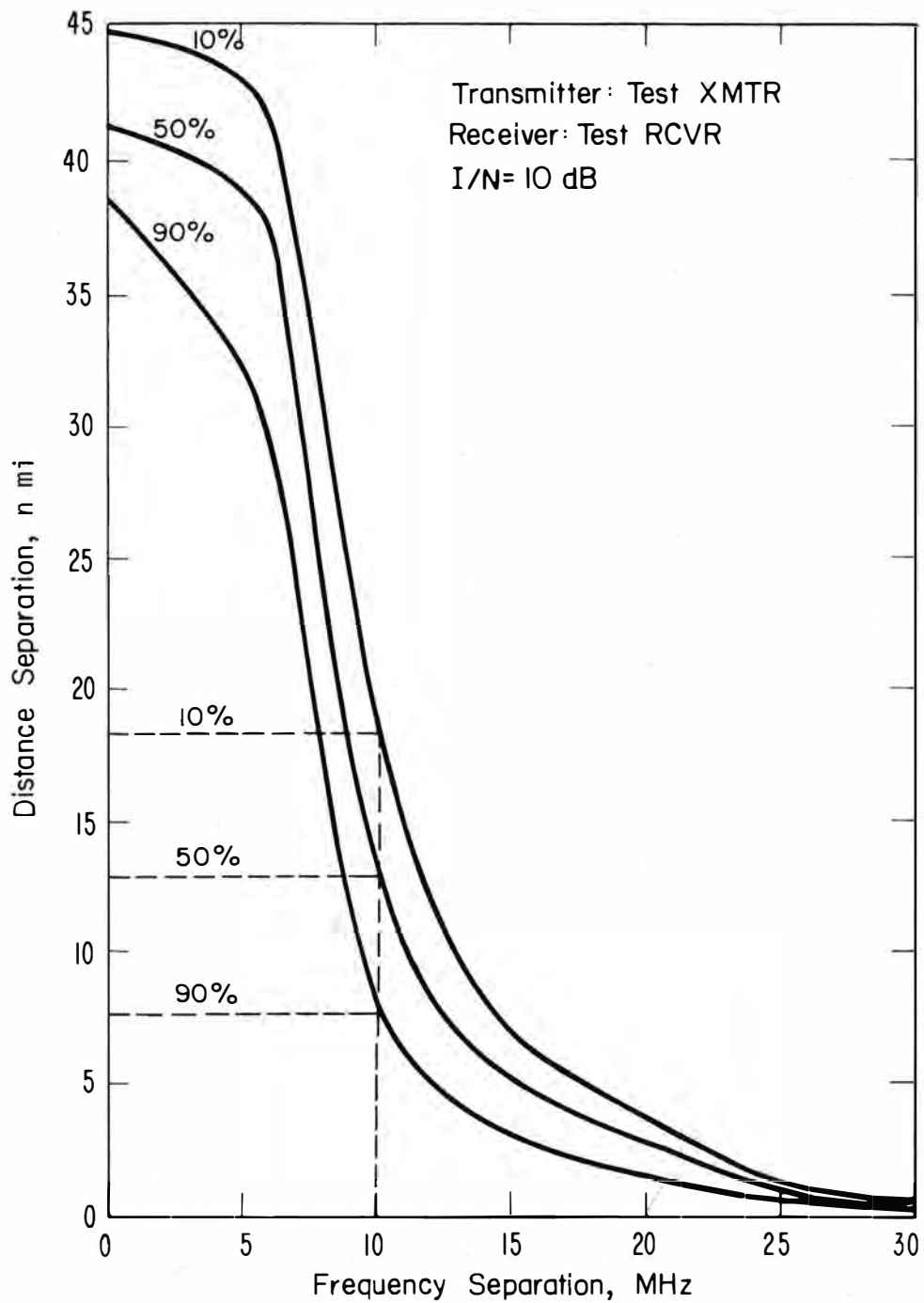


Figure 1-4. Sample statistical frequency-distance separation curve illustrating application for a specified frequency separation (1 n mi = 1.85 km).

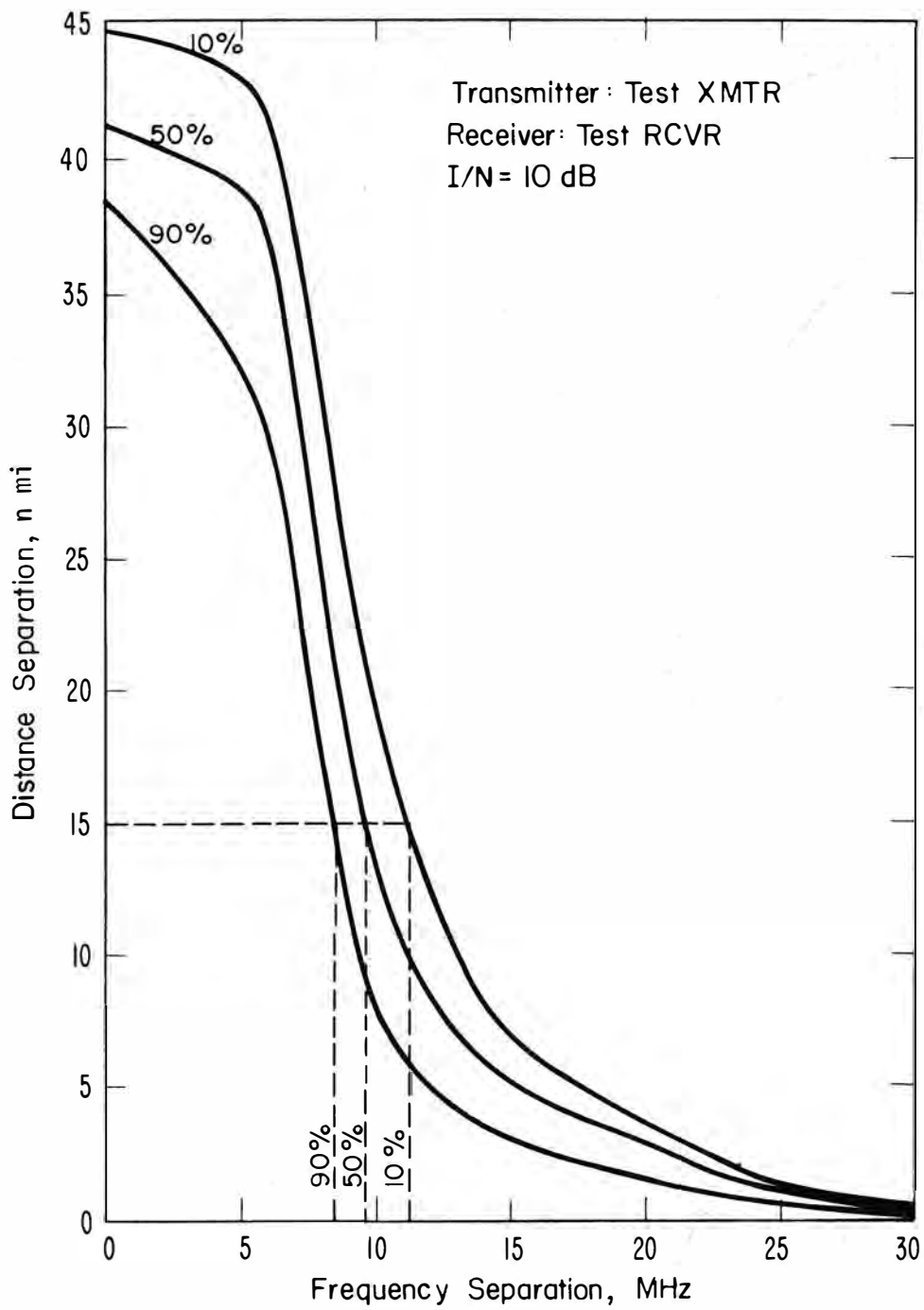


Figure 1-5. Sample statistical frequency-distance separation curve illustrating application for a specified distance separation (1 n mi = 1.85 km).

Other workers concerned with electromagnetic compatibility have applied a statistical treatment to the frequency-distance separation concept (Lustgarten, 1966; Lustgarten and Mayher, 1968; and U. S. Army Electronic Proving Ground, 1968). These and other unreported results have been used where possible in this development.

2. GENERAL DESIGN

The concepts and ideas described in the previous section have been worked into an approach that will meet the objectives of the Office of Telecommunications Policy (OTP) and the Interdepartment Radio Advisory Committee (IRAC). The model development has been an evolutionary one.

2.1 Design Objectives

(1) The techniques used must be realistic models of the system components so that the probabilistic nature of the variables can be accurately considered and the appropriate trade-offs examined.

(2) The model developed must be one that is easily accessible and can be used readily by the frequency management community as well as system designers. This means that the interface with the user must be simple and easily understood.

(3) This model must provide a natural interface with the probabilistic performance and operational factors affecting electromagnetic compatibility.

2.2 General Structure

A generally useful technique for computing the probabilistic trade-offs in frequency and distance must provide for statistical considerations of each of the

factors in figure 1-1. Also, it must provide for valid statistical combinations of these factors.

The structure of the model can be examined in two major divisions: those components that are frequency dependent and those components that are primarily distance dependent.

The major frequency dependent parts of the model are the transmitter and the receiver. Their frequency dependent characteristics (transmitter emission spectrum and the receiver selectivity) can be input to the model manually from known or approximated data, or they can be synthesized from time domain wave shapes and filter types. The combined frequency dependence of the transmitter and receiver is termed the spectrum dependency, SD, characteristic.* This can be expressed for any frequency difference (Δf) between the pair as:

$$SD_{\Delta f} = \int_0 P_T(f_T) S(f_T, \Delta f) df$$

*Off-frequency rejection (OFR) as discussed by Fleck (1967) is the spectrum dependency at a specified frequency separation ($\Delta f =$ specified value) normalized to the spectrum dependency when the receiver and transmitter are tuned to their normal operating frequencies ($\Delta f = f_T - f_R$). OFR as defined in Appendix E of this report is normalized by the spectrum dependency for the receiver and transmitter tuned to the same frequency, i.e. $f_R = f_T$ ($\Delta f = 0$).

where:

$P_T(f)$ is the transmitter power spectral density function,

$S(f,\Delta f)$ is the receiver selectivity or transfer function, and

Δf is the difference between tuned frequencies.

This quantity can be considered to be the effective power of the received spectra when a transmitter and receiver are connected back-to-back. It is a convenient parameter in that it is dependent on hardware, and can be measured in the laboratory.

The factor that is primarily distance dependent is propagation. An inverse solution to the propagation loss algorithm then must be found. An "inverse" solution means that one starts with a value of loss and then must compute a corresponding value of distance. Many of the propagation models that exist are not easily amenable to an inverse solution. The other parameters involved in the F-D calculation (transmitter power, antenna gains, receiver sensitivity, and SD) determine the required loss between the transmitting and receiving antennas.

Depending upon the application of the F-D model, an appropriate propagation sub-model must be used. Currently both an air-ground model (Gierhart and Johnson, 1973) and a ground-to-ground model derived from work reported by Longley and Rice (1968) are incorporated into the program.

The major technical problem in the development of a statistical frequency-distance separation model is in the proper combination of probability distributions of the several contributing factors. The block diagram in figure 2-1 gives the logical flow between the sub-models which represent each contributing factor or statistical variable. Details of each sub-model are given either in references or in the appendices of this report.

The emission spectrum and receiver selectivity blocks (shown in the upper-left corner) are combined as an SD characteristic of the pair. Note also that the normalization process which produces OFR tabular data is available as an optional output. The input parameters may be synthesized internally or input by the user. Appendix C gives a detailed technical discussion of the synthesization techniques. After determining the SD characteristics of the equipment, the necessary interference protection or attenuation that is required between that pair for a given I/N (or another interference criterion) is calculated. This value then is input to the propagation equation which is solved for the distance that produces this loss.

Actually, since we are dealing with statistical values for both antenna patterns and propagation loss, the cumulative distribution functions for the antennas and the propagation loss must be combined by convolution to obtain a

Statistical Frequency-Distance Curves Model Functional Block Diagram

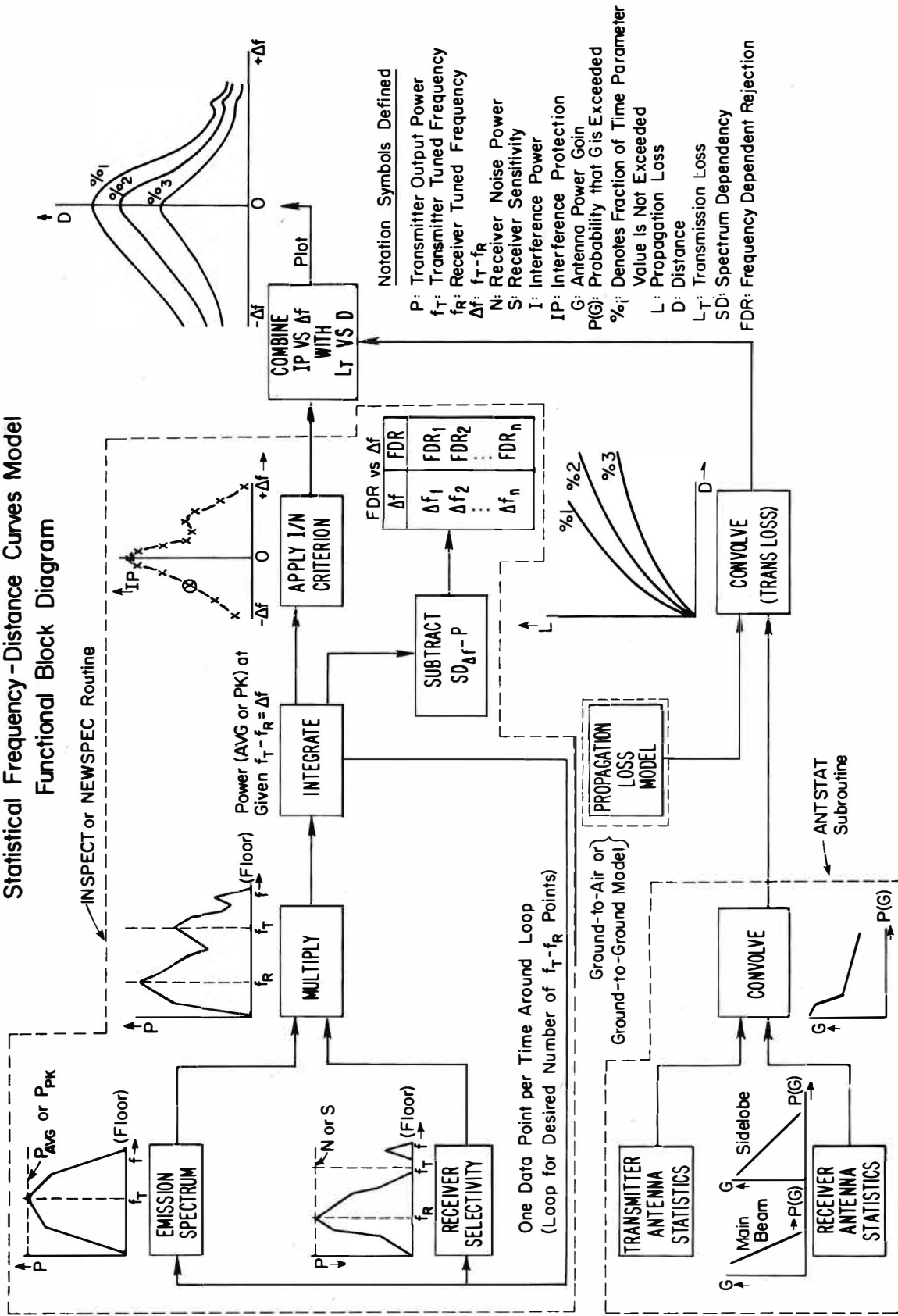


Figure 2-1. Functional block diagram of the statistical frequency-distance curves model.

composite cumulative distribution function for both parameters. This is illustrated at the bottom of figure 2-1.

Once the distance values are known for the required probability levels, they are used as one point on the F-D curve, and the frequency is incremented. The process of determining the SD, and then convolving the statistics of the antenna gain and propagation loss is repeated over the range of frequencies and distances of interest. This process is the basis for the initial model development, as well as the future extensions of the model.

2.3 Design of the Statistical Frequency-Distance Curves Model

The initial model has been organized around existing computer models for various components. These programs have been modified to fit together into a useful tool that will be expanded to work with a broad class of problems that face the OTP and IRAC.

The existing programs used in the F-D model are:

- (1) Statistical propagation prediction routines from the Air-Ground model (Gierhart and Johnson, 1973).
- (2) Propagation prediction routines from the Longley-Rice Irregular Terrain Model (Longley and Rice, 1968).

- (3) Emission spectrum and filtering routines the NEWSPEC synthesis model developed during a study of spectrum sharing (E. Haakinson and H. Kimball, Spectrum assessment for the 1535-1660 MHz band, phase II analysis, private communication).

Each of these programs was restructured for its application to F-D curve generation.

The computational routines require input in special forms. The program design allows the user flexibility in supplying input data and unspecified input is supplied from a table of default values.

These input variables then are adjusted (e.g., feet to miles or milliseconds to microseconds) as necessary. The initial F-D model allows a user the choice of supplying data for the pulse emissions in the time domain, as well as supplying filter types with their number of poles for the receiver. This option is NEWSPEC as described in Appendix C. A second option allows the user to supply data in the frequency domain in the form of amplitudes for specific frequencies (point-amplitude) or as slopes of the emission envelope and receiver response at specific frequencies (point-slope) for input data. This option gives maximum flexibility in that if measured spectrum data and measured receiver data are available, they can be input to the program in the detail desired or necessary. However, it also allows the introduction of approximated spectrum and

receiver response data for those systems that have not been developed.

The fixed system characteristics (transmitter power, receiver noise, terrain type, etc) that are required for calculation of F-D are described in Appendix A.

All of the original sub-elements were designed for specific applications, hence each has some built-in limitations. Although the objective has been to remove as many of these as possible, there are some limitations that should be pointed out.

1. Frequency Range is 20 MHz to 20 GHz.
2. The transmitter antenna heights in the ground-air model must be from 1.6 ft to 9,840 ft (0.5 m to 3000 m), and the receiving antenna heights must be greater than the transmitting antenna height up to 300,000 ft (91,440 m) maximum.
3. Antenna heights in the ground-ground model must be between 1.6 ft to 9,840 ft (0.5 m to 3000 m) for each antenna.
4. The plotting capability imposes some practical restrictions which are identified in the user's guide, Appendix A.

5. The number of point-amplitude or point-slope data pairs used to specify an emission spectrum or a receiver response is limited to 100 data pairs for each envelope.

6. The maximum number of frequency separations which can be used to plot statistical frequency-distance curves is 101. However, Appendix A contains an advisory to use fewer frequency separations when the NEWSPEC routine is selected to synthesize the emission spectrum and receiver response.

3. TYPICAL APPLICATIONS

This model, which portrays the probabilistic nature of radio interference, can be particularly useful in analyzing and avoiding or resolving EMC problems of two types (or from two points-of-view). These applications are (1) the problems faced by the frequency managers in assuring that users of the spectrum will realize satisfactory system performance and (2) the problems faced by an agency in planning and developing a new system or a new use of an existing system. The utility of statistical frequency-distance curves in evaluating each type of problem is demonstrated in the discussion of the following two sections.

3.1 Frequency Management Problem

For this discussion, suppose that some agency of the Federal Government has determined a need to establish a new Land Mobile Radio (LMR) voice net. This net will consist of a fixed base station and several mobile units. The plans call for the base station to use a commercially-available antenna installed 100 ft (30.48 m) above the surrounding terrain. The mobile units will be required to operate within 15 mi (24.1 km) of an existing LMR fixed base station which operates in the 162-174 MHz frequency band with an antenna installed 150 ft (45.72 m) above the terrain and within 10 mi (16.1 km) of an LMR repeater which

operates in the 406-420 MHz frequency band with an antenna installed 200 ft (60.96 m) above the terrain.

Assume that the agency has applied for authorization to operate in the 406-420 MHz frequency band. How can statistical frequency-distance curves be utilized by the frequency management analyst to evaluate this problem? At least two aspects of the problem must be evaluated. These are (1) interference from the existing repeater to the new mobile units and (2) interference from the repeater to the base station for the new voice communications net and vice versa. Interference from the new base station to the existing repeater will be the same as interference from the repeater to the base station, since transmitter and receiver technical characteristics for each installation are assumed to be identical.

The analyst assembles the best data he can obtain for emission characteristics of the repeater and new base station transmitters; receiver selectivity characteristics for the repeater, new base station and new mobile equipments; antenna characteristics for the antenna used by each equipment; and factors influencing propagation between each transmitting and receiving system. These data are provided as input to the statistical frequency-distance curves model. In addition, the analyst must specify an interference criterion and the three probabilities of interference to be considered. Upon execution, the model then will produce the curves that are shown in figures 3-1 and 3-2. Tables 3-1 and 3-2 are the tabular data

STATISTICAL FREQUENCY-DISTANCE CURVES

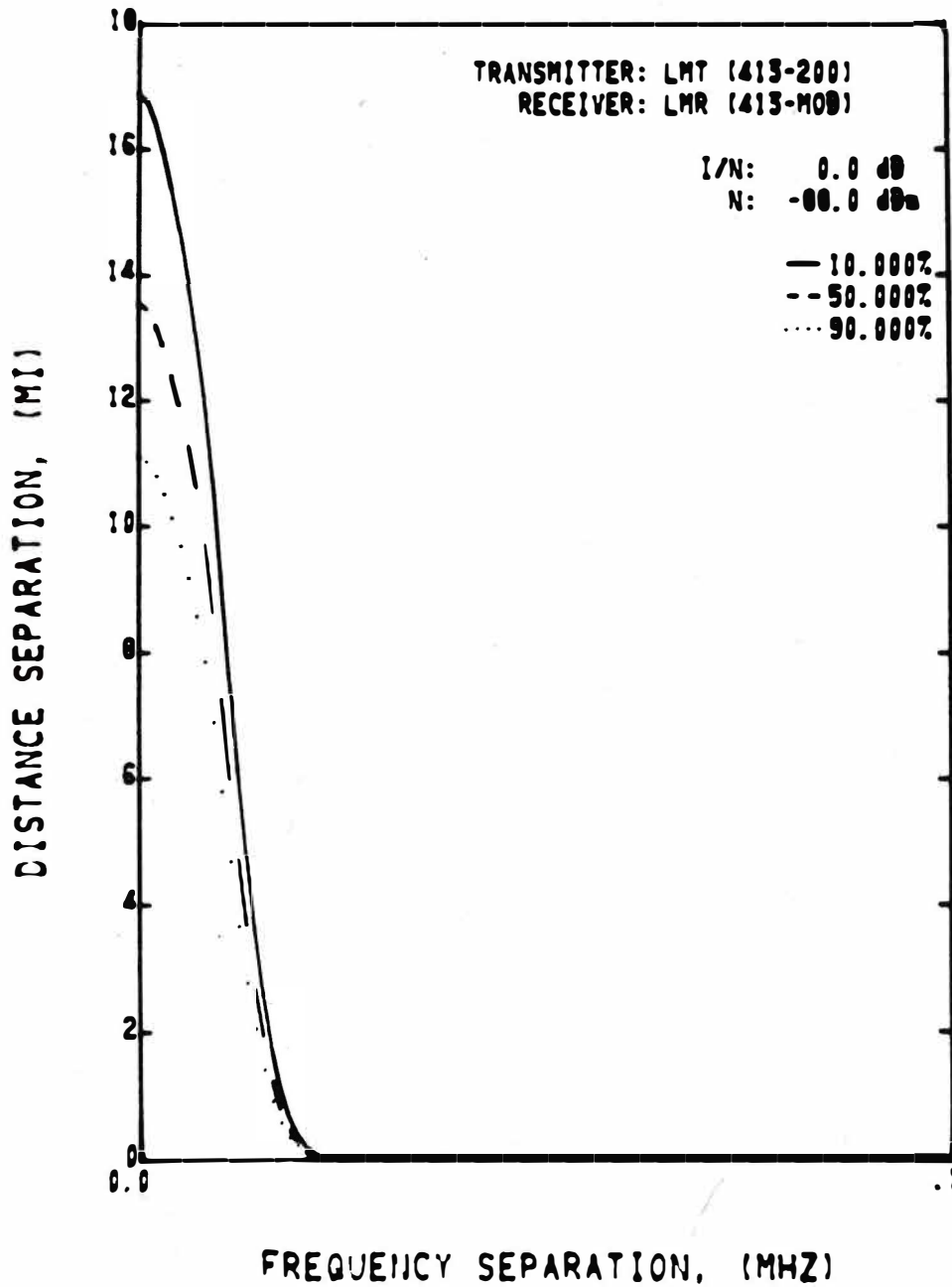


Figure 3-1. Statistical frequency-distance curves for Land Mobile Radio systems operating in the 406-420 MHz band-- fixed equipment transmitter with antenna 200 ft (60.96 m) above terrain vs. mobile receiver for interference criterion I/N = 0 dB (1 mi = 1.6 km).

STATISTICAL FREQUENCY-DISTANCE CURVES

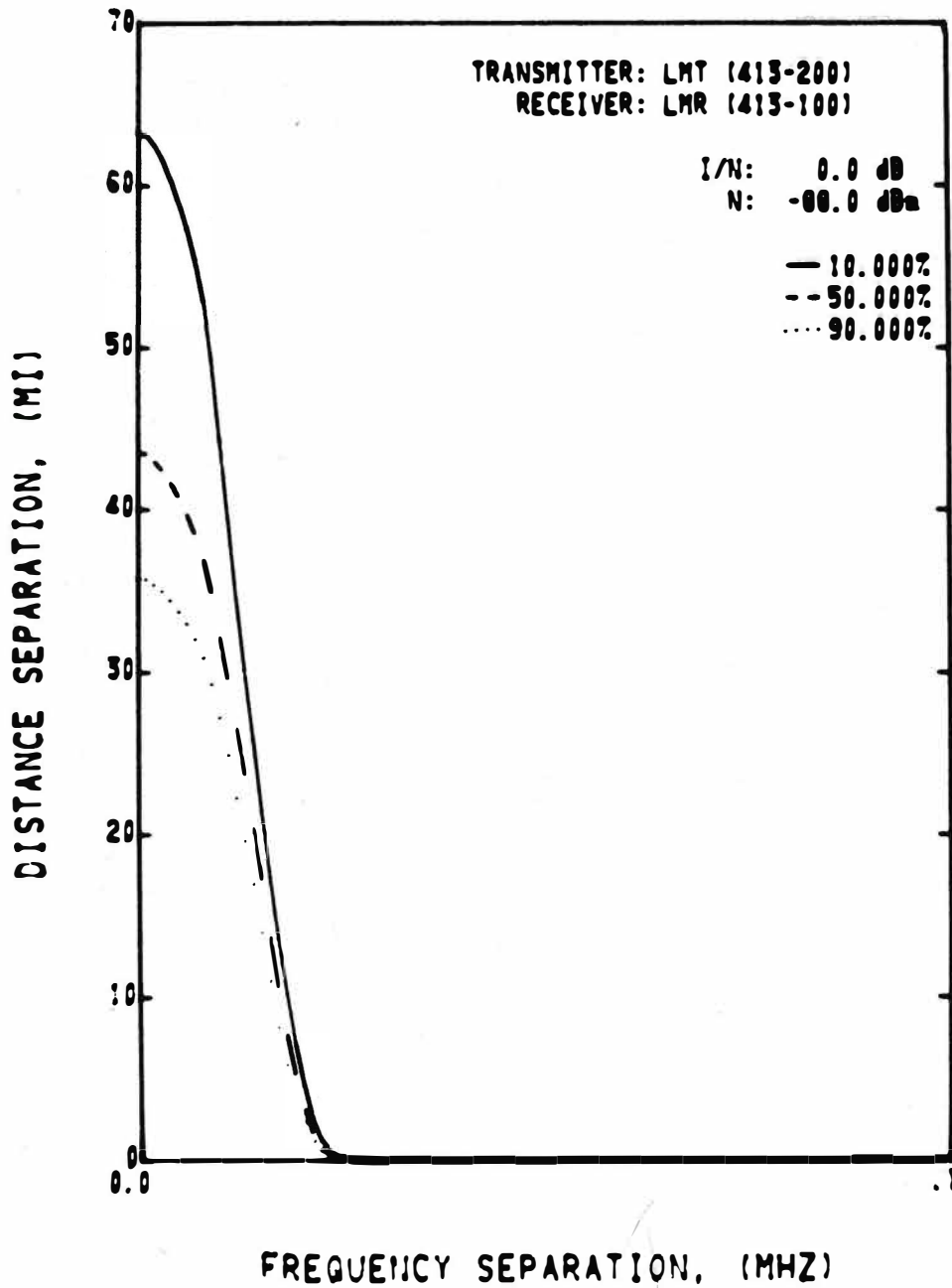


Figure 3-2. Statistical frequency-distance curves for Land Mobile Radio systems operating in the 406-420 MHz band -- fixed equipment transmitter with antenna 200 ft (60.96 m) above terrain vs. fixed equipment receiver with antenna 100 ft (30.48 m) above terrain for interference criterion I/N = 0 dB (1 mi = 1.6 km).

Table 3-1. Tabular Data for Land Mobile Radio Systems Operating in the 406-420 MHz Band with Transmitting Antenna 200 ft (60.96 m) High and Mobile Unit Receiving Antenna

TRANSMITTER: LMT (413-2J0)
 RECEIVER: LMR (413-M0B)

DELTA F (MHZ)	TRANS LOSS (DB)	PROP LOSS (DB)	OFR (DB)	FCR (DB)	DISTANCE SEPARATION, MI	
					(10.000)	(50.000) (90.000
0.000J	134.55	144.55	3.0000	-4.481	16.86	13.53 11.08
.0010	134.43	144.43	-1.185	-5.568	16.73	13.43 10.93
.0020	134.12	144.12	-4.343	-8.824	15.38	13.17 10.77
.0030	133.68	143.68	-8.740	-13.221	15.90	12.81 10.46
.0040	133.14	143.14	-14.128	-18.610	15.32	12.37 10.08
.005J	132.50	142.50	-20.544	-25.025	14.64	11.85 9.64
.0060	131.73	141.73	-28.230	-33.2711	13.87	11.26 9.13
.007J	130.79	140.79	-38.7655	-44.2137	13.01	10.55 8.54
.008J	129.58	139.58	-52.9727	-59.4208	12.02	9.53 7.81
.009J	127.91	137.91	-76.6390	-87.0872	10.70	8.58 6.86
.010J	125.75	135.75	-108.3067	-129.2549	9.11	7.27 5.75
.011J	123.28	133.28	-151.2737	-184.7218	7.51	5.95 4.65
.0120	120.60	130.60	-210.9512	-264.3993	6.07	4.73 3.65
.013J	117.73	127.73	-295.8263	-374.2744	4.75	3.65 2.76
.0140	114.59	124.59	-424.9651	-534.4132	3.55	2.69 2.04
.0150	111.03	121.03	-608.5262	-764.9743	2.52	1.91 1.41
.0160	107.06	117.06	-874.4963	-1114.9444	1.70	1.25 .92
.017J	102.81	112.81	-1201.7429	-1614.1910	1.08	.73 .57

Table 3-2. Tabular Data for Land Mobile Radio Systems Operating in the 406-420 MHz Band with Transmitting Antenna 200 ft (60.96 m) and Receiving Antenna 100 ft. (30.48 m) High

TRANSMITTER: LMT (413-200)
 RECEIVER: LMR (413-100)

DELTA F (MHZ)	TRANS LOSS (DB)	PROP LOSS (DB)	JFR (DB)	FCR (DB)	(10.000)	(50.000)	(90.000)
0.0000	134.55	154.55	0.0000	-.4481	63.19	43.52	35.63
.0010	134.43	154.43	-.1135	-.5668	62.97	43.36	35.56
.0020	134.12	154.12	-.4343	-.8824	62.34	42.92	35.24
.0030	133.68	153.68	-.8740	-1.3221	61.40	42.31	34.80
.0040	133.14	153.14	-1.4128	-1.8610	60.17	41.57	34.25
.0050	132.50	152.50	-2.0544	-2.5025	58.70	40.69	33.63
.0060	131.73	151.73	-2.8230	-3.2711	57.04	39.63	32.88
.0070	130.79	150.79	-3.7555	-4.2137	55.10	38.37	31.95
.0080	129.58	149.58	-4.8727	-5.4208	52.61	36.80	30.79
.0090	127.91	147.91	-6.2390	-7.0872	48.88	34.73	29.13
.0100	125.75	145.75	-8.0067	-9.2549	44.09	32.19	27.11
.0110	123.28	143.28	-10.2737	-11.7218	39.13	29.45	24.75
.0120	120.60	140.60	-13.0512	-14.3993	34.16	26.55	22.14
.0130	117.73	137.73	-16.3263	-17.2744	29.81	23.54	19.50
.0140	114.59	134.59	-20.0951	-20.4132	25.60	20.45	16.86
.0150	111.03	131.03	-23.5252	-23.9743	21.27	17.12	13.94
.0160	107.06	127.06	-27.4963	-27.9444	17.15	13.77	10.93
.0170	102.81	122.81	-31.7429	-32.1910	13.40	10.57	8.19
.0180	98.30	118.30	-36.2514	-36.6995	10.01	7.71	5.82
.0190	93.44	113.44	-41.1111	-41.5592	7.05	5.27	3.84
.0200	87.94	107.94	-46.6103	-47.0584	4.51	3.24	2.23
.0210	81.51	101.51	-53.3393	-53.4874	2.48	1.74	1.13
.0220	74.84	94.84	-63.7070	-60.1552	1.27	.86	.57

corresponding respectively to the figures. Figure 3-1 shows the frequency separation-distance separation relationships that apply to potential interference from the existing repeater transmitter to the new mobile receivers. Because of the reciprocity explained above, the curves in figure 3-2 show the trade-offs in frequency and distance separation which apply either to potential interference from the repeater transmitter to the receiver of the new base station or to potential interference from the new base station transmitter to the repeater receiver.

Considering potential interference from the repeater transmitter to a new mobile receiver, figure 3-1 shows a distance separation of 16.9 mi (27.2 km) would be required if the systems were co-channel ($\Delta f=0$). This value comes from the 10% curve which means that interference power would not exceed the interference criterion more than 10% of the time. The interpretation also can be thought of as at least 90% probability of interference-free operation. If interference could be tolerated as much as 50% of the time, then a distance separation of 13.5 mi (21.7 km) would be needed, and separation of 11 mi (17.7 km) would allow 90% probability of interference. The change from 10% to 50% probability of interference reduced the required distance separation by only 20%. Furthermore, the performance penalty thus incurred would not be accepted by most users. Under co-channel and, perhaps, adjacent channel operating conditions, the probability of interference is an important consideration, as noted. However, it also should be

noted that for frequency separations greater than about 30 kHz (two channel widths), the probability of interference is insignificant, since the required distance separation apparently is much less than the valid minimum distance for which the propagation loss model can be employed. (That minimum distance is considered to be about 1 km.)

A much more desirable scheme for achieving compatible operation under conditions of small distance separations is to operate the new voice net systems with some frequency separation from known sources of interference. In defining the problem, operation of the new mobile units within 10 mi (16.1 km) of the repeater was listed as a requirement. Ten miles (16.1 km) corresponds to a 40% reduction in the necessary distance separation for co-channel operation with 10% probability of interference. With a little effort one can read from the 10% curve in figure 3-1 a frequency separation of about 9 kHz corresponding to 10 mi (16.1 km). Assuming the LMR equipments employ 15 kHz channel spacing, the repeater operation and new voice net operation must be separated by 1 channel. However, one might properly ask if, in fact, the mobile units of the new net always will be at least 10 mi (16.1 km) from the repeater. Figure 3-1 shows that two channels separation (30 kHz) would allow the systems to operate within less than 1 mi (1.61 km) distance separation with at least 90% probability of no interference. If the assumption had been that the agency was applying for authorization to operate in the 162-174 MHz band, an

evaluation similar to the discussion of this paragraph would have been presented for interference from the fixed base station to mobile units operating within a 15 mi (24.1 km) radius.

Now consider interference between the repeater and the new base station. Figure 3-2 shows a maximum distance separation of 63 mi (101 km) would be required if the systems were co-channel ($\Delta f=0$). Such separation would result in interference power exceeding the interference criterion no more than 10% of the time. If performance requirements for the fixed installation were such that interference could be tolerated up to 50% of the time, then a distance separation of 43.5 mi (70 km) would be required. Similar to the preceding situation, this change in probability of interference from 10% to 50% reduces the required distance separation by only 31%. However, few users of the LMR net would be willing to tolerate a 50% probability of interference to their service.

Compatible operation can be achieved by employing frequency separation. Looking at the curves in figure 3-2, it is seen that frequency separation of about 0.03 MHz will allow low probability of interference as well as small required distance separation. The ground-to-ground propagation loss model (as well as the ground-to-air model) is a far field model. No inferences of cosite and/or near field coupling effects are intended by the statistical frequency-distance curves in figures 3-1 and 3-2. By consulting the tabular data in table 3-2, one observes that a frequency

separation of 0.022 MHz (22 kHz) with an associated distance separation of 1.27 mi (2 km) will provide operation with no more than 10% probability of interference. A frequency separation of 22 kHz is midway between one and two channel widths.

At least one factor influencing the curves in figure 3-2 deserves discussion. Antenna-to-antenna coupling has been computed assuming each antenna has power gain of 10 dBi and that main beam-to-main beam coupling will occur. Further, it has been assumed that one antenna will be 200 ft (60.96 m) above the terrain and the other antenna will be 100 ft (30.48 m) above the terrain. Antennas for fixed installations such as the existing repeater and the new base station likely would have some directivity and be installed so that main beam-to-main beam coupling would not occur. A reduction in net coupling gain would reduce the required distance separation. However, one can observe that at 30 kHz (0.03 MHz) frequency separation, the required distance separation is so small that modeling capabilities which consider antenna near field and/or cosite effects must be employed if realistic computations are to be made of required distance separation.

3.2 Engineering/System Design Problem

This problem is an examination of interference that could occur in the 7.25 to 8.40 GHz frequency band. There are many terrestrial microwave links now in operation which employ the RML-4 class of receivers. These systems can operate on any of 24 frequencies in the 7.125 to 7.650 GHz frequency band and on any of 36 frequencies in the 7.650 to

8.400 GHz frequency band. The MILSATCOM system also is scheduled to operate in the 7.25 to 8.40 GHz frequency band. The possible interference that could result to the RML-4 terrestrial receivers from MILSATCOM Airborne Platform transmissions is the problem which will be analyzed. Two questions might concern a system engineer for the MILSATCOM Airborne Platform transmitter:

1. What spectral emission control (how much filtering, etc?) must be applied to achieve compatibility with the RML-4 receivers?
2. Could some additional filtering be incorporated into the RML-4 receivers to help achieve compatibility?

The system designer must collect the best available data on the emission characteristics of the Airborne Platform transmitter and on the selectivity characteristics of the RML-4 receiver, as well as for the antennas used by each system. The antenna patterns reveal that both systems employ high main beam gain antennas. Thus, the antenna gain patterns will be highly directive, and the designer must be concerned with defining the regions of each antenna pattern that provide the energy coupling between systems. A study of the coupling geometry reveals that only side- and back-lobe regions of the Airborne Platform antenna will couple energy to only side- and back-lobe regions of the RML-4 receiver antenna.

Two assumptions for the emission spectrum envelope of the MILSATCOM Airborne Platform transmitter and two assumptions for the selectivity curve of the RML-4 receiver are considered to generate the four plots of statistical frequency-distance curves shown in figures 3-3 through 3-6. Tables 3-3 through 3-6 are the tabular data associated with each respective figure. The assumptions for the emission spectrum envelope are:

- (1) 60 dB/decade roll-off rate at frequencies differing by ± 20 MHz or more from the carrier frequency. This transmitter assumption is designated AB MILSATCOM(7) in figures 3-3 and 3-4.
- (2) a theoretical estimate presented in the ECAC (1975) report which analyzes MILSATCOM compatibility. This transmitter assumption is designated AB MILSATCOM (R) in figures 3-5 and 3

The assumptions for the receiver selectivity curve are:

- (1) 100 dB/decade fall-off rate outside the 3 dB passband, corresponding to a receiver front-end containing five tuned stages. This receiver is designated RML-4 (1) in figures 3-3 and 3-5.
- (2) 140 dB/decade fall-off rate outside the 3 dB passband, corresponding to a receiver front-end containing ten tuned stages. This receiver is designated RML-4 (2) in figures 3-4 and 3-6.

STATISTICAL FREQUENCY-DISTANCE CURVES

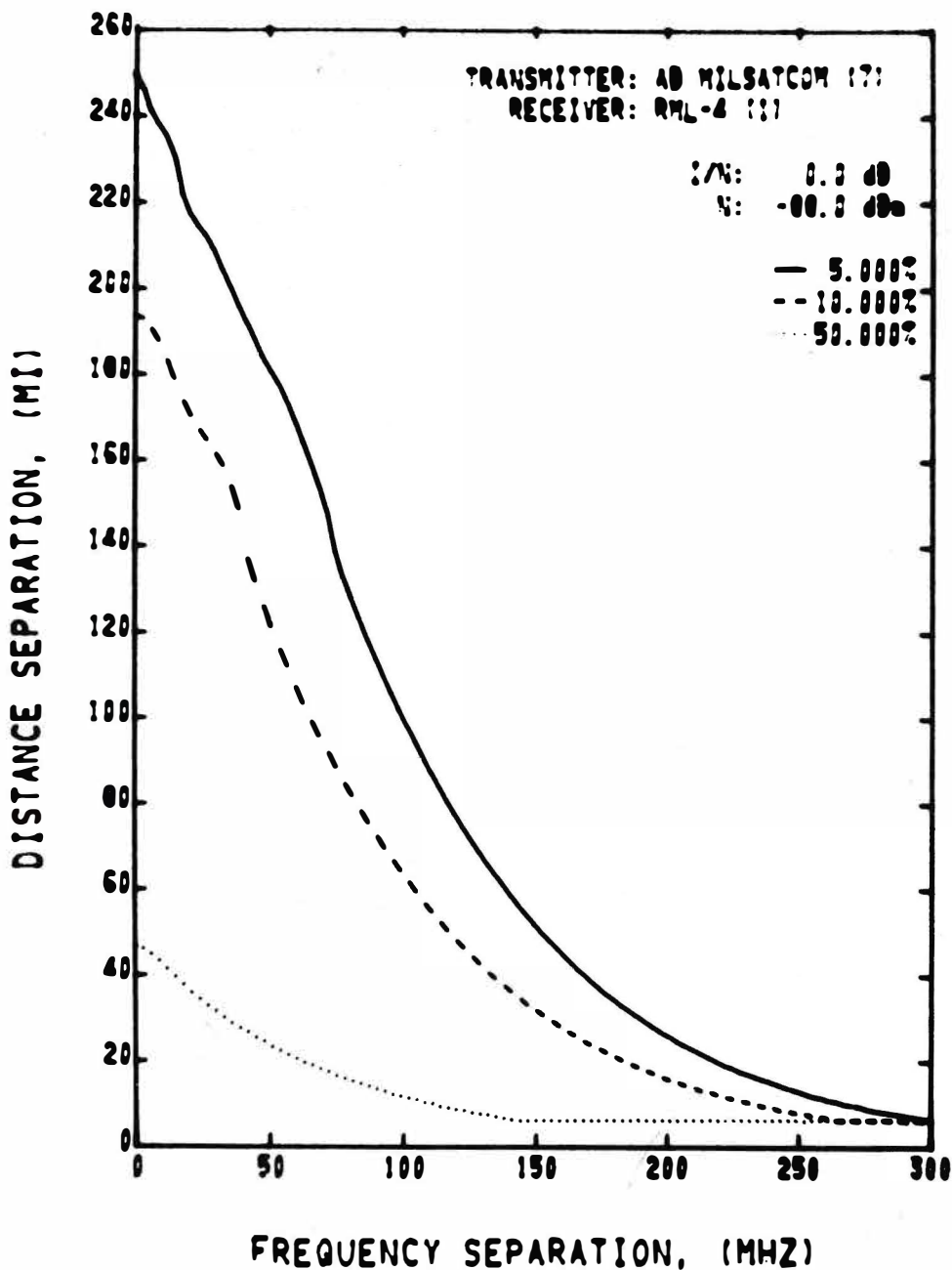


Figure 3-3. Statistical frequency-distance curves for MILSATCOM Airborne transmitter (60 dB/decade roll-off rate) vs. RML-4 receiver (100 dB/decade fall-off rate; 1 mi = 1.6 km).

STATISTICAL FREQUENCY-DISTANCE CURVES

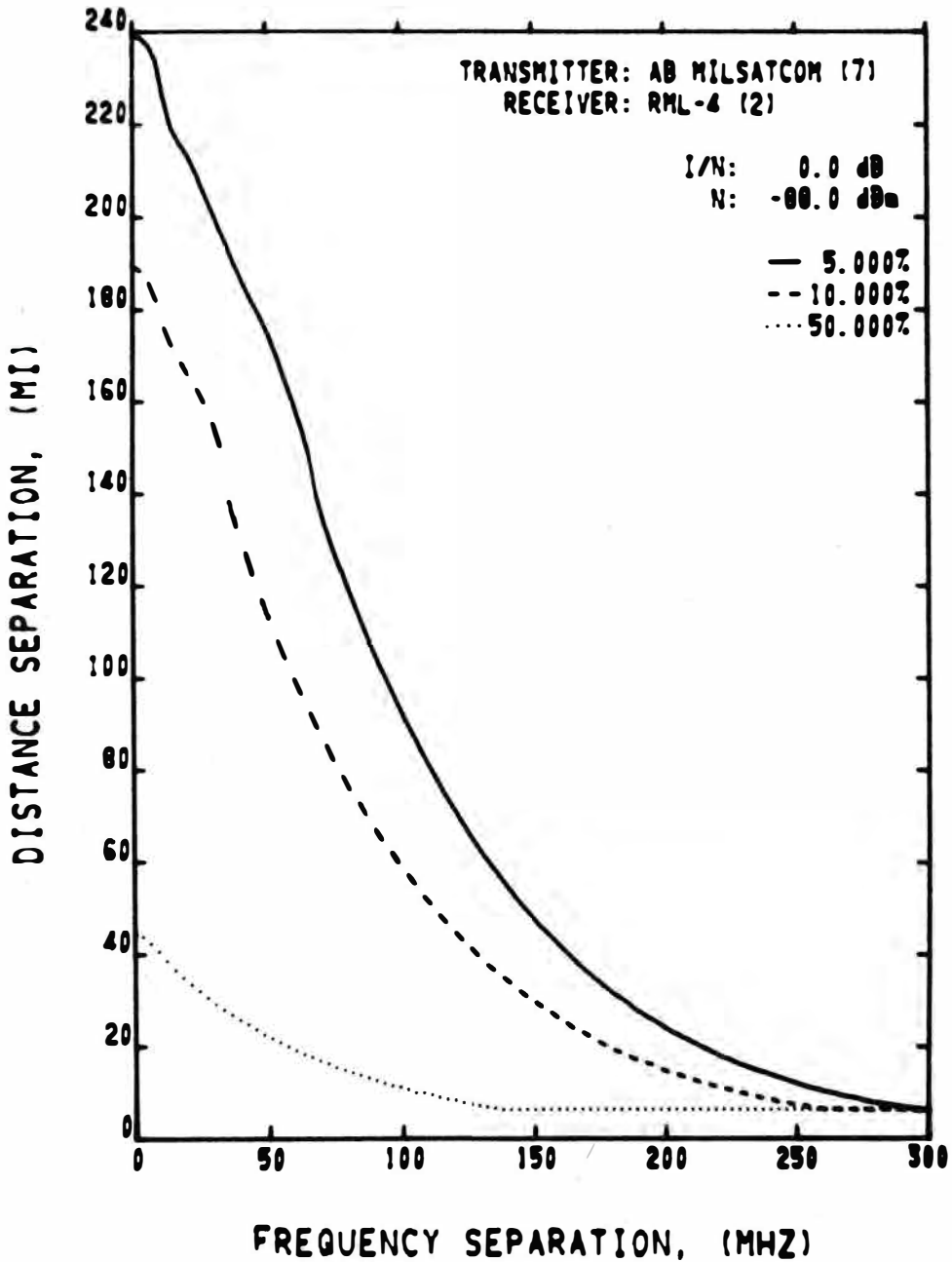


Figure 3-4. Statistical frequency-distance curves for MILSATCOM Airborne transmitter (60 dB/decade roll-off rate) vs. RML-4 receiver (140 dB/decade fall-off rate), (1 mi = 1.6 km).

STATISTICAL FREQUENCY-DISTANCE CURVES

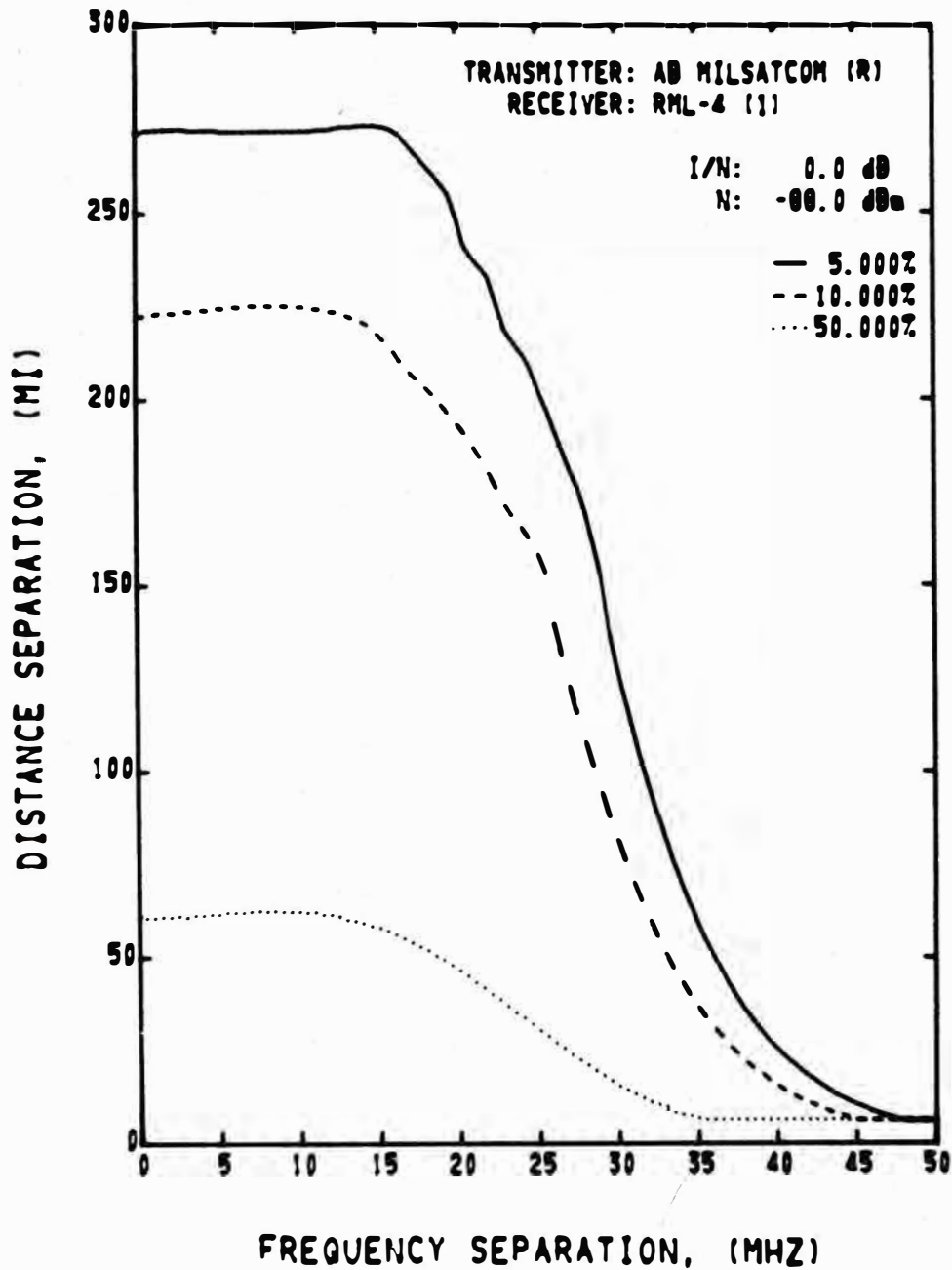


Figure 3-5. Statistical frequency-distance curves for MILSATCOM Airborne transmitter (ECAC emission envelope) vs. RML-4 receiver (100 dB/decade fall-off rate; 1 mi = 1.6 km).

STATISTICAL FREQUENCY-DISTANCE CURVES

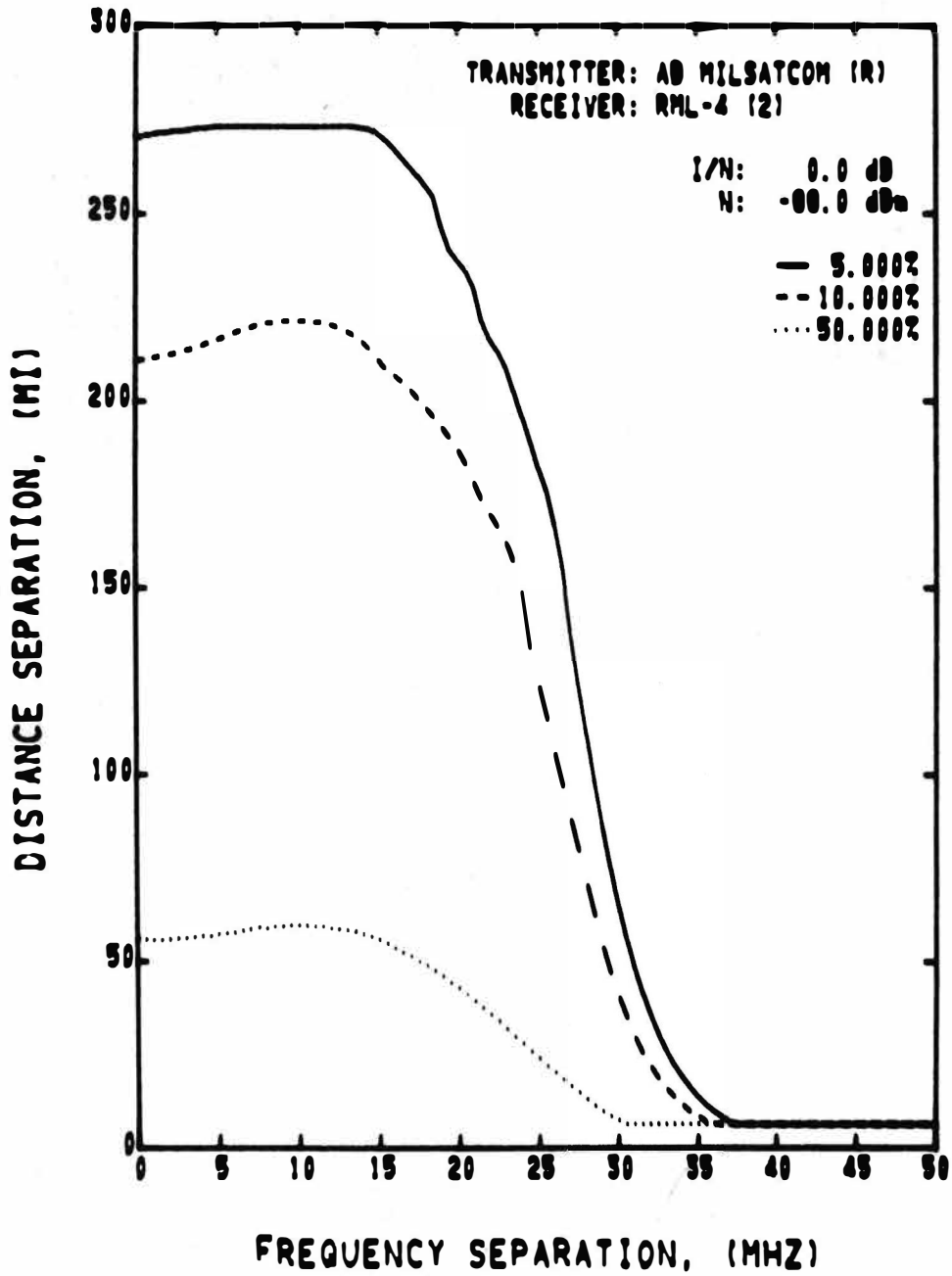


Figure 3-6. Statistical frequency-distance curves for MILSATCOM Airborne transmitter (ECAC emission envelope) vs. RML-4 receiver (140 dB/decade fall-off rate; 1 mi = 1.6 km).

Table 3-3. Tabular Data for MILSATCOM Airborne Transmitter
(60dB/Decade Roll-Off) vs. RML-4 Receiver
(100 dB/Decade Fall-Off)

TRANSMITTER: AB MILSATCOM (7)
RECEIVER: RML-4 (1)

DELTA F (MHZ)	TRANS LOSS (DB)	PROP LOSS (DB)	DFF (DB)	FDR (DB)	DISTANCE SEPARATION, MI		
					(5.000)	(10.000)	(50.000)
0.0000	150.52	148.52	0.0000	-7.4504	249.31	193.07	46.30
3.0000	150.44	148.44	-1.0832	-7.5636	245.94	192.26	45.88
6.0000	150.21	148.21	-1.3051	-7.7865	240.26	190.09	44.77
9.0000	149.88	147.88	-1.6424	-8.1229	236.73	186.83	43.14
12.0000	149.47	147.47	-1.8463	-8.5267	233.97	182.75	41.25
15.0000	149.05	147.05	-1.4723	-8.9524	229.31	177.88	39.34
18.0000	148.62	146.62	-1.8993	-9.3797	220.35	173.06	37.51
21.0000	148.20	146.20	-2.3179	-9.7983	215.70	169.29	35.80
24.0000	147.80	145.80	-2.7235	-10.2039	212.97	166.38	34.24
27.0000	147.40	145.40	-3.1179	-10.5974	210.41	163.75	32.77
30.0000	147.02	145.02	-3.5009	-10.9813	206.98	160.92	31.38
33.0000	146.64	144.64	-3.8799	-11.3603	202.83	157.57	30.06
36.0000	146.26	144.26	-4.2571	-11.7375	198.69	153.51	28.81
39.0000	145.89	143.89	-4.6334	-12.1138	194.60	147.75	27.63
42.0000	145.51	143.51	-5.0094	-12.4898	190.55	136.96	26.51
45.0000	145.13	143.13	-5.3851	-12.8655	186.52	130.93	25.43
48.0000	144.75	142.75	-5.7606	-13.2410	182.60	125.59	24.37
51.0000	144.38	142.38	-6.1360	-13.6164	179.42	120.54	23.36
54.0000	144.01	142.01	-6.5113	-13.9917	176.40	115.75	22.38
57.0000	143.63	141.63	-6.8864	-14.3668	172.64	111.23	21.45
60.0000	143.26	141.26	-7.2613	-14.7417	167.95	106.94	20.56
63.0000	142.88	140.88	-7.6362	-15.1166	163.10	102.83	19.71
66.0000	142.51	140.51	-8.0109	-15.4913	158.05	98.89	18.89
69.0000	142.13	140.13	-8.3855	-15.8658	152.96	95.09	18.11
72.0000	141.76	139.76	-8.7599	-16.2403	146.70	91.42	17.35
75.0000	141.39	139.39	-9.1342	-16.6146	137.62	87.89	16.63
78.0000	141.01	139.01	-9.5083	-16.9887	131.63	84.49	15.94
81.0000	140.64	138.64	-9.8824	-17.3628	126.50	81.21	15.28
84.0000	140.26	138.26	-10.2563	-17.7366	121.94	78.05	14.64
87.0000	139.89	137.89	-10.6300	-18.1104	117.52	75.01	14.03
90.0000	139.52	137.52	-11.0036	-18.4840	113.18	72.09	13.45
93.0000	139.14	137.14	-11.3771	-18.8575	108.96	69.26	12.89
96.0000	138.77	136.77	-11.7504	-19.2308	104.90	66.54	12.36
99.0000	138.40	136.40	-12.1237	-19.6041	100.95	63.91	11.84
102.0000	138.02	136.02	-12.4967	-19.9771	97.13	61.38	11.35
105.0000	137.65	135.65	-12.8697	-20.3501	92.46	58.94	10.88
108.0000	137.29	135.28	-13.2425	-20.7229	89.91	56.59	10.42
111.0000	136.93	134.93	-13.6152	-21.0956	86.46	54.33	9.99
114.0000	136.53	134.53	-13.9877	-21.4681	83.14	52.15	9.57
117.0000	136.16	134.16	-14.3601	-21.8405	79.93	50.07	9.18
120.0000	135.79	133.79	-14.7324	-22.2128	76.83	48.07	8.79
123.0000	135.42	133.42	-15.1045	-22.5849	73.84	46.15	8.43
126.0000	135.04	133.04	-15.4755	-22.9569	70.94	44.29	8.08
129.0000	134.67	132.67	-15.8484	-23.3288	68.15	42.51	7.74
132.0000	134.30	132.30	-16.2201	-23.7005	65.48	40.78	7.42
135.0000	133.93	131.93	-16.5917	-24.0721	62.91	39.13	7.11
138.0000	133.56	131.56	-16.9632	-24.4436	60.43	37.54	6.82
141.0000	133.19	131.19	-17.3345	-24.8149	58.04	36.03	6.53
144.0000	132.81	130.81	-17.7057	-25.1861	55.75	34.59	6.26
147.0000	132.44	130.44	-18.0758	-25.5572	53.54	33.19	6.21
150.0000	132.07	130.07	-18.4477	-25.9281	51.42	31.83	6.21
153.0000	131.70	129.70	-18.8185	-26.2989	49.36	30.52	6.21
156.0000	131.33	129.33	-19.1892	-26.6695	47.38	29.27	6.21
159.0000	130.96	128.96	-19.5597	-27.0401	45.48	28.09	6.21

Table 3-3. Continued

162.0000	130.59	128.59	-13.9331	-27.4105	43.67	26.95	6.21
165.0000	130.22	128.22	-20.3004	-27.7808	41.92	25.33	6.21
168.0000	129.35	127.85	-20.6705	-28.1509	40.24	24.83	6.21
171.0000	129.48	127.48	-21.3405	-28.5209	38.61	23.81	6.21
174.0000	129.11	127.11	-21.4104	-28.8909	37.05	22.83	6.21
177.0000	128.74	126.74	-21.7801	-29.2605	35.55	21.89	6.21
180.0000	128.37	126.37	-22.1497	-29.6301	34.13	20.99	6.21
183.0000	128.00	126.00	-22.5192	-29.9996	32.75	20.14	6.21
186.0000	127.63	125.63	-22.8885	-30.3689	31.42	19.31	6.21
189.0000	127.26	125.26	-23.2577	-30.7381	30.14	18.52	6.21
192.0000	126.89	124.89	-23.6268	-31.1072	28.91	17.76	6.21
195.0000	126.52	124.52	-23.9957	-31.4761	27.75	17.03	6.21
198.0000	126.16	124.16	-24.3645	-31.8449	26.64	16.34	6.21
201.0000	125.79	123.79	-24.7332	-32.2136	25.57	15.67	6.21
204.0000	125.42	123.42	-25.1018	-32.5822	24.53	15.03	6.21
207.0000	125.05	123.05	-25.4702	-32.9506	23.52	14.41	6.21
210.0000	124.68	122.68	-25.8385	-33.3189	22.55	13.82	6.21
213.0000	124.31	122.31	-26.2066	-33.6870	21.64	13.25	6.21
216.0000	123.94	121.94	-26.5746	-34.0550	20.76	12.71	6.21
219.0000	123.58	121.58	-26.9425	-34.4229	19.91	12.19	6.21
222.0000	123.21	121.21	-27.3103	-34.7907	19.11	11.69	6.21
225.0000	122.84	120.84	-27.6779	-35.1583	18.32	11.21	6.21
228.0000	122.47	120.47	-28.0454	-35.5258	17.58	10.75	6.21
231.0000	122.11	120.11	-28.4128	-35.8932	16.86	10.31	6.21
234.0000	121.74	119.74	-28.7800	-36.2604	16.17	9.88	6.21
237.0000	121.37	119.37	-29.1471	-36.6275	15.51	9.48	6.21
240.0000	121.01	119.01	-29.5141	-36.9945	14.89	9.09	6.21
243.0000	120.64	118.64	-29.8810	-37.3613	14.27	8.72	6.21
246.0000	120.27	118.27	-30.2477	-37.7281	13.69	8.36	6.21
249.0000	119.91	117.91	-30.6142	-38.0946	13.13	8.02	6.21
252.0000	119.54	117.54	-30.9807	-38.4611	12.59	7.69	6.21
255.0000	119.17	117.17	-31.3470	-38.8274	12.08	7.37	6.21
258.0000	118.81	116.81	-31.7132	-39.1936	11.59	7.07	6.21
261.0000	118.44	116.44	-32.0793	-39.5597	11.11	6.78	6.21
264.0000	118.07	116.07	-32.4452	-39.9256	10.66	6.50	6.21
267.0000	117.71	115.71	-32.8110	-40.2914	10.23	6.23	6.21
270.0000	117.34	115.34	-33.1767	-40.6571	9.81	6.21	6.21
273.0000	116.98	114.98	-33.5422	-41.0226	9.41	6.21	6.21
276.0000	116.61	114.61	-33.9077	-41.3880	9.02	6.21	6.21
279.0000	116.25	114.25	-34.2729	-41.7533	8.65	6.21	6.21
282.0000	115.88	113.88	-34.6381	-42.1185	8.30	6.21	6.21
285.0000	115.52	113.52	-35.0031	-42.4835	7.95	6.21	6.21
288.0000	115.15	113.15	-35.3680	-42.8484	7.64	6.21	6.21
291.0000	114.79	112.79	-35.7328	-43.2132	7.33	6.21	6.21
294.0000	114.42	112.42	-36.0974	-43.5778	7.03	6.21	6.21
297.0000	114.06	112.06	-36.4619	-43.9423	6.74	6.21	6.21
300.0000	113.69	111.69	-36.8263	-44.3067	6.46	6.21	6.21

Table 3-4. Tabular Data for MILSATCOM Airborne Transmitter
(60 dB/Decade Roll-Off) vs. RML-4 Receiver
(140 dB/Decade Fall-Off)

TRANSMITTER: AB MILSATCOM (7)
RECEIVER: RML-4 (2)

DELTA F (MHZ)	TRANS LOSS (DB)	PROP LOSS (DB)	OFR (DB)	FDR (DB)	DISTANCE SEPARATION, MI		
					(5.000)	(10.000)	(50.000)
0.0000	149.97	147.97	1.0000	-8.0277	237.52	187.73	43.53
3.0000	147.87	147.87	-0.9980	-8.1258	236.71	186.77	43.12
6.0000	149.61	147.61	-0.3634	-8.3912	234.90	184.15	41.87
9.0000	149.20	147.20	-0.7673	-8.7950	231.48	179.73	40.03
12.0000	148.76	146.76	-1.2153	-9.2431	223.23	174.52	38.03
15.0000	148.31	146.31	-1.6605	-9.6883	216.61	170.19	36.24
18.0000	147.88	145.88	-2.0955	-10.1233	213.47	166.93	34.54
21.0000	147.46	145.46	-2.5157	-10.5435	210.80	164.12	32.97
24.0000	147.05	145.05	-2.9186	-10.9464	207.36	161.20	31.50
27.0000	146.67	144.67	-3.3067	-11.3344	203.12	157.82	30.15
30.0000	146.29	144.29	-3.6845	-11.7123	198.97	153.81	28.89
33.0000	145.91	143.91	-4.0608	-12.0885	194.88	148.47	27.71
36.0000	145.54	143.54	-4.4363	-12.4645	190.82	137.27	26.58
39.0000	145.16	143.16	-4.8127	-12.8405	186.79	131.31	25.50
42.0000	144.78	142.78	-5.1885	-13.2162	182.83	125.93	24.44
45.0000	144.41	142.41	-5.5641	-13.5919	179.61	120.86	23.42
48.0000	144.03	142.03	-5.9396	-13.9674	176.61	116.05	22.44
51.0000	143.66	141.66	-6.3150	-14.3427	172.93	111.51	21.51
54.0000	143.28	141.28	-6.6902	-14.7179	168.27	107.20	20.62
57.0000	142.91	140.91	-7.0653	-15.0930	163.31	103.08	19.76
60.0000	142.53	140.53	-7.4403	-15.4680	158.36	99.13	18.94
63.0000	142.16	140.16	-7.8151	-15.8428	153.28	95.32	18.15
66.0000	141.78	139.78	-8.1897	-16.2175	147.26	91.64	17.40
69.0000	141.41	139.41	-8.5643	-16.5920	138.00	88.10	16.68
72.0000	141.03	139.03	-8.9387	-16.9664	131.97	84.69	15.98
75.0000	140.66	138.66	-9.3130	-17.3407	126.77	81.40	15.32
78.0000	140.29	138.29	-9.6871	-17.7148	122.20	78.23	14.68
81.0000	139.91	137.91	-10.0611	-18.0888	117.77	75.18	14.07
84.0000	139.54	137.54	-10.4350	-18.4627	113.42	72.25	13.48
87.0000	139.16	137.16	-10.8087	-18.8364	109.20	69.42	12.92
90.0000	138.79	136.79	-11.1823	-19.2100	105.12	66.69	12.39
93.0000	138.42	136.42	-11.5558	-19.5835	101.16	64.05	11.87
96.0000	138.04	136.04	-11.9291	-19.9569	97.33	<u>61.51</u>	<u>11.38</u>
99.0000	137.67	135.67	-12.3023	-20.3300	93.66	59.07	10.90
102.0000	137.30	135.30	-12.6753	-20.7031	90.09	56.71	10.45
105.0000	136.92	134.92	-13.0482	-21.0760	<u>86.64</u>	<u>54.44</u>	<u>10.01</u>
108.0000	136.55	134.55	-13.4210	-21.4488	83.31	52.26	9.60
111.0000	136.18	134.18	-13.7937	-21.8214	80.10	50.17	9.20
114.0000	135.81	133.81	-14.1662	-22.1939	<u>76.39</u>	<u>48.17</u>	<u>8.81</u>
117.0000	135.43	133.43	-14.5386	-22.5663	73.98	46.24	8.45
120.0000	135.06	133.06	-14.9109	-22.9386	71.08	44.38	8.09
123.0000	134.69	132.69	-15.2829	-23.3107	<u>68.29</u>	<u>42.59</u>	<u>7.76</u>
126.0000	134.32	132.32	-15.6549	-23.6827	65.60	40.86	7.43
129.0000	133.95	131.95	-16.0268	-24.0545	63.03	39.20	7.12
132.0000	133.57	131.57	-16.3985	-24.4262	<u>60.54</u>	<u>37.61</u>	<u>6.83</u>
135.0000	133.20	131.20	-16.7701	-24.7978	58.15	36.10	6.54
138.0000	132.83	130.83	-17.1415	-25.1692	55.85	34.65	6.27
141.0000	132.46	130.46	-17.5129	-25.5405	<u>53.64</u>	<u>33.25</u>	<u>6.21</u>
144.0000	132.09	130.09	-17.8840	-25.9117	51.51	31.89	6.21
147.0000	131.72	129.72	-18.2550	-26.2829	49.45	30.58	6.21
150.0000	131.35	129.35	-18.6259	-26.6537	<u>47.46</u>	<u>29.32</u>	<u>6.21</u>
153.0000	130.98	128.98	-18.9967	-27.0244	45.56	28.13	6.21
156.0000	130.60	128.60	-19.3674	-27.3951	43.74	27.00	6.21
159.0000	130.23	128.23	-19.7379	-27.7656	41.99	25.92	6.21

Table 3-4. Continued

162.000J	129.86	127.86	-20.1082	-26.1360	40.30	24.87	6.21
165.000J	129.49	127.49	-20.4735	-28.5062	33.67	23.85	6.21
168.000J	129.12	127.12	-20.8436	-28.8763	37.11	22.87	6.21
171.000J	128.75	126.75	-21.2196	-29.2463	35.61	21.93	6.21
174.000J	128.38	126.38	-21.5884	-29.6162	34.18	21.02	6.21
177.000J	128.01	126.01	-21.9581	-29.9859	32.80	20.17	6.21
180.000J	127.64	125.64	-22.3277	-30.3555	31.47	19.34	6.21
183.000J	127.28	125.28	-22.6972	-30.7249	30.18	18.55	6.21
186.000J	126.91	124.91	-23.0665	-31.0942	28.96	17.79	6.21
189.000J	126.54	124.54	-23.4357	-31.4634	27.79	17.06	6.21
192.000J	126.17	124.17	-23.8047	-31.8325	26.68	16.36	6.21
195.000J	125.80	123.80	-24.1735	-32.2014	25.61	15.69	6.21
198.000J	125.43	123.43	-24.5424	-32.5702	24.56	15.05	6.21
201.000J	125.06	123.06	-24.9111	-32.9388	23.55	14.43	6.21
204.000J	124.69	122.69	-25.2795	-33.3073	22.58	13.83	6.21
207.000J	124.32	122.32	-25.6480	-33.6757	21.56	13.27	6.21
210.000J	123.96	121.96	-26.0163	-34.0440	20.79	12.72	6.21
213.000J	123.59	121.59	-26.3844	-34.4121	19.94	12.20	6.21
216.000J	123.22	121.22	-26.7524	-34.7801	19.13	11.70	6.21
219.000J	122.85	120.85	-27.1203	-35.1480	18.34	11.22	6.21
222.000J	122.48	120.48	-27.4880	-35.5157	17.60	10.76	6.21
225.000J	122.12	120.12	-27.8555	-35.8833	16.88	10.32	6.21
228.000J	121.75	119.75	-28.2231	-36.2509	16.19	9.89	6.21
231.000J	121.38	119.38	-28.5904	-36.6182	15.53	9.49	6.21
234.000J	121.01	119.01	-28.9576	-36.9854	14.90	9.10	6.21
237.000J	120.65	118.65	-29.3247	-37.3525	14.29	8.73	6.21
240.000J	120.28	118.28	-29.6917	-37.7194	13.71	8.37	6.21
243.000J	119.91	117.91	-30.0585	-38.0862	13.15	8.02	6.21
246.000J	119.55	117.55	-30.4252	-38.4529	12.61	7.69	6.21
249.000J	119.18	117.18	-30.7918	-38.8195	12.09	7.38	6.21
252.000J	118.81	116.81	-31.1582	-39.1859	11.60	7.07	6.21
255.000J	118.45	116.45	-31.5245	-39.5522	11.12	6.79	6.21
258.000J	118.08	116.08	-31.8907	-39.9184	10.67	6.51	6.21
261.000J	117.72	115.72	-32.2567	-40.2844	10.23	6.24	6.21
264.000J	117.35	115.35	-32.6226	-40.6504	9.82	6.21	6.21
267.000J	116.98	114.98	-32.9884	-41.0161	9.41	6.21	6.21
270.000J	116.62	114.62	-33.3541	-41.3813	9.03	6.21	6.21
273.000J	116.25	114.25	-33.7195	-41.7473	8.56	6.21	6.21
276.000J	115.89	113.89	-34.0850	-42.1127	8.31	6.21	6.21
279.000J	115.52	113.52	-34.4502	-42.4780	7.97	6.21	6.21
282.000J	115.16	113.16	-34.8154	-42.8431	7.64	6.21	6.21
285.000J	114.79	112.79	-35.1804	-43.2081	7.33	6.21	6.21
288.000J	114.43	112.43	-35.5453	-43.5730	7.03	6.21	6.21
291.000J	114.06	112.06	-35.9100	-43.9377	6.74	6.21	6.21
294.000J	113.70	111.70	-36.2746	-44.3024	6.47	6.21	6.21
297.000J	113.33	111.33	-36.6391	-44.6669	6.21	6.21	6.21
300.000J	112.97	110.97	-37.0035	-45.0312	6.21	6.21	6.21

Table 3-5. Tabular Data for MILSATCOM Airborne Transmitter
(ECAC Emission Envelope) vs. RML-4 Receiver
(100 dB/Decade Fall-Off)

TRANSMITTER: AB MILSATCOM (R)
RECEIVER: RML-4 (1)

DELTA F (MHZ)	TRANS LOSS (DB)	PROP LOSS (DB)	OFR (DB)	FDR (DB)	DISTANCE SEPARATION, MI		
					(5.000)	(10.000)	(50.000)
0.0000	152.95	150.95	.0000	-5.0463	271.12	222.06	60.43
.5000	152.96	150.96	.0020	-5.0443	271.11	222.08	60.44
1.0000	152.96	150.96	.0078	-5.0385	271.09	222.13	60.43
1.5000	152.97	150.97	.0172	-5.0291	271.06	222.21	60.54
2.0000	152.98	150.98	.0298	-5.0165	271.01	222.31	60.63
2.5000	153.00	151.00	.0453	-5.0010	270.96	222.44	60.73
3.0000	153.02	151.02	.0634	-4.9829	270.90	222.59	60.85
3.5000	153.04	151.04	.0837	-4.9627	270.83	222.76	60.93
4.0000	153.06	151.06	.1055	-4.9408	270.75	222.93	61.13
4.5000	153.08	151.08	.1285	-4.9173	270.67	223.12	61.23
5.0000	153.11	151.11	.1521	-4.8942	270.59	223.30	61.43
5.5000	153.13	151.13	.1755	-4.8708	270.51	223.48	61.59
6.0000	153.15	151.15	.1981	-4.8483	270.43	223.66	61.74
6.5000	153.17	151.17	.2188	-4.8275	270.36	223.82	61.83
7.0000	153.19	151.19	.2368	-4.8096	270.30	223.96	62.00
7.5000	153.20	151.20	.2507	-4.7956	270.26	224.07	62.09
8.0000	153.21	151.21	.2595	-4.7863	270.23	224.13	62.15
8.5000	153.22	151.22	.2625	-4.7837	270.22	224.15	62.17
9.0000	153.21	151.21	.2597	-4.7866	270.23	224.14	62.15
9.5000	153.20	151.20	.2534	-4.7959	270.26	224.06	62.09
10.0000	153.19	151.19	.2433	-4.8121	270.31	223.94	61.93
10.5000	153.16	151.16	.2193	-4.8355	270.39	223.76	61.83
11.0000	153.13	151.13	.1735	-4.8663	270.49	223.52	61.62
11.5000	153.09	151.09	.1337	-4.9066	270.63	223.20	61.35
12.0000	153.04	151.04	.0906	-4.9553	270.80	222.81	61.03
12.5000	152.98	150.98	.0311	-5.0152	271.01	222.32	60.63
13.0000	152.91	150.91	-.0395	-5.0853	271.25	221.72	60.17
13.5000	152.83	150.83	-.1217	-5.1680	271.49	220.96	59.64
14.0000	152.74	150.74	-.2158	-5.2622	271.72	220.00	59.03
14.5000	152.63	150.63	-.3229	-5.3692	271.87	218.73	58.35
15.0000	152.51	150.51	-.4438	-5.4902	271.85	217.13	57.58
15.5000	152.37	150.37	-.5793	-5.6262	271.53	214.83	56.73
16.0000	152.22	150.22	-.7306	-5.7769	270.72	212.06	55.81
16.5000	152.06	150.06	-.8958	-5.9421	269.14	209.20	54.81
17.0000	151.88	149.83	-1.0752	-6.1215	266.84	206.85	53.75
17.5000	151.68	149.68	-1.2633	-6.3152	264.37	204.82	52.62
18.0000	151.48	149.48	-1.4771	-6.5235	261.82	202.66	51.43
18.5000	151.25	149.25	-1.7004	-6.7468	259.28	200.38	50.19
19.0000	151.01	149.01	-1.9395	-6.9853	256.64	197.95	48.89
19.5000	150.76	148.76	-2.1953	-7.2416	253.71	195.42	47.53
20.0000	150.48	148.43	-2.4691	-7.5154	247.93	192.73	46.12
20.5000	150.19	148.19	-2.7621	-7.8084	239.96	189.87	44.66
21.0000	149.88	147.88	-3.0740	-8.1203	236.75	186.83	43.15
21.5000	149.55	147.55	-3.4045	-8.4508	234.50	183.55	41.60
22.0000	149.20	147.20	-3.7542	-8.8006	231.42	179.67	40.01
22.5000	148.83	146.83	-4.1245	-9.1703	224.38	175.33	38.39
23.0000	148.44	146.44	-4.5167	-9.5630	217.79	171.28	36.75
23.5000	148.02	146.02	-4.9300	-9.9763	214.42	167.96	35.11
24.0000	147.59	145.59	-5.3637	-10.4100	211.69	165.01	33.46
24.5000	147.14	145.14	-5.8173	-10.8636	208.19	161.84	31.80
25.0000	146.66	144.66	-6.2909	-11.3373	203.09	157.80	30.14
25.5000	146.17	144.17	-6.7850	-11.8313	197.67	152.36	28.51
26.0000	145.65	143.65	-7.3003	-12.3466	192.09	139.65	26.93
26.5000	145.12	143.12	-7.8381	-12.8845	186.32	130.65	25.37

Table 3-5. Continued

27.0000	144.55	142.55	-8.4804	-13.4467	180.78	122.79	23.81
27.5000	143.96	141.96	-3.9895	-14.0358	176.01	115.20	22.27
28.0000	143.35	141.35	-3.6070	-14.6533	169.11	107.93	20.77
28.5000	142.70	140.70	-11.2439	-15.2952	160.64	100.93	19.31
29.0000	142.04	140.04	-11.3107	-15.9570	151.68	94.18	17.92
29.5000	141.36	139.36	-11.5888	-16.6352	137.28	87.70	16.59
30.0000	140.67	138.67	-12.2805	-17.3269	126.94	81.52	15.34
30.5000	139.97	137.97	-12.3836	-18.0299	118.46	75.66	14.16
31.0000	139.26	137.26	-13.6962	-18.7425	110.25	70.12	13.06
31.5000	138.54	136.54	-14.4168	-19.4631	102.42	64.89	12.03
32.0000	137.81	135.81	-15.1443	-20.1906	95.02	59.97	11.03
32.5000	137.08	135.08	-15.8775	-20.9239	88.04	55.36	10.19
33.0000	136.34	134.34	-16.6158	-21.6621	81.46	51.06	9.37
33.5000	135.60	133.60	-17.3583	-22.4046	75.28	47.07	8.60
34.0000	134.85	132.85	-18.1044	-23.1508	69.47	43.35	7.91
34.5000	134.10	132.10	-18.8537	-23.9000	64.03	39.88	7.25
35.0000	133.35	131.35	-19.6056	-24.6520	59.03	36.63	6.65
35.5000	132.59	130.59	-20.3539	-25.4062	54.43	33.75	6.21
36.0000	131.84	129.84	-21.1162	-26.1625	50.11	31.00	6.21
36.5000	131.08	129.08	-21.8742	-26.9205	46.08	28.45	6.21
37.0000	130.32	128.32	-22.6338	-27.6801	42.39	26.17	6.21
37.5000	129.56	127.56	-23.3947	-28.4410	38.95	24.03	6.21
38.0000	128.80	126.80	-24.1568	-29.2031	35.78	22.04	6.21
38.5000	128.03	126.03	-24.9200	-29.9663	32.87	20.21	6.21
39.0000	127.27	125.27	-25.6842	-30.7305	30.17	18.54	6.21
39.5000	126.50	124.50	-26.4493	-31.4956	27.69	17.00	6.21
40.0000	125.74	123.74	-27.2153	-32.2616	25.43	15.58	6.21
40.5000	124.97	122.97	-27.9822	-33.0285	23.31	14.28	6.21
41.0000	124.20	122.20	-28.7498	-33.7961	21.33	13.09	6.21
41.5000	123.44	121.44	-29.5177	-34.5641	19.60	12.00	6.21
42.0000	122.67	120.67	-30.2859	-35.3322	17.97	10.99	6.21
42.5000	121.90	119.90	-31.0541	-36.1004	16.47	10.07	6.21
43.0000	121.13	119.13	-31.8223	-36.8687	15.09	9.22	6.21
43.5000	120.36	118.36	-32.5907	-37.6370	13.83	8.45	6.21
44.0000	119.59	117.59	-33.3591	-38.4054	12.63	7.74	6.21
44.5000	118.83	116.83	-34.1275	-39.1739	11.61	7.08	6.21
45.0000	118.06	116.06	-34.8959	-39.9423	10.64	6.49	6.21
45.5000	117.29	115.29	-35.6645	-40.7109	9.75	6.21	6.21
46.0000	116.52	114.52	-36.4331	-41.4794	8.93	6.21	6.21
46.5000	115.75	113.75	-37.2016	-42.2481	8.18	6.21	6.21
47.0000	114.98	112.98	-37.9702	-43.0165	7.49	6.21	6.21
47.5000	114.21	112.21	-38.7388	-43.7851	6.86	6.21	6.21
48.0000	113.45	111.45	-39.5074	-44.5538	6.29	6.21	6.21
48.5000	112.68	110.68	-40.2760	-45.3224	6.21	6.21	6.21
49.0000	111.91	109.91	-41.0447	-46.0910	6.21	6.21	6.21
49.5000	111.14	109.14	-41.8132	-46.8596	6.21	6.21	6.21
50.0000	110.37	108.37	-42.5818	-47.6281	6.21	6.21	6.21

Table 3-6. Tabular Data for MILSATCOM Airborne Transmitter
(ECAC Emission Envelope) vs. RML-4 Receiver
(140 dB/Decade Fall-Off)

TRANSMITTER: AB MILSATCOM (R)
RECEIVER: RML-4 (2)

DELTA F (MHZ)	TRANS LOSS (DB)	PROP LOSS (DB)	DFR (DB)	FDR (DB)	DISTANCE SEPARATION, MI		
					(5.000)	(10.000)	(50.000)
0.0000	152.13	150.13	0.0000	-5.8652	269.97	210.48	55.27
.5000	152.14	150.14	.0030	-5.8622	270.00	210.53	55.29
1.0000	152.15	150.15	.0120	-5.8533	270.08	210.59	55.35
1.5000	152.16	150.16	.0265	-5.8387	270.22	210.94	55.43
2.0000	152.18	150.18	.0465	-5.8188	270.39	211.30	55.55
2.5000	152.21	150.21	.0715	-5.7938	270.59	211.75	55.71
3.0000	152.24	150.24	.1013	-5.7639	270.81	212.30	55.89
3.5000	152.27	150.27	.1356	-5.7296	271.03	212.94	56.10
4.0000	152.31	150.31	.1742	-5.6911	271.25	213.65	56.33
4.5000	152.35	150.35	.2166	-5.6486	271.44	214.43	56.60
5.0000	152.40	150.40	.2625	-5.6027	271.61	215.25	56.88
5.5000	152.45	150.45	.3114	-5.5538	271.75	216.10	57.18
6.0000	152.50	150.50	.3626	-5.5027	271.84	216.93	57.50
6.5000	152.55	150.55	.4150	-5.4503	271.88	217.72	57.83
7.0000	152.60	150.60	.4669	-5.3983	271.88	218.42	58.16
7.5000	152.65	150.65	.5153	-5.3499	271.85	219.01	58.47
8.0000	152.69	150.69	.5562	-5.3090	271.80	219.49	58.73
8.5000	152.72	150.72	.5881	-5.2771	271.75	219.84	58.93
9.0000	152.75	150.75	.6108	-5.2544	271.70	220.09	59.08
9.5000	152.76	150.76	.6243	-5.2410	271.68	220.23	59.17
10.0000	152.76	150.76	.6284	-5.2358	271.67	220.27	59.19
10.5000	152.76	150.76	.6230	-5.2422	271.68	220.21	59.16
11.0000	152.74	150.74	.6078	-5.2575	271.71	220.05	59.06
11.5000	152.72	150.72	.5820	-5.2832	271.76	219.78	58.89
12.0000	152.68	150.68	.5447	-5.3205	271.82	219.35	58.66
12.5000	152.63	150.63	.4936	-5.3716	271.87	218.75	58.33
13.0000	152.56	150.56	.4263	-5.4389	271.89	217.88	57.90
13.5000	152.48	150.48	.3428	-5.5224	271.81	216.62	57.38
14.0000	152.38	150.38	.2434	-5.6218	271.55	214.91	56.76
14.5000	152.26	150.26	.1278	-5.7374	270.98	212.79	56.05
15.0000	152.13	150.13	-.0050	-5.8702	269.92	210.39	55.24
15.5000	151.98	149.98	-.1560	-6.0212	268.12	208.03	54.34
16.0000	151.81	149.81	-.3249	-6.1901	265.96	206.13	53.35
16.5000	151.62	149.62	-.5114	-6.3767	263.59	204.18	52.27
17.0000	151.42	149.42	-.7156	-6.5808	261.15	202.07	51.11
17.5000	151.20	149.20	-.9377	-6.8023	258.65	199.81	49.88
18.0000	150.96	148.96	-1.1785	-7.0438	255.99	197.38	48.58
18.5000	150.70	148.70	-1.4391	-7.3043	252.96	194.80	47.21
19.0000	150.41	148.41	-1.7249	-7.5861	245.03	192.04	45.77
19.5000	150.11	148.11	-2.0258	-7.8910	238.91	189.07	44.25
20.0000	149.78	147.78	-2.3565	-8.2218	236.02	185.83	42.67
20.5000	149.42	147.42	-2.7157	-8.5810	233.55	182.17	41.00
21.0000	149.03	147.03	-3.1048	-8.9700	229.92	177.67	39.26
21.5000	148.61	146.61	-3.5257	-9.3909	220.14	172.94	37.46
22.0000	148.15	146.15	-3.9821	-9.8473	215.33	168.91	35.61
22.5000	147.66	145.66	-4.4792	-10.3444	212.10	165.44	33.71
23.0000	147.11	145.11	-5.0211	-10.8863	207.97	161.67	31.72
23.5000	146.53	144.53	-5.6017	-11.4670	201.66	156.51	29.70
24.0000	145.92	143.92	-6.2165	-12.0819	194.95	148.64	27.73
24.5000	145.27	143.27	-6.8659	-12.7303	187.97	133.01	25.81
25.0000	144.59	142.59	-7.5490	-13.4142	181.05	123.23	23.90
25.5000	143.86	141.86	-8.2728	-14.1381	175.07	113.95	22.01
26.0000	143.09	141.09	-9.0438	-14.9090	165.76	105.08	20.18
26.5000	142.26	140.26	-9.8722	-15.7374	154.73	96.38	18.37

Table 3-6. Continued

27.0000	141.36	139.36	-11.7733	-16.6385	137.22	87.67	16.59
27.5000	140.36	138.36	-11.7701	-17.6354	123.16	78.90	14.81
28.0000	139.25	137.25	-12.9818	-18.7471	110.20	70.09	13.06
28.5000	138.06	136.06	-14.1797	-19.9449	97.45	61.59	11.39
29.0000	136.80	134.80	-15.3356	-21.2009	85.51	53.70	9.87
29.5000	135.50	133.50	-16.6318	-22.4971	74.53	46.59	8.51
30.0000	134.18	132.18	-17.9566	-23.8218	64.63	40.23	7.32
30.5000	132.83	130.83	-19.3018	-25.1671	55.87	34.66	6.27
31.0000	131.47	129.47	-20.6620	-26.5273	48.13	29.74	6.21
31.5000	130.10	128.10	-22.0333	-27.8985	41.38	25.54	6.21
32.0000	128.72	126.72	-23.4130	-29.2782	35.48	21.85	6.21
32.5000	127.34	125.34	-24.7993	-30.6645	30.39	18.68	6.21
33.0000	125.94	123.94	-26.1911	-32.0564	26.02	15.95	6.21
33.5000	124.55	122.55	-27.5880	-33.4533	22.21	13.61	6.21
34.0000	123.15	121.15	-29.9894	-34.8547	18.97	11.60	6.21
34.5000	121.74	119.74	-31.3953	-36.2605	16.17	9.88	6.21
35.0000	120.33	118.33	-32.8050	-37.6712	13.78	8.41	6.21
35.5000	118.91	116.91	-34.2224	-39.0876	11.73	7.15	6.21
36.0000	117.49	115.49	-35.6457	-40.5110	9.97	6.21	6.21
36.5000	116.06	114.06	-37.0731	-41.9433	8.47	6.21	6.21
37.0000	114.61	112.61	-38.5221	-43.3873	7.18	6.21	6.21
37.5000	113.15	111.15	-39.9815	-44.8468	6.21	6.21	6.21
38.0000	111.67	109.67	-41.4630	-46.3282	6.21	6.21	6.21
38.5000	110.15	108.15	-42.9790	-47.8442	6.21	6.21	6.21
39.0000	108.59	106.59	-44.5431	-49.4133	6.21	6.21	6.21
39.5000	106.94	104.94	-46.1872	-51.0624	6.21	6.21	6.21
40.0000	105.17	103.17	-47.9694	-52.8347	6.21	6.21	6.21
40.5000	103.19	101.19	-49.9405	-54.8057	6.21	6.21	6.21
41.0000	101.95	99.95	-51.1895	-57.0457	6.21	6.21	6.21

Let us now examine the information contained in the statistical F-D curves. First, notice that all curves are for an interference criterion $I/N = 0$ dB. (In most cases, this interference criterion would be a safe, perhaps even conservative assumption.) The criterion is specified by the model user when supplying the input data. Secondly, notice on these figures that curves are plotted for 5%, 10%, and 50% probabilities of interference. In the preceding example 10%, 50%, and 90% probabilities of interference were used. These values also are specified by the model user when supplying the input data.

Figure 3-3 shows curves for the AB MILSATCOM (7) vs. RML-4 (1) pair. In the figure, a maximum distance separation of ~ 249 mi (401 km) is required if the systems are tuned to the same frequency ($\Delta f=0$). This value is shown by the 5% curve which has the meaning that interference power will not exceed the interference criterion more than 5% of the time. The 5% curve also can be thought of as portraying at least 95% probability of interference-free operation. If the RML-4 receiver can tolerate 10% probability of interference, the required distance separation drops to ~ 193 mi (311 km) - a 22% reduction in required distance separation when the systems are tuned to the same frequency.

One would need to examine channel frequencies and bandwidths to determine frequency separations (between the

airborne transmitter and the microwave receiver) which could be used. But, assume that 25 MHz is a workable frequency separation. Then figure 3-3 shows that about 212 mi (341 km) separation is required for 5% probability of interference and about 166 mi (267 km) separation is required for 10% probability of interference. Compared to the distance separation requirements when $\Delta f=0$, the reductions in required distance separation when $\Delta f=25$ MHz are 14.9% and 14.0% respectively.

Now consider the effect of assuming sharper selectivity of 140 dB/decade roll-off rate outside the 3 dB bandwidth for the RML-4 receiver. The transmitter emission spectrum is still assumed to be 60 dB/decade roll-off rate. Figure 3-4 shows the statistical F-D curves for this transmitter-receiver pair, i.e. AB MILSATCOM (7) vs. RML-4 (2). At $\Delta f=0$, the required distance separation now is ~ 238 mi (383 km) for 5% probability of interference and ~ 188 mi (302 km) for 10% probability of interference. Allowing the probability of interference to increase from 5% to 10% now provides a 21% reduction in required distance separation at $\Delta f=0$. At $\Delta f=25$ MHz, the required distance separation is ~ 206 mi (332 km) for 5% probability of interference and ~ 160 mi (258 km) for 10% probability of interference. When 25 MHz of frequency separation are employed, the reductions in required distance separation are 13.3% for 5% probability of interference and 14.8% for 10% probability of interference.

Comparing required distance separations between figures 3-3 and 3-4, one observes that at $\Delta f=0$ the sharper receiver fall-off rate reduces the required separation by only 4.8% and at $\Delta f=25$ MHz the reduction is only about 2.4%.

Statistical frequency-distance curves portraying the influence of the theoretical emission spectrum envelope published in the ECAC (1975) report now will be examined. Figure 3-5 shows curves for the AB MILSATCOM (R) vs. RML-4 (1) combination. The distance separation at $\Delta f=0$ is shown to be ~ 271 mi (436 km) for 5% probability of interference and ~ 222 mi (357 km) for 10% probability of interference. These required separations are larger than the comparable values shown in figures 3-3 and 3-5. The reason is that the revised emission spectrum envelope has considerably reduced spectral power density at frequencies greater than ± 20 MHz away from the carrier frequency, yet the total output power has been assumed to be the same. Thus, the spectral power density at frequencies less than ± 20 MHz is greater for the revised spectral envelope than for the envelope with 60 dB/decade roll-off rate.

Returning to discussion of the information contained in figure 3-5, one observes that allowing 10% probability of interference reduces the required distance separation by 18.1% at $\Delta f=0$. As before, if frequency separation of 25 MHz is employed, the required distance separations are ~ 203 mi (327 km) for 5% and ~ 158 mi (254 km) for 10% probabilities

of interference. The respective reductions in required distance separation are 25.1% and 28.9%. The revised emission spectrum envelope and frequency separation combine to yield an important reduction in required distance separation.

Finally, consider figure 3-6 which is statistical F-D curves for the AB MILSATCOM (R) vs. RML-4 (2) transmitter-receiver combination. The required distance separations at $\Delta f=0$ are ~ 270 mi (435 km) for 5% and ~ 210 mi (338 km) for 10% probabilities of interference. Accepting 10% probability of interference, rather than 5% probability of interference would reduce the required distance separation by 22% when the more selective RML-4 receiver is used. However, comparing similar data at $\Delta f=0$ for 5% and 10% probabilities of interference shows that the respective required distance separations are reduced by only 0.4% and 5.2%. At frequency separation of 25 MHz, the required distance separations on figure 3-6 are ~ 181 mi (241 km) for 5% and ~ 123 mi (198 km) for 10% probabilities of interference. These separations compared to the required distance separations at $\Delta f=0$ represent reductions of 32.9% and 91.5% respectively.

The reader will notice in figures 3-5 and 3-6 that the curves show maximum required distance separations at about 10 MHz frequency separation. This phenomenon occurs because the receiver bandwidth is narrower than the emission

spectrum width. Under such conditions, the statistical F-D curves tend to follow the slope of the spectral power density envelope which is maximum at $\Delta f=15$ MHz.

In summary, the statistical frequency-distance curves in this example lead to and support the following conclusions:

1. Separation between the operating frequencies of two systems can be very effective in reducing the required distance separation between the systems.
2. The shape of the emission spectrum is a dominant influence upon required distance separation when the 3 dB bandwidth of the victim receiver is narrower than the 3 dB emission spectrum width. The shape of the receiver selectivity curve is a relatively insignificant influence.
3. When the interfering transmitter and victim receiver are tuned to the same frequency ($\Delta f=0$), the dominant factors which influence required distance separation are (1) the relationship between emission spectrum width and receiver bandwidth (2) the receiver noise power, (3) the interference criterion, and (4) the total output power of the interfering transmitter.
4. Probability of interference has a significant influence upon required distance separation when a given frequency separation applies.

4. CONCLUSIONS AND RECOMMENDATIONS

Conclusions

1. A method of calculating trade-offs in frequency and distance separations between interference sources and potential victim receivers has been developed which considers the probabilistic nature of contributing technical factors.
2. This technique provides trade-offs of direct interest to frequency managers and incorporates a more realistic description of key technical factors affecting interference than has been generally available in the past.
3. The technique is user-oriented and allows various options for the description of input characteristics.
4. The technique is based on a general structure capable of expansion to consider additional statistical data as they become available.
5. The technique allows consideration of a wide range of interference situations including ground-to-ground and ground-to-air combinations.
6. The use of this technique is limited primarily by the availability of valid statistical descriptions of input factors. This initial model uses statistical descriptions of propagation loss and antenna power gain. As recommended,

additional work is needed to adapt and develop statistical descriptions of other technical and system performance factors for incorporation into the model.

Recommendations

To improve the validity and general utility of the Statistical Frequency-Distance Curves Model, it is recommended that:

- 1) A capability to incorporate statistical emission spectra and receiver response curves be added.
- 2) The validity of available antenna models be verified with empirical data.
- 3) Statistical data be acquired for emission spectra and antenna gain patterns using the Radio Spectrum Measurement System, bench measurements, and other sources as available.
- 4) A data base and data analysis procedure be established for the storage and use of statistical characteristics.
- 5) The techniques be expanded to allow consideration of probabilistic performance factors (S/I, D/U) such as those that are contained in the FMC Degradation Handbook (Kravitz, 1973).
- 6) The techniques be expanded to allow consideration

of temporal and spatial characteristics of telecommunications systems as determined by their operational use.

- 7) Additional options for synthesis of equipment characteristics be incorporated.
- 8) Freespace propagation loss calculations be available as a selectable option for the loss model.

5. REFERENCES

- Abramowitz, M. and I. A. Stegun (1964), Handbook of Mathematical Functions With Formulas, Graphs, and Mathematical Tables, (U.S. Government Printing Office, Washington, DC 20402), 297.
- C.C.I.R. (1970), Propagation in non-ionized media, XIIth Plenary Assembly, II, Pt. 1, New Delhi.
- ECAC (1975), Analysis of SHF AIRSATCOM earth station compatibility with unique SHF communications systems, Final Report No. ECAC-PR-75-013, under contract F-19628-75C-0002 for the Department of Defense.
- Fleck, R. (1967), Procedures for computing separation criteria and off-frequency rejection in electromagnetic compatibility problems, DoD Report No. ESD-TR-67-5, under ECAC No. AF19(628)-5049.
- Geisinger, K. (1965), Removing receiver characteristics effects from measured power spectra, ECAC Technical Note No. ECAC-TN-003-199.
- Gierhart, G.D., and M. E. Johnson (1973), Computer programs for air/ground propagation and interference analysis, 0.1 to 20 GHz, DoT Report No. FAA-RD-73-103.
- Jasik, H. (1961), Antenna Engineering Handbook (McGrawHill Book Company, Inc., New York, New York).
- Kravitz, F. (1973), Communications/electronics receiver performance degradation handbook, DoD Report No. ESD-TR-73-014.
- Longley, A.G., and P. L. Rice (1968), Prediction of tropospheric radio transmission loss over irregular terrain, a computer method - 1968, ESSA Tech. Report ERL 79-ITS 67.
- Lustgarten, M. N. (1970), COSAM (Co-site analysis model), Symposium Record, IEEE International Symposium on Electromagnetic Compatibility, Anaheim, California, July 14-16, 1970.

- Lustgarten, M. N. (1966), Application of frequency/distance characteristics to VHF FM mobile communications problems, ECAC-TN-002-3.
- Lustgarten, M. N. and R. Mayher (1968), Application of degradation considerations to a UHF AM communications systems problem, ECAC-TN-002-20.
- Rice, P. L., A. G. Longley, K. A. Norton, and A. P. Barsis (1967), Transmission loss predictions for tropospheric communication circuits (revised), NBS Tech. Note 101.
- Rome Air Development Center (1966), Interference Notebook, Report No. RADC-TR-66-1, I and II.
- Sachs/Freeman Associates, Inc. (1971), Identification of information and associated analytical techniques for the solution of frequency management problems, III, Contract OEP-SE-70-101.
- U. S. Army Electronic Proving Ground (1968), Statistical antenna and propagation model for the EMETF interference prediction model, Publication No. USAEPG-DR-416.
- U. S. Army Electronic Proving Ground (1968), Interference prediction model theory, III, Bell Report No. A70009-408.
- Weinberg, L. (1962), Network Analysis and Synthesis, (McGraw-Hill Book Company, Inc.), Chapter 11.

APPENDIX A. USER'S GUIDE
FREQUENCY-DISTANCE CURVES MODEL

A.1 Functional Nature of the Model

The general characteristics of any interference condition are dependent upon knowledge (real or assumed) about the emission spectrum of the transmitter, the power gains of the transmitting and receiving antennas, the attenuation of the propagation medium, and the selectivity and sensitivity of the receiver.

Emission spectra and receiver response characteristics are primarily frequency dependent phenomena. Transmitter frequencies may be adjusted and radiated and/or received signals may be filtered to reduce interference. Propagation loss is both frequency and distance dependent, but the distance dependency is the primary consideration in analyzing an interference problem.

The procedure for developing a curve that relates frequency separation and distance separation (F-D curve) requires one to determine the isolation that is required between two systems for a given frequency separation and performance condition. In this model the interference criterion is interference power-to-receiver noise power ratio. Knowing the isolation that is required between systems, the propagation loss expression is solved

implicitly to obtain distance (rather than knowing the distance and solving explicitly for propagation loss).

The detailed and lengthy computations which are required to produce frequency-distance curves are ideally suited to programming for computer solution. This model is a computer-based model that calculates these frequency separation-distance separation relationships. Further, the model is enhanced by its statistical characterization of propagation loss and antenna gains.

The functional organization and operation of the model are depicted by figure A-1. Three principal sub-sections of the model are indicated by lightly dashed lines.

The upper left portion of the figure depicts the specification of emission and receiver characteristics, the process of combining the emission spectrum and receiver selectivity to obtain the amount of interference power that is at the output of the receiver filtering, and the utilization of the information to provide frequency-dependent rejection (FDR) data and/or the interference protection (IP) as a function of frequency. These operations are performed by the models INSPECT or NEWSPEC, depending upon the selection of the user. The detailed mathematics of these models is contained in Appendix C. INSPECT provides a general capability for specifying bounds (in straight-line segments on semi-logarithmic paper) for

Statistical Frequency-Distance Curves Model Functional Block Diagram

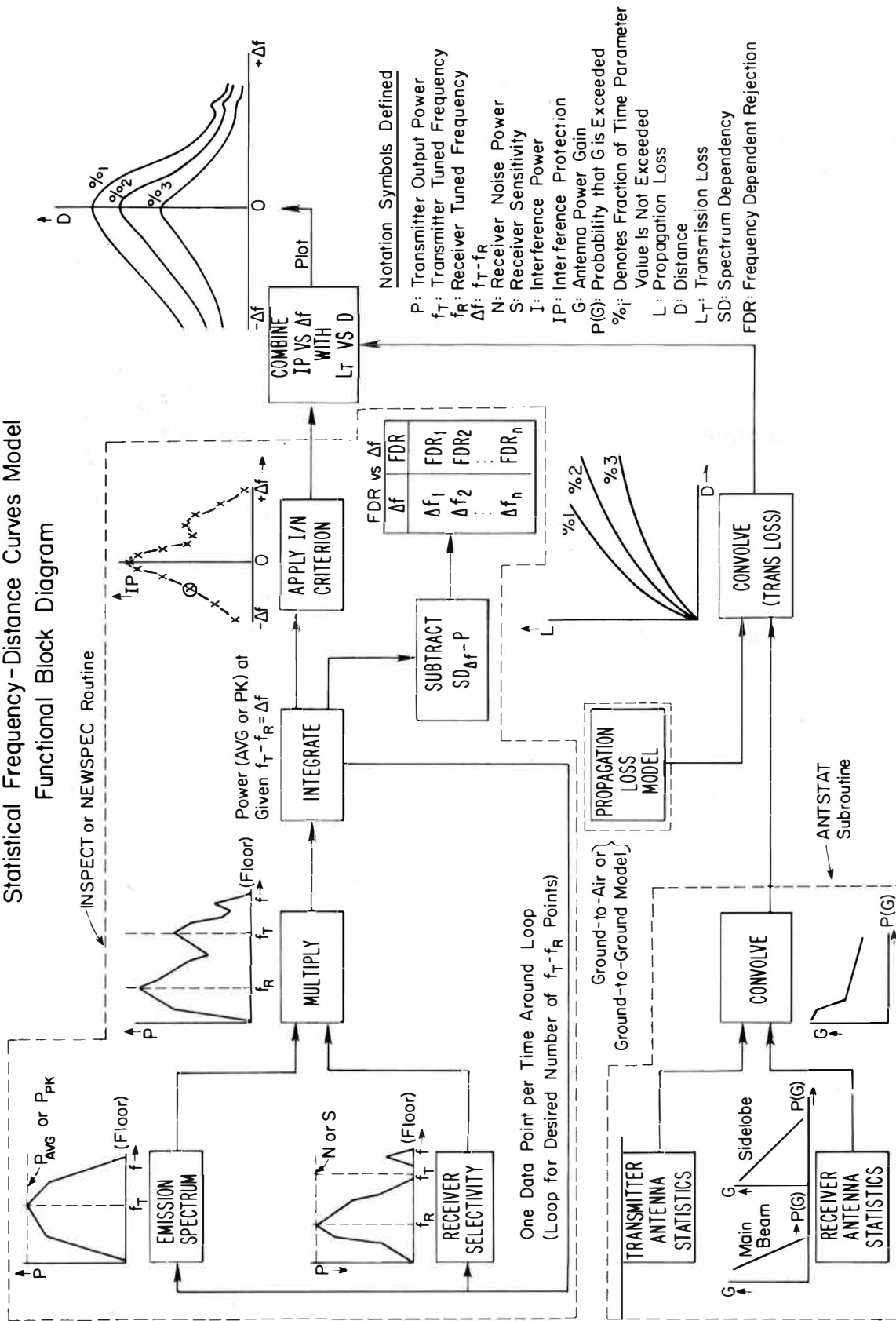


Figure A-1. Functional block diagram of the statistical frequency-distance curves model.

the emission spectrum and receiver selectivity curve, whereas NEWSPEC provides a capability for theoretically modeling the emission spectrum for a pulsed emitter and the power admitted by a filter which may be specified as Butterworth, Chebyshev or elliptic.

The lower left portion of figure A-1 illustrates the capability for specifying antenna power gains in statistical terms. The antenna power gain model characterizes the mainbeam power gain by a cumulative distribution with mean value, G_M , and standard deviation, σ_M . The side- and back-lobe regions are characterized by another cumulative distribution with mean value, G , and standard deviation, σ_B . These distributions are convolved to obtain a mutual gain distribution with mean value and standard deviation. Details of the statistical characterization of antenna power gain are contained in Appendix D, and the convolution routine mathematics is shown in Appendix G.

A single box in the lower, central portion of figure A-1 portrays utilization of a propagation loss model. The models currently available are: (1) a ground-to-air propagation loss model known as POWAV and (2) a ground-to-ground propagation loss model known as Q-AREA. The user selects the propagation loss model to be used.

Remaining functions of the statistical frequency-distance curves model involve the convolution of the

selected propagation model with the mutual antenna power gain expression to obtain the probabilistic transmission loss vs. distance data. These data are then combined with the interference protection vs. frequency separation data to provide plots, with statistical character, of required distance separation as a function of frequency separation--the statistical frequency-distance curves.

A.2 Input Data for the Model

Input data must correspond to the requirements of the particular subroutines selected. For example, the input data for INSPECT are different from those required by NEWSPEC. Certain basic data, of course, are common to more than one subroutine.

The five pages of table A-1 are the data forms which are used to provide input data for the model. If the point-amplitude or point-slope method of specifying the emission spectrum and receiver selectivity (INSPECT subroutine) is selected, page 3 of the data form is not required. When the NEWSPEC subroutine (which produces synthesized emission spectra from time domain data describing pulsed systems) is used, page 2 is not required. The required user-input data are denoted by asterisks. All other variables have default values which are automatically used if those data are not input.

Table A-1. Sample Forms to Provide Input Data for the Statistical Frequency-Distance Curves Model

DATA FORM
STATISTICAL FREQUENCY-DISTANCE CURVES MODEL

General Data

- _____ Transmitter identification (16 characters maximum)
- _____ Receiver identification (16 characters maximum)
1. _____ *Carrier frequency, f_T , MHz
 2. _____ *Output power, dBm
 3. _____ Type of output power (0.)
=0. if output power is average power, I_{AVG}
=1. if output power is peak power, I_{PK}
 4. _____ *Receiver noise, N, dBm
 5. _____ Interference-to-noise criterion, I/N, dB (0.)
 6. _____ Transmitter polarization (1.)
=1. for horizontal
=2. for vertical
 11. _____ Number of frequency separations (101.)
 12. _____ Lowest frequency separation, MHz (0.)
 13. _____ Highest frequency separation, MHz (100.)
 14. _____ Maximum distance separation to be plotted, n mi (0.)
=0. for model to calculate maximum
 15. _____ (10.)
 16. _____ (50.)
 17. _____ (90.)
- } Probability of interference, percent
18. _____ Units for the distance (1.)
=1. for nautical miles (n mi)
=2. for statute miles (mi)
=3. for kilometers (km)
 19. _____ Type of output (1.)
=1. for statistical F-D and FDR curves
=2. for FDR curves only
 21. _____ Emission spectrum/receiver selectivity model (1.)
=1. for INSPECT, input 22
=2. for NEWSPEC, input 23 through 27

* Denotes required input data on each data sheet.

() Denotes values used if user does not specify.

Table A-1. Continued

Subroutine INSPECT

22. ----- *Emission spectrum and receiver selectivity envelopes
 =1. to input Δf and amplitude (point-amplitude)
 =2. to input Δf and "slope" in dB/decade (point-slope)
 =3. to input Δf and "slope" in dB/octave (point-slope)

Spectrum Envelope

Normalized Receiver Response

(Point - Amplitude)

<u>Δf, MHz</u>	<u>Amplitude, dBm/Hz</u>	<u>Δf, MHz</u>	<u>Amplitude, dB</u>
-----	-----	-----	-----
-----	-----	-----	-----
-----	-----	-----	-----
-----	-----	-----	-----
-----	-----	-----	-----
-----	-----	-----	-----
-----	-----	-----	-----
-----	-----	-----	-----
-----	-----	-----	-----
-----	-----	-----	-----

(Point - Slope)

<u>Δf, MHz</u>	<u>Slope, dB/decade or dB/octave</u>	<u>Δf, MHz</u>	<u>Slope, dB/decade or dB/octave</u>
-----	-----	-----	-----
-----	-----	-----	-----
-----	-----	-----	-----
-----	-----	-----	-----
-----	-----	-----	-----
-----	-----	-----	-----
-----	-----	-----	-----
-----	-----	-----	-----
-----	-----	-----	-----
-----	-----	-----	-----

Table A-1. Continued

Subroutine NEWSPEC

- 23. _____ *Receiver (filter) bandwidth, MHz
- 24. _____ *Half amplitude pulse width, microseconds
- 25. _____ *10% - 90% rise time, microseconds
- 26. _____ *90% - 10% fall time, microseconds
- 27. _____ *Pulse repetition rate, pulses/second
- 28. _____ Type of filter (2.)
=1. for Chebyshev, input 27., 28., and 29.
=2. for Butterworth, input 27.
=3. for Elliptic, input 28., 29., 30., and 31.
- 29. _____ Number of poles or ripples (5.)
- 30. _____ Maximum Z-squared in pass band
- 31. _____ Minimum (allowable) Z-squared in pass band
- 32. _____ Maximum (allowable) Z-squared in stop band
- 33. _____ Beginning frequency of the stop band

Table A-1. Continued

Subroutine ANTSTAT (Antenna Statistics)

Transmitter

41. _____ Coupling (1.)
 (Interference Notebook Tables)
 =1. for main beam only, input 42.
 =2. for side- and back-lobe only, input 42. and 44.
 =3. for full pattern, input 42., 44., and 45.
 (User-provided statistics)
 =4. for main beam only, input 42. and 46.
 =5. for side- and back-lobe only, input 47. and 48.
 =6. for full pattern, input 42. and 45. through 48.
42. _____ *Median main-beam gain, G_{TM} , dBi
44. _____ Site condition (2.)
 =1. for open
 =2. for average
 =3. for crowded
45. _____ 10 dB main-beam width, α_T , degrees
46. _____ Standard deviation, main-beam gain, σ_{TM} , dB
47. _____ Median side- and back-lobe gain, G_{TB} , dBi
48. _____ Standard deviation, side- and back-lobe gain, σ_{TB} , dB

Receiver

51. _____ Coupling (1.)
 (Interference Notebook Tables)
 =1. for main beam only, input 52. and 53.
 =2. for side- and back-lobe only, input 52. and 54.
 =3. for full pattern, input 52. through 55.
 (User-provided statistics)
 =4. for main beam only, input 52. and 56.
 =5. for side- and back-lobe only, input 57. and 58.
 =6. for full pattern, input 52. and 55. through 58.
52. _____ *Median main-beam gain, G_{RM} , dBi
53. _____ Polarization (1.)
 =1. for horizontal
 =2. for vertical
54. _____ Site condition (2.)
 =1. for open
 =2. for average
 =3. for crowded
55. _____ 10 dB main-beam width, α_R , degrees
56. _____ Standard deviation, main-beam gain, σ_{RM} , dB
57. _____ Median side- and back-lobe gain, G_{RB} , dBi
58. _____ Standard deviation, side- and back-lobe gain, σ_{RB} , dB

Table A-1. Continued

Loss Data

61. _____ Loss model (1.)
=1. for ground-to-air, input 62. through 66.
=2. for ground-to-ground, input 62. through 66.
and 91. through 95.
62. _____ Transmitter antenna height above terrain, H_T , feet (50.)
63. _____ Receiver antenna height above terrain, H_R , feet (1000.)
64. _____ Surface refractivity, N-units (301.)
65. _____ Terrain roughness, ΔH , feet (0.)
66. _____ Transmitter site elevation above MSL, feet (0.)
67. _____ Surface types and constants (3.)
=1. sea water
=2. good ground
=3. average ground
=4. poor ground
=5. fresh water
=6. concrete
=7. metal

Ground-to-ground only

91. _____ Transmitter antenna siting (1.)
=1. for random siting
=2. for some selection in siting
=3. for good selection in siting
92. _____ Receiver antenna siting (1.)
=1. for random siting
=2. for some selection in siting
=3. for good selection in siting
93. _____ Climate (5.)
=1. for equatorial
=2. for continental subtropical
=3. for maritime subtropical
=4. for desert
=5. for continental temperate
=6. for maritime temperate overland
=7. for maritime temperate oversea

The first page of the data form contains all variables to be general inputs that are used by two or more subroutines. The second page of the data form contains variables used only by subroutine INSPECT. Note that two options are available. These are discussed later in this section. A detailed description of INSPECT is contained in Appendix C, part 1. Page 3 of the data form lists the variables for using subroutine NEWSPEC. A detailed description of NEWSPEC is provided in Appendix C, part 2. The variables for antenna statistics are on page 4 of the data form. Appendix D discusses the statistical antenna power gain model. Finally, page 5 lists the variables required for propagation loss computations. Appendix F presents summary discussions of each propagation loss model. An item-by-item discussion of each variable is provided in the following sections.

A.2.1 General Data

On the general data sheet (page 1 of the data form), the first two blocks are for identifying the interfering transmitter and the victim receiver. A maximum of 16 characters are provided for each.

Numbers preceding the subsequent variable entries are for convenience in discussing the entry and compiling the input data cards. The value in parentheses following the item description is the default value for that item.

Item 1 is the carrier frequency of the interfering transmitter, specified in MHz. This is the reference frequency in computing frequency difference, Δf . Carrier frequency is a required input.

Item 2 is the total output power of the transmitter, specified in decibels referenced to 1 milliwatt (dBm). This value is treated as average power or peak power according to the specification of item 3. The output power is a required input.

Item 3 provides definition of the type of output power (average or peak) being considered. This is not a required input. The default specification is that average power is being used.

Item 4 is the noise power of the victim receiver, specified in dBm. The criterion for interference is interference-to-noise ratio, I/N , which is discussed as item 5. The receiver noise power is a required input.

Item 5, as mentioned, is the interference-to-noise ratio, specified in decibels (dB). This ratio is used as the criterion for interference. That is, if one wishes to portray the frequency separation-distance separation

relationship for interference power 5 dB less than the victim receiver's noise power, he specifies I/N to be -5 dB. If desired, one can consider item 5 as actually a specification of tolerable interference relative to some operating threshold of the receiver; then, item 4 specification must be understood as the receiver's operating threshold. When item 5 is not specified, the default value is $I/N = 0$ dB.

Item 6 is specification of polarization for the transmitting antenna. The choices for polarization are horizontal, specified by inserting a 1, and vertical, specified by inserting a 2. When specification is not provided, the model assumes horizontal polarization.

Item 11 is a specification of the number of frequency separations to be used in computing the frequency separation-distance separation data. The default value of 101 is appropriate when using the INSPECT routine. If the NEWSPEC routine is selected to synthesize the emission spectrum and receiver response, considerably fewer than 101 frequency separations should be used in order that computer running time not exceed a practical limit. One will note in Appendix B that 21 frequency separations were used for sample 3. Of course, fewer frequency separations provide more coarse data for plotting the final curves.

Items 12 and 13 define the frequency separation span, specified in MHz. Item 12, the lowest frequency separation, has a default value of 0 MHz which is appropriate whenever the emission spectrum and receiver selectivity are symmetrical. When symmetry does not exist, item 12 must be specified with a negative value. Item 13, the highest frequency separation, has a default value of 100 MHz. In specifying items 12 and 13, the frequency separation span must include $\Delta f = 0$. This requirement arises from the definition of off-frequency rejection in Appendix E. A practical constraint in specifying these limits results from the output plotting of the statistical frequency-distance curves. If frequency separations greater than ± 300 MHz or 0 to 600 MHz are used, the abscissa scale (frequency separation axis) is very difficult to read.

Item 14 allows specification, in nautical miles (n mi), of the maximum distance separation to be shown by the ordinate of the statistical frequency-distance curves plot. This feature is useful when two or more plots are generated which one desires to compare directly (by overlay or other similar technique). The default option, denoted by zero, calculates the maximum distance separation required and automatically scales the ordinate of the plot to correspond with that calculated value.

Items 15, 16 and 17 allow specification of three values, in percent, for probability of not exceeding the specified I/N criterion. The three plotted statistical frequency-distance curves will be for these specified probabilities. Default values are 10% for item 15, 50% for item 16, and 90% for item 17.

Item 18 provides opportunity for the model user to specify the units for distance to be used in plotting the statistical frequency-distance curve. Option 1 provides distance scaled in nautical miles; option 2 provides distance scaled in statute miles. The default option provides distance scaled in nautical miles, option 1.

Item 19 defines the type of output data desired by the model user. Statistical frequency distance curves and frequency-dependent rejection (FDR) curves are provided through option 1, which is the default option. Specification of option 2 directs the model to produce only FDR plots.

Item 21 is specification of the method to be used in specifying the emission spectrum and receiver selectivity curve. The subroutines INSPECT (discussed in section A.2.2) or NEWSPEC (discussed in section A.2.3), are the options. The INSPECT subroutine is utilized through option 1 which requires that item 22 be specified. The NEWSPEC subroutine is utilized through option 2. This option uses the data

which are provided as items 23 through 33. The INSPECT subroutine, option 1, is the default condition for item 21.

A.2.2 Data for INSPECT

Page 2 of the data form itemizes data for subroutine INSPECT. INSPECT utilizes straight-line segments (when plotted on semi-logarithmic graph paper) which bound the emission spectrum and receiver selectivity curve. Use of this subroutine requires the data to be specified in either point-amplitude or point-slope form.

The point-amplitude specification is used when each straight-line segment is defined as the amplitude and frequency difference of each end point. Amplitude data for an emission spectrum may be either normalized or absolute from the power spectral density curve. Amplitude data for a receiver selectivity curve must be normalized (0 dB for maximum sensitivity and negative values for other points of the curve). The frequency difference (Δf) values that are required for the input data are the frequencies of the data points relative to the carrier frequency of the transmitter or relative to the tuned frequency of the receiver as appropriate.

The point-slope specification is used when the straight-line segment is defined in terms of its slope and

the frequency difference at one end of the line segment. The model is programmed to accept input data which specify the difference frequency for the line segment end with smaller absolute value difference frequency. Slope must be defined in terms of change in amplitude per frequency interval. Definitions in terms of dB/decade or dB/octave are programmed into the model. Again, difference frequency associated with the slope is the frequency of the right end of the line segment for negative difference frequency and the left end of the line segment for positive difference frequency referenced to the carrier frequency of the interfering transmitter or tuned frequency of the receiver. Input data for INSPECT must correspond to the selection for item 22. A numeral 1 shown in item 22 selects the point-amplitude method; a numeral 2 shown in item 22 selects the point-slope method.

Point-amplitude data must be input in ascending order of Δf values beginning with the largest negative Δf value for non-symmetrical curves or with $\Delta f = 0$ for symmetrical curves. Amplitudes from a spectral power density plot and amplitudes from a normalized emission spectrum must not be mixed.

In summary, the Δf for spectrum data is the difference between the frequency for the data point and the carrier frequency of the transmitter. Spectrum envelope amplitude

data are the numerical values for amplitude on either a spectral power density curve (units of dBm/Hz) or a normalized emission spectrum (negative numbers expressed in dB). The spectrum envelope is integrated to obtain power. The particular integral then is compared with the power (specified by items 2 and 3 on the general data page). When these values are different, as will be the case if the input data are normalized amplitudes, the "total" power from the integration is adjusted to agree with the input power data.

The Δf for receiver selectivity data is the difference between the frequency of the data point and the tuned frequency of the receiver. Receiver selectivity amplitude data are negative numerical values (in dB) for amplitude on a normalized receiver selectivity curve.

Point-slope data must be properly ordered for input. The required order is that data be organized to provide point-slope pairs starting with $\Delta f = 0$ and list data pairs in increasing absolute value of negative difference frequency (when appropriate), then start with $\Delta f = 0$ and list data pairs in increasing value of positive difference frequency. Symmetry is assumed when data pairs for positive difference frequency only are provided.

When using the INSPECT subroutine, in either point-amplitude or point-slope form, the emission spectrum envelopes and receiver selectivity curves should be

specified at least 80 dB below the maximum amplitude. If available data do not provide specification to -80 dB normalized amplitude, the following recommendations should be employed. For emission spectrum envelopes, continue the defined envelope slope to -80 dB normalized amplitude. For receiver selectivity curves, assume a fall-off rate of 20 dB/decade continuing from the last defined datum until -80 dB normalized amplitude is reached.

A.2.3 Data for NEWSPEC

The NEWSPEC subroutine is useful when the interferer is a pulsed emitter and the emission spectrum is not known, but the pulse shape is known. For these conditions, this subroutine will model the pulse, the emission spectrum, and filtering of the energy which may be characteristic (in concept) of filtering at either the emitter output or the receiver input.

Item 23 on the NEWSPEC data sheet (page 3 of the data form) defines the filter bandwidth in MHz. This is the bandwidth of the filter at which power response is decreased by 3 dB. This filter may be a final filter on the transmitter, but more likely, it will be the filtering of the victim receiver. Bandwidth specification is required to use this subroutine.

Item 24 is a specification of the half amplitude pulse width of the transmitter expressed in microseconds. The pulse width is a required input.

Item 25 specifies the pulse rise time expressed in microseconds. This is the time between 10% amplitude and 90% amplitude for the leading edge of the pulse. Pulse rise time is a required input.

Item 26 specifies the pulse fall time expressed in microseconds. This is the time between 90% amplitude and 10% amplitude for the trailing edge of the pulse. Pulse fall time is a required input.

Item 27 specifies the frequency at which pulses occur, expressed in pulses per second. The pulse repetition rate is a required datum.

Item 28 provides for selection of the type of filter to be considered. Three options are available. These are (1) Chebyshev, (2) Butterworth, and (3) elliptic. When specification of filter type is not provided, the subroutine automatically uses a Butterworth filter.

Item 29 defines the number of poles for the Butterworth filter or the number of ripples for the Chebyshev filter depending upon the selection made for item 28. When no selection is made for items 28 and 29, the subroutine automatically uses the Butterworth filter with 5 poles.

Items 30 and 31 pertain only to a Chebyshev or elliptic filter selection. The transfer impedance of the filter is denoted by Z . Passband ripple is defined by the values used for items 30 and 31 where

$$\text{ripple (dB)} = 10 \log \frac{Z^2_{\text{max}} (\text{item 30})}{Z^2_{\text{min}} (\text{item 31})}$$

Items 32 and 33 pertain only to an elliptic filter specification. Item 32 is the maximum squared value to be considered for the transfer impedance, Z , of the filter at frequencies outside the passband, i.e., in the stop band. As an example, if one wants the stop band characteristics to provide at least 70 dB of attenuation (relative to signals within the passband) the normalized Z value used in item 32 would be $Z^2 = 1 \times 10^{-7}$ or $Z \approx 3.16228 \times 10^{-4}$. Item 33 is the frequency in MHz at which the stop band attenuation characteristic is to begin. Note that the ratio of the frequency at which the filter bandwidth is achieved to the frequency at which the stop band characteristic begins is a measure of the steepness of the filter's rejection characteristic.

Users not familiar with Chebyshev and elliptic filter specification should consult some good reference (i.e., Weinberg, 1962) before attempting to use this subroutine.

A.2.4 Antenna Data

The subroutine which computes the mutual antenna power gain statistical distribution is named ANTSTAT. Data for this subroutine are provided by page 4 of the data form. Two basic options are contained in the subroutine for specifying antenna characteristics. These can either (1) utilize antenna power gain statistics from the RADC Interference Notebook (1966) which have been incorporated into the subroutine, (Appendix D provides a summary of the RADC statistical characterizations of antenna power gain.), or (2) require as user-provided input data the statistical characterizations of antenna power gains. These desired antenna coupling options are selected by the data input in items 41 and 51.

Item 41 defines the transmitting antenna coupling to be used by specifying one of 6 options.

Option 1 (the default value for item 41) selects main-beam coupling only, and requires the user to specify median main-beam gain in item 42. The subroutine then utilizes the RADC data for standard deviation of the main-beam gain.

Option 2 selects side- and back-lobe coupling only. The user must specify median main-beam gain in item 42. Under this option the subroutine utilizes the RADC data to select appropriate

values that are dependent on the main-beam gain for a median side- and back-lobe gain and a standard deviation of the side- and back-lobe gain. If option 2 is selected for Item 41, then the site condition, item 44, needs to be supplied. Option 3 selects full pattern coupling. This selection requires the main-beam width, item 45, to be specified in addition to items 42 and 44 (the median main beam gain and the site condition respectively). The full pattern selection is appropriate for rotating and randomly oriented antennas. "Full pattern" weights the median gains for main beam and side- and back-lobe according to the ratio of main-beam width to 360° . The statistical antenna power gain characterizations discussed in Appendix D consider the main-beam region gain to be normally distributed. The gain in the side- and back-lobe region also is assumed to be normally distributed (a different distribution from that for the mainbeam region, of course). Recall that for a normal distribution the mean and median are equal and that the distribution is characterized completely by specification of the mean (or median) and standard deviation for the

distribution. The same tabular data from Appendix D as are built into the statistical F-D curves model also are shown in Tables A-2, A-3, and A-4 as a convenience to the model user. He is not required to provide any data from these tables as part of his input data, but he may desire to know what values are used by the model for a particular logic of antenna coupling defined by him in specifying items 41 and 51.

For example, suppose his problem involved coupling between a transmitting antenna with median main-beam region gain of 0 dBi and a well-engineered (open site) receiving antenna with median main-beam region gain of 20 dBi. Further, suppose items 41 and 51 defined the coupling to occur from the mainbeam region of the transmitting antenna to the side- and back-lobe region of the receiving antenna. From table A-4, one can see, then, that the model will use 0 dBi as the median gain with associated standard deviation of 1 dB for the transmitting antenna. From table A-3, one can see that the model will use -15 dBi as the median gain with associated standard deviation of 8 dB for the side- and back-lobe region of the receiving antenna.

Table A-2. Statistics for Typical High-Gain Antennas ($G > 25\text{dBi}$)

Operational Conditions		Side and Back Lobe Region		Main Beam Region		
Polarization	Site	G_B	σ_B	α_M	G_M	σ_M
		dB/Iso	dB	deg	dB/Iso	dB
Design	Open	-15	8			
	Average	-10	6	α_o	G_o	2
	Crowded	- 5	4			
Orthogonal to Design	Open	-15	8			
	Average	-10	6	$7\alpha_o$	$G_o - 15$	3
	Crowded	- 5	4			

Table A-3. Statistics for Typical Medium-Gain Antennas (10 dBi \leq G \leq 25 dBi)

Operational Conditions		Side and Back Lobe Region		Main Beam Region		
		G_B	σ_B	α_M	G_M	σ_M
Polarization	Site	dB/Iso	dB	deg	dB/Iso	dB
Design	Open	-10	6			2
	Average	- 8	5	α_O	G_O	
	Crowded	- 5	4			
Orthogonal to Design	Open	-10	6			
	Average	- 8	5	$3\alpha_O$	$G_O - 10$	3
	Crowded	- 5	4			

Table A-4. Statistics for Typical Low-Gain Antennas ($G < 10\text{dBi}$)

Operational Conditions		Extraneous Lobe Region		Major Lobe Region		
		G_B	σ_B	α_M	G_M	σ_M
Polarization	site	dB/Iso	dB	deg	dB/Iso	dB
Design	Open	-7	4		G_O	1
	Average	-5	3	α_O		
	Crowded	-3	2			
Orthogonal to Design	Open	-7	4			
	Average	-5	3	$1.4\alpha_O$	$(G_O - 3)$	2
	Crowded	-3	2			

Option 4 selects main-beam coupling only, but with this selection, the main-beam median gain, item 42 and standard deviation, item 46, must be input.

Option 5 selects side- and back-lobe coupling only.

With this selection the side- and back-lobe median gain, item 47, and standard deviation, item 48, must be input.

Option 6 selects full pattern coupling utilizing users' input data, which requires specification of items 42 and 45 through 48.

Item 42 is the median main-beam gain expressed in dB relative to the gain of an isotropic (dBi) antenna. This is a required item of input data. However, when median main-beam gain is the only item of input data for the transmitting antenna, the only coupling selection that can be made for item 41 is option 1 which uses the RADC data for standard deviation of the main-beam gain.

Item 44 defines the site conditions for the transmitting antenna. This is an important consideration whenever the coupling selection (in item 41) involves any consideration of side- and back-lobes (options 2 or 3).

Site condition 1 defines an antenna location virtually free of objects which will scatter and/or reflect the antenna radiation.

Site condition 2 defines an antenna site for which there is an "average" number of objects within the vicinity which will scatter and/or reflect the radiation.

Site condition 3 defines a very crowded site with many objects to scatter and reflect the antenna radiation.

When no site condition is specified, an average condition is assumed.

Item 45 is the 10 dB main-beam width of the azimuthal antenna power gain pattern. That is, this beam width is the width in degrees of the power gain pattern at the points where gain is 10 dB less than the maximum gain. This is a required datum only if coupling option 3 or 6 is selected in item 41.

Item 46 is the standard deviation, expressed in dB, of the main-beam gain. This is a required datum only if coupling option 4 or 6 is selected in item 41.

Item 47 is the median side- and back-lobe gain expressed in dBi. This is a required datum only if coupling option 5 or 6 is selected for item 41.

Item 48 is the standard deviation, expressed in dB, of the side-and back-lobe gain. This is a required datum only if coupling option 5 or 6 is selected for item 41.

Items 51-58 provide characterization of the receiving antenna exactly analogous to the characterization of the transmitting antenna provided by items 41-48, with one exception. Polarization of the transmitting antenna is defined by item 6 of the general data sheet (page 1 of the data form). Polarization of the receiving antenna is defined by item 53 of the ANTSTAT data sheet (page 4 of the data form). The choices for polarization are horizontal, specified by a numeral 1, and vertical, specified by a numeral 2. When polarization is not specified, the model assumes horizontal polarization.

A.2.5 Propagation Data

It has been stated in section A.1 that the statistical frequency-distance curves model incorporates two propagation loss models. These are (1) a ground-to-air loss model and (2) a ground-to-ground loss model. Page 5 of the input data form, the propagation data sheet, contains the data requirements for both propagation models. Some required data inputs for computing propagation loss are common to other subroutines of the statistical frequency-distance curves model and these inputs are listed on the general data sheet (page 1 of the data form). Examples are frequency

(item 2) and transmitter polarization (item 6). Most other input data are used by both propagation loss routines in the statistical frequency-distance curves model.

On the propagation data sheet, item 61 provides selection of the desired propagation loss model. Option 1 selects the ground-to-air model; option 2 selects the ground-to-ground model. If a selection is not indicated the ground-to-air model is used.

Item 62 defines the transmitting antenna height, in feet, above the surrounding terrain. This value must be greater than 1.6 ft (0.5 m) but less than 9,840 ft (3,000 m), If transmitting antenna height is not specified, a height of 50 ft (15.2 m) is assumed.

Item 63 defines the receiving antenna height, in feet. When the ground-to-air model is used, this value must be greater than the transmitting antenna height but less than 300,000 ft (91,440 m). When the ground-to-ground model is used, this value must be between 1.6 ft (0.5 m) but less than 9,840 ft (3,000 m). If a receiving antenna height is not specified, a height of 1,000 ft (305 m) is used.

Item 64 is the surface refractivity referred to sea level, expressed in N-units, The input value must be at least 250 but no larger than 400 N-units. The surface refractivity default value is 301 N-units when item 64 is

not provided. This value corresponds to an effective $4/3$ earth radius.

Item 65 characterizes the terrain over which propagation is to occur as an irregularity factor or roughness expressed in feet. This terrain irregularity may be calculated directly from path profiles or estimated from table A-5. Terrain roughness of zero (0) defines a smooth earth condition; this is the assumed value when roughness is not defined by the input data.

Table A-5. Estimates of Terrain Roughness

Type of Terrain	Terrain Roughness (feet) (1 ft = 0.30 m)
Water or very smooth plains	0 - 16
Smooth plains	16 - 65
Slightly rolling plains	65 - 130
Rolling plains	130 - 260
Hills	260 - 490
Mountains	490 - 980
Rugged mountains	980 - 2300
Extremely rugged mountains	>2300

Item 66 specifies the elevation above mean sea level (msl) in feet for the transmitting antenna site. The

default value for site elevation is 0 ft.

Item 67 defines a conductivity and dielectric constant selection to be used in the propagation loss computation. The seven options are quantitatively defined in table A-6. When specification is not provided, average ground conditions (option 3) are assumed.

Table A-6. Surface Types and Constants

	Surface Type	Conductivity (mhos/m)	Dielectric Constant
1	Sea water	5	81
2	Good Ground	0.02 ██████	25
3	Average ground	0.005	15
4	Poor ground	0.001	4
5	Fresh water	0.010	81
6	Concrete	0.01	5
7	Metal	10^7	1

Several additional data are required only for the ground-to-ground model. Items 91 and 92 specify the quality of site selection to be considered for the transmitting and receiving antennas respectively. When the quality of site selection is not known, random siting, specified by numeral 1, is appropriate. When the quality of site selection is known, one of the other options for "some selection" or "good selection" is appropriate and should be specified by

either a numeral 2 or numeral 3. The default option for each item is "random siting."

Item 93 specifies the climate for the geographic region containing the systems being considered. Seven selections are available as itemized on the data sheet. The default selection is continental temperate climate, denoted by numeral 5.

APPENDIX B. SAMPLE MODEL APPLICATIONS

Three samples illustrating various ways in which the statistical frequency-distance curves model may be used are shown and discussed in this appendix. Each sample includes the appropriate "raw" data available to a frequency manager's analyst (emission spectrum, receiver selectivity, pulse shape, etc.), translation of those data to the worksheets for the F-D model, the statistical F-D curves which are generated by the model, and discussion of the salient features of each step in the sample.

The first sample is for a transmitter emission spectrum and receiver selectivity that were specified using point-amplitude data pairs for the INSPECT subroutine. For this sample the ground-to-air propagation loss model has been used.

The second sample again uses the point-amplitude specification for the transmitter emission spectrum and the receiver selectivity. However, the ground-to-ground propagation loss model has been used for this sample.

The third sample uses the NEWSPEC subroutine to synthesize an emission spectrum for a pulsed transmitter and a 5-pole Butterworth filter to model the receiver. The ground-to-air propagation loss model has been used.

B.1 Sample Number 1. Example of the Statistical F-D Model
Using the Ground-to-Air Propagation Loss Model and
Point-Amplitude Spectrum and Receiver Response Data

The systems considered in this sample operate at 5000 MHz and are identified simply as transmitter 1 and receiver 1. The data forms as they were completed for this example are shown in figures B-1 through B-4. The items referred to are shown in these figures.

The general data sheet, figure B-1, shows the transmitter has peak power output of 60 dBm, and the receiver has an operating threshold of -96 dBm (noise power would be somewhat less than this operating threshold) to which the interference criterion is related. Therefore, -96 dBm is shown in item 4. The criterion for interference is that peak interference power be 3 dB greater than the operating threshold of the receiver. This is entered as $I/N = 3$ dB in item 5. Other data provided on the general data sheet are the frequency separation (Δf) limits to be used in plotting the F-D curves.

Figure B-5 shows the emission spectrum for transmitter 1 and the receiver selectivity curve is shown by figure B-6. The emission spectrum is symmetrical, but the receiver selectivity is non-symmetrical. Therefore, the frequency

DATA FORM
 STATISTICAL FREQUENCY-DISTANCE CURVES MODEL

General Data

- 1 Transmitter identification (16 characters maximum)
- 1 Receiver identification (16 characters maximum)
1. 5000. *Carrier frequency, f_T , MHz
2. 60. *Output power, dBm
3. 1. Type of output power (0.)
 =0. if output power is average power, I_{AVG}
 =1. if output power is peak power, I_{PK}
4. -96. *Receiver noise, N, dBm
5. 3. Interference-to-noise criterion, I/N, dB (0.)
6. Transmitter polarization (1.)
 =1. for horizontal
 =2. for vertical
11. Number of frequency separations (101.)
12. -350. Lowest frequency separation, MHz (0.)
13. 300. Highest frequency separation, MHz (100.)
14. Maximum distance separation to be plotted, n mi (0.)
 =0. for model to calculate maximum
15. (10.)
16. (50.)
17. (90.)
- } Probability of interference, percent
18. Units for the distance (1.)
 =1. for nautical miles (n mi)
 =2. for statute miles (mi)
 =3. for kilometers (km)
19. Type of output (1.)
 =1. for statistical F-D and FDR curves
 =2. for FDR curves only
21. Emission spectrum/receiver selectivity model (1.)
 =1. for INSPECT, input 22
 =2. for NEWSPEC, input 23 through 27

* Denotes required input data on each data sheet.

() Denotes values used if user does not specify.

Figure B-1. Completed general data sheet for Sample 1.

Subroutine INSPECT

22. 1. *Emission spectrum and receiver selectivity envelopes
 =1. to input Δf and amplitude (point-amplitude)
 =2. to input Δf and "slope" in dB/decade (point-slope)
 =3. to input Δf and "slope" in dB/octave (point-slope)

<u>Spectrum Envelope</u>		<u>Normalized Receiver Response</u>	
(Point - Amplitude)			
<u>Δf, MHz</u>	<u>Amplitude, dBm/Hz</u>	<u>Δf, MHz</u>	<u>Amplitude, dB</u>
<u>-350.</u>	<u>-70.</u>	<u>-60.</u>	<u>-70.</u>
<u>-19.</u>	<u>-20.</u>	<u>-25.</u>	<u>-21.8</u>
<u>-3.6</u>	<u>-3.</u>	<u>-15.</u>	<u>-3.</u>
<u>0.</u>	<u>0.</u>	<u>0.</u>	<u>0.</u>
<u>3.6</u>	<u>-3.</u>	<u>60.</u>	<u>-3.</u>
<u>19.</u>	<u>-20.</u>	<u>83.</u>	<u>-70.</u>
<u>350.</u>	<u>-70.</u>	-----	-----
-----	-----	-----	-----
(Point - Slope)			
<u>Δf, MHz</u>	<u>Slope, dB/decade or dB/octave</u>	<u>Δf, MHz</u>	<u>Slope, dB/decade or dB/octave</u>
-----	-----	-----	-----
-----	-----	-----	-----
-----	-----	-----	-----
-----	-----	-----	-----
-----	-----	-----	-----
-----	-----	-----	-----
-----	-----	-----	-----
-----	-----	-----	-----

Figure B-2. Completed data sheet for subroutine INSPECT for Sample 1.

Subroutine ANTSTAT (Antenna Statistics)
Transmitter

41. _____ Coupling (1.)
(Interference Notebook Tables)
=1. for main beam only, input 42.
=2. for side- and back-lobe only, input 42. and 44.
=3. for full pattern, input 42., 44., and 45.
(User-provided statistics)
=4. for main beam only, input 42. and 46.
=5. for side- and back-lobe only, input 47. and 48.
=6. for full pattern, input 42. and 45. through 48.
42. 3.5 *Median main-beam gain, G_{TM} , dBi
44. _____ Site condition (2.)
=1. for open
=2. for average
=3. for crowded
45. _____ 10 dB main-beam width, α_T , degrees
46. _____ Standard deviation, main-beam gain, σ_{TM} , dB
47. _____ Median side- and back-lobe gain, G_{TB} , dBi
48. _____ Standard deviation, side- and back-lobe gain, σ_{TB} , dB

Receiver

51. _____ Coupling (1.)
(Interference Notebook Tables)
=1. for main beam only, input 52. and 53.
=2. for side- and back-lobe only, input 52. and 54.
=3. for full pattern, input 52. through 55.
(User-provided statistics)
=4. for main beam only, input 52. and 56.
=5. for side- and back-lobe only, input 57. and 58.
=6. for full pattern, input 52. and 55. through 58.
52. 3.5 *Median main-beam gain, G_{RM} , dBi
53. _____ Polarization (1.)
=1. for horizontal
=2. for vertical
54. _____ Site condition (2.)
=1. for open
=2. for average
=3. for crowded
55. _____ 10 dB main-beam width, α_R , degrees
56. _____ Standard deviation, main-beam gain, σ_{RM} , dB
57. _____ Median side- and back-lobe gain, G_{RB} , dBi
58. _____ Standard deviation, side- and back-lobe gain, σ_{RB} , dB

Figure B-3. Completed data sheet for subroutine ANTSTAT for Sample 1.

Loss Data

61. _____ Loss model (1.)
=1. for ground-to-air, input 62. through 66.
=2. for ground-to-ground, input 62. through 66.
and 91. through 95.
62. 1000. Transmitter antenna height above terrain, H_T , feet (50.)
63. 10,000. Receiver antenna height above terrain, H_R , feet (1000.)
64. _____ Surface refractivity, N-units (301.)
65. _____ Terrain roughness, ΔH , feet (0.)
66. _____ Transmitter site elevation above MSL, feet (0.)
67. _____ Surface types and constants (3.)
=1. sea water
=2. good ground
=3. average ground
=4. poor ground
=5. fresh water
=6. concrete
=7. metal

Ground-to-ground only

91. _____ Transmitter antenna siting (1.)
=1. for random siting
=2. for some selection in siting
=3. for good selection in siting
92. _____ Receiver antenna siting (1.)
=1. for random siting
=2. for some selection in siting
=3. for good selection in siting
93. _____ Climate (5.)
=1. for equatorial
=2. for continental subtropical
=3. for maritime subtropical
=4. for desert
=5. for continental temperate
=6. for maritime temperate overland
=7. for maritime temperate oversea

Figure B-4. Completed loss data sheet for Sample 1.

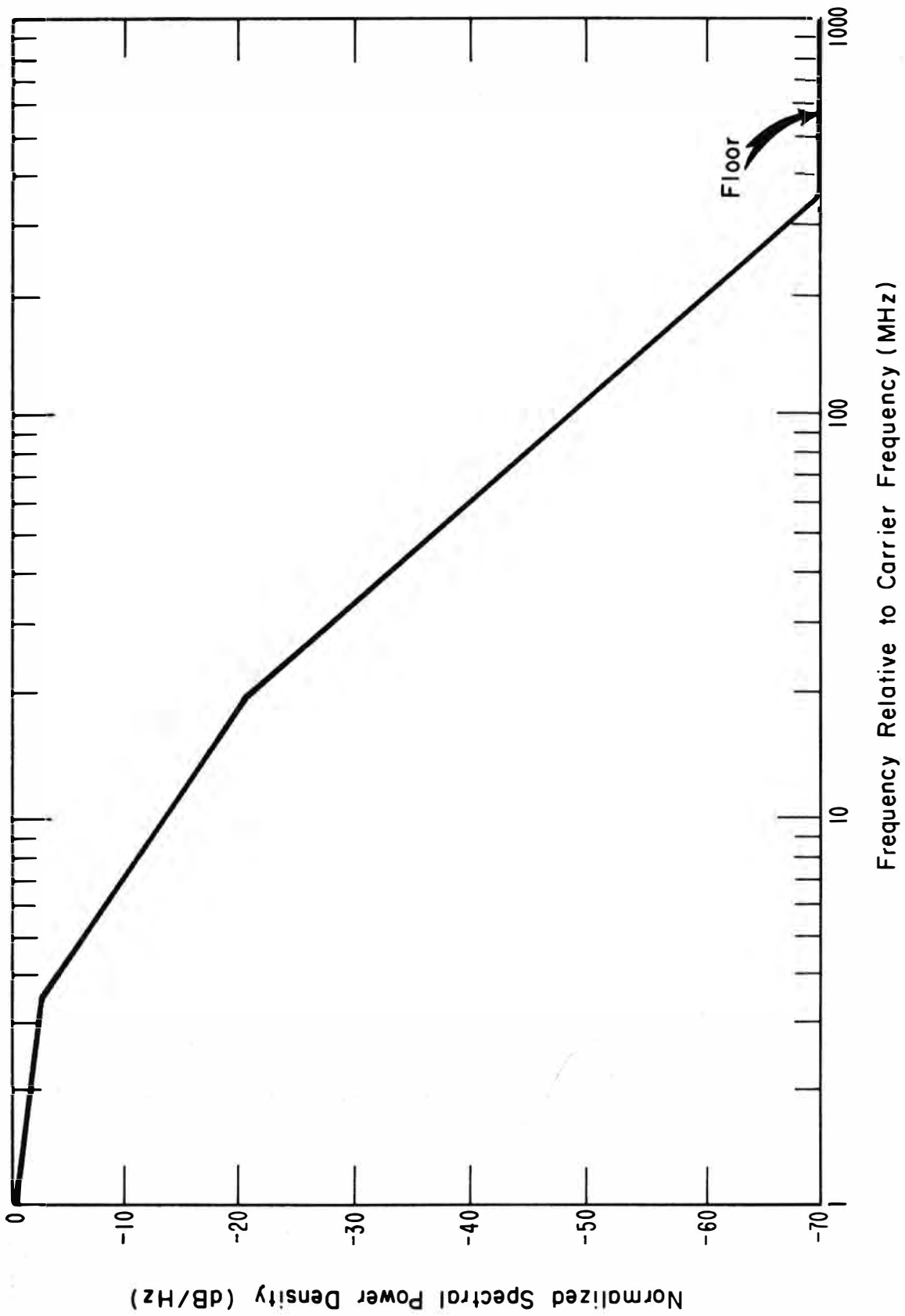


Figure B-5. Normalized spectral power density envelope for transmitter 1 used in Sample 1.

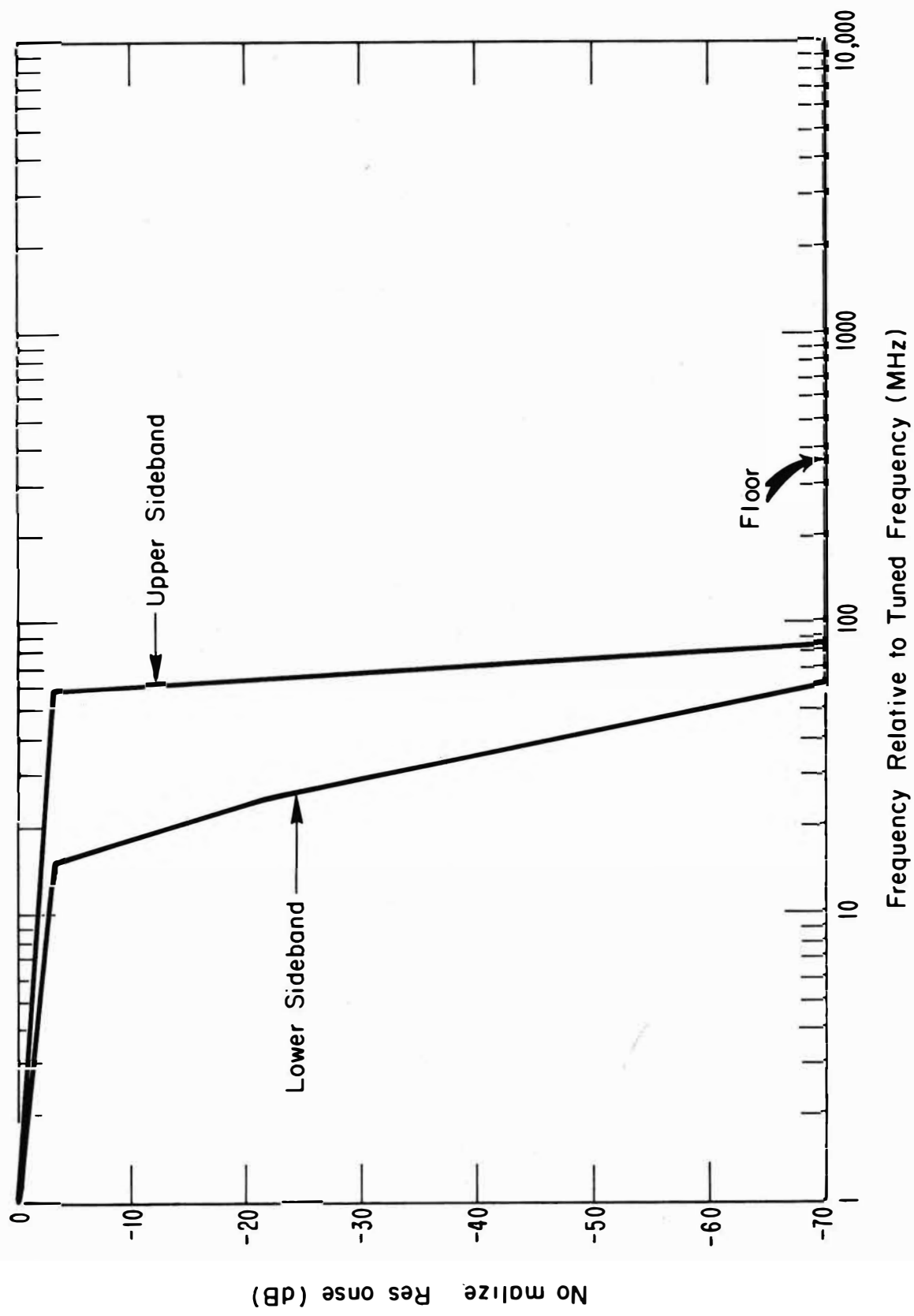


Figure B-6. Normalized receiver selectivity curve for receiver 1 used in Sample 1.

separation limits have been specified from -350 MHz to 300 MHz in items 12 and 13.

Nine items of input data have been left blank on the general data sheet, figure B-1, which simply means that the default values are the best estimates for these quantities.

The emission spectrum and receiver selectivity curve shown in figures B-5 and B-6 provide the input data for subroutine INSPECT. These data are shown on figure B-2. Note that the spectrum and selectivity curves are "bounding" straight-line segment estimates. The relative frequency and normalized amplitude for each line segment intersection are entered as data pairs on the data sheet for the INSPECT subroutine. The point-amplitude option has been selected in item 22. Up to 100 point-amplitude or point-slope data pairs may be used to specify the emission spectrum and the receiver response curve, but only seven were required for the spectrum and six for the selectivity curves of this example.

Many options are built into the selections of the data sheet for antenna statistics.* Note that only two required items of data have been specified in this example (see figure B-3). These are the main-beam gain for both the transmitting and receiving antennas.

*The options are discussed in detail in the User's Guide, Appendix A.

It is important to review the default conditions and the data that result. Leaving blank the antenna coupling (items 41 and 51) results in main beam-to-main beam antenna coupling, and the F-D model then utilizes the RADC Interference Notebook data for antenna statistics. Since main-beam gains are specified, the only additional data needed by the model are the standard deviations for main-beam gain for both antennas. These values are automatically selected from the tabular data as described in Appendix D.

For the user's information, observe that both antennas have been specified with median main-beam gain of 3.5 dBi. Reference to Table D-3 (in Appendix D) shows the main-beam standard deviation is 1 dB, and that site conditions (items 44 and 54) do not influence the main-beam standard deviations. Horizontal polarization is the default option for polarization.

Looking now at the input data sheet for computing propagation loss, figure B-4, the ground-to-air loss model has been used by default in item 61. Transmitter antenna height has been specified as 1000 ft (304.8 m) above its surrounding terrain (item 62) and receiver antenna height has been specified (item 63) as 10,000 ft (3048 m). Omitting the remaining data means that the loss calculations are made using a smooth earth with effective 4/3 earth radius (default values of items 64, 65 and 67). Further,

the earth dielectric and resistive properties are considered to be "average" (item 67). (Refer to table A-4, Appendix A, for quantitative values for "average" earth reflection material.)

Figure B-7 shows the statistical F-D curves which are generated using the data of this example. The transmitter and receiver identifications are labeled automatically on the plot along with the values for receiver noise and the I/N criterion. The curves have the following interpretation: for a given frequency separation, a related distance separation defined by the appropriate curve will allow the interference power to be greater than the 3 dB I/N criterion 10% of the time for the solid curve, 50% of the time for the dashed curve, or 90% of the time for the dotted curve.

The shapes of the statistical F-D curves have two characteristics deserving comment. First, the non-symmetrical shape of the receiver selectivity curve in figure B-6 is reflected in the F-D curves. Since the transmitter carrier frequency is used as the reference frequency, one can see that the broader upper sideband character of the receiver selectivity results in a greater distance separation for the constant I/N of the example when the receiver tuned frequency is less than the transmitter carrier frequency (negative Δf values). When the receiver

STATISTICAL FREQUENCY-DISTANCE CURVES

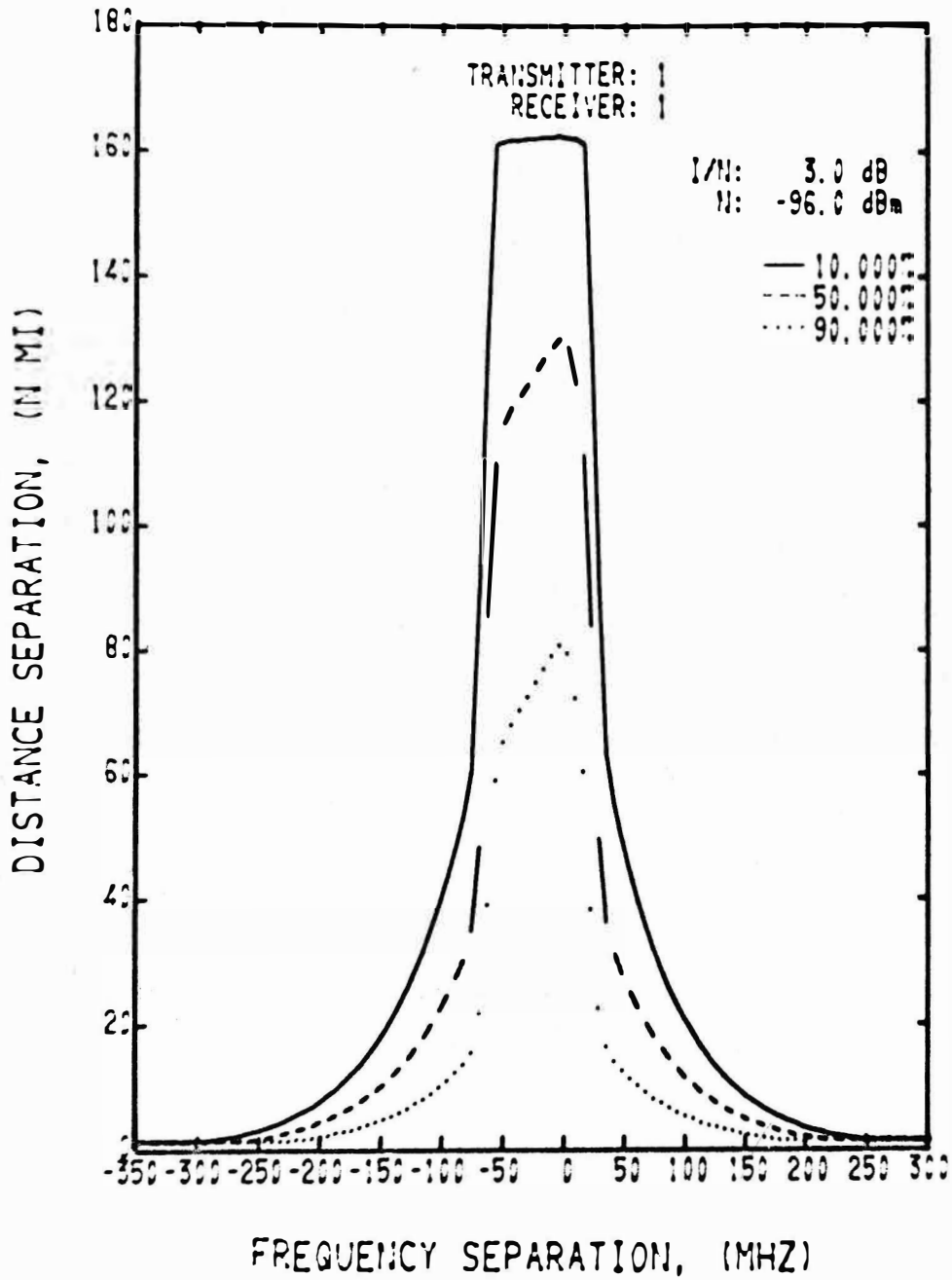


Figure B-7. Statistical frequency-distance curves for transmitter 1-receiver 1 pair for Sample 1 using the ground-to-air propagation loss model (1 n mi = 1.85 km).

is tuned above the transmitter operating frequency, the receiver can operate closer in distance to the transmitter.

A second characteristic of the F-D curves of this example is that near $\Delta f=0$ the solid curve has a flat top, whereas the other curves do not. This flatness is an influence of the propagation loss model. For any propagation path, as distance increases there is, first, a region of line-of-sight propagation, then a region of diffraction-mode propagation, and, finally, a region of scatter-mode propagation. Loss in these regions is influenced by antenna heights, terrain characteristics, etc. As the propagation goes from line-of-sight to diffraction mode, a rapid increase occurs in the propagation loss. In addition, when considering statistical propagation loss curves, the standard deviations become much greater for diffraction and scatter modes than for line-of-sight modes. For the conditions specified in this example, the transition from line-of-sight to diffraction mode propagation occurred at about 160 n mi (296 km).

B.2 Sample Number 2. Example of the Statistical F-D Model
Using the Ground-to-Ground Propagation Loss Model and
Point-Amplitude Spectrum and Receiver Response Data
The data forms as they were completed for this example

are shown in figures B-8 through B-11. The items referred to are shown in these figures.

This sample considers systems which operate at 5000 MHz. The systems are identified simply as transmitter 3A and receiver 6A. The transmitter has average output power of 53 dBm (items 2 and 3, figure B-8). The receiver noise power is -110 dBm (item 4), and the interference criterion is that average interference power be 5 dB greater than the noise power (item 5 showing $I/N = 5$ dB).

The remaining items on the general data sheet, except item 13 (the highest frequency separation) are not specified, hence the default values are used by the model. Item 13 is specified by consulting the emission spectrum and receiver selectivity plots, figures B-12 and B-13. The emission spectrum is symmetrical and reaches its minimum value at a frequency of about 60 MHz above the transmitter center frequency ($\Delta f = 60$ MHz). The receiver selectivity is also symmetrical, except for the image response at 120 MHz below the tuned frequency of the receiver. The selectivity curve reaches its minimum value about 50 MHz above the tuned frequency and about 180 MHz below the tuned frequency except for the image response. Considering the frequencies at which the transmitted spectrum and the receiver selectivity reach their minimum values, frequencies of 120 MHz and 240 MHz would be entered in items 12 and 13 for the lowest and

DATA FORM
 STATISTICAL FREQUENCY-DISTANCE CURVES MODEL

General Data

- 3A Transmitter identification (16 characters maximum)
- 6A Receiver identification (16 characters maximum)
1. 5000. *Carrier frequency, f_T , MHz
2. 53. *Output power, dBm
3. Type of output power (0.)
 =0. if output power is average power, I_{AVG}
 =1. if output power is peak power, I_{PK}
4. -110. *Receiver noise, N, dBm
5. 5. Interference-to-noise criterion, I/N, dB (0.)
6. Transmitter polarization (1.)
 =1. for horizontal
 =2. for vertical
11. Number of frequency separations (101.)
12. -100. Lowest frequency separation, MHz (0.)
13. 220. Highest frequency separation, MHz (100.)
14. Maximum distance separation to be plotted, n mi (0.)
 =0. for model to calculate maximum
15. (10.)
16. (50.)
17. (90.)
- } Probability of interference, percent
18. Units for the distance (1.)
 =1. for nautical miles (n mi)
 =2. for statute miles (mi)
 =3. for kilometers (km)
19. Type of output (1.)
 =1. for statistical F-D and FDR curves
 =2. for FDR curves only
21. Emission spectrum/receiver selectivity model (1.)
 =1. for INSPECT, input 22
 =2. for NEWSPEC, input 23 through 27

* Denotes required input data on each data sheet.

() Denotes values used if user does not specify.

Figure B-8. Completed general data sheet for Sample 2.

Subroutine INSPECT

22. 1. *Emission spectrum and receiver selectivity envelopes
 =1. to input Δf and amplitude (point-amplitude)
 =2. to input Δf and "slope" in dB/decade (point-slope)
 =3. to input Δf and "slope" in dB/octave (point-slope)

<u>Spectrum Envelope</u>		<u>Normalized Receiver Response</u>	
(Point - Amplitude)			
<u>Δf, MHz</u>	<u>Amplitude, dBm/Hz</u>	<u>Δf, MHz</u>	<u>Amplitude, dB</u>
<u>-60.</u>	<u>-70.</u>	<u>-180.</u>	<u>-60.</u>
<u>-1.22</u>	<u>-12.5</u>	<u>-140.</u>	<u>-2.0</u>
<u>-0.47</u>	<u>0.</u>	<u>-100.</u>	<u>-2.0</u>
<u>0.</u>	<u>0.</u>	<u>-70.</u>	<u>-60.</u>
<u>0.47</u>	<u>0.</u>	<u>-50.</u>	<u>-60.</u>
<u>1.22</u>	<u>-12.5</u>	<u>-20.</u>	<u>0.</u>
<u>60.</u>	<u>-70.</u>	<u>0.</u>	<u>0.</u>
<u>_____</u>	<u>_____</u>	<u>20.</u>	<u>0.</u>
		<u>50.</u>	<u>-60.</u>
(Point - Slope)			
<u>Δf, MHz</u>	<u>Slope, dB/decade or dB/octave</u>	<u>Δf, MHz</u>	<u>Slope, dB/decade or dB/octave</u>
<u>_____</u>	<u>_____</u>	<u>_____</u>	<u>_____</u>
<u>_____</u>	<u>_____</u>	<u>_____</u>	<u>_____</u>
<u>_____</u>	<u>_____</u>	<u>_____</u>	<u>_____</u>
<u>_____</u>	<u>_____</u>	<u>_____</u>	<u>_____</u>
<u>_____</u>	<u>_____</u>	<u>_____</u>	<u>_____</u>
<u>_____</u>	<u>_____</u>	<u>_____</u>	<u>_____</u>
<u>_____</u>	<u>_____</u>	<u>_____</u>	<u>_____</u>
<u>_____</u>	<u>_____</u>	<u>_____</u>	<u>_____</u>

Figure B-9. Completed data sheet for subroutine INSPECT for Sample 2.

Subroutine ANTSTAT (Antenna Statistics)
Transmitter

41. _____ Coupling (1.)
(Interference Notebook Tables)
=1. for main beam only, input 42.
=2. for side- and back-lobe only, input 42. and 44.
=3. for full pattern, input 42., 44., and 45.
(User-provided statistics)
=4. for main beam only, input 42. and 46.
=5. for side- and back-lobe only, input 47. and 48.
=6. for full pattern, input 42. and 45. through 48.
42. 0. *Median main-beam gain, G_{TM} , dBi
44. _____ Site condition (2.)
=1. for open
=2. for average
=3. for crowded
45. _____ 10 dB main-beam width, α_T , degrees
46. _____ Standard deviation, main-beam gain, σ_{TM} , dB
47. _____ Median side- and back-lobe gain, G_{TB} , dBi
48. _____ Standard deviation, side- and back-lobe gain, σ_{TB} , dB

Receiver

51. _____ Coupling (1.)
(Interference Notebook Tables)
=1. for main beam only, input 52. and 53.
=2. for side- and back-lobe only, input 52. and 54.
=3. for full pattern, input 52. through 55.
(User-provided statistics)
=4. for main beam only, input 52. and 56.
=5. for side- and back-lobe only, input 57. and 58.
=6. for full pattern, input 52. and 55. through 58.
52. 20. *Median main-beam gain, G_{RM} , dBi
53. _____ Polarization (1.)
=1. for horizontal
=2. for vertical
54. _____ Site condition (2.)
=1. for open
=2. for average
=3. for crowded
55. _____ 10 dB main-beam width, α_R , degrees
56. _____ Standard deviation, main-beam gain, σ_{RM} , dB
57. _____ Median side- and back-lobe gain, G_{RB} , dBi
58. _____ Standard deviation, side- and back-lobe gain, σ_{RB} , dB

Figure B-10. Completed data sheet for subroutine ANTSTAT for Sample 2.

Loss Data

61. 2. Loss model (1.)
=1. for ground-to-air, input 62. through 66.
=2. for ground-to-ground, input 62. through 66.
and 91. through 95.
62. 25. Transmitter antenna height above terrain, H_T , feet (50.)
63. 50. Receiver antenna height above terrain, H_R , feet (1000.)
64. _____ Surface refractivity, N-units (301.)
65. _____ Terrain roughness, ΔH , feet (0.)
66. _____ Transmitter site elevation above MSL, feet (0.)
67. _____ Surface types and constants (3.)
=1. sea water
=2. good ground
=3. average ground
=4. poor ground
=5. fresh water
=6. concrete
=7. metal

Ground-to-ground only

91. _____ Transmitter antenna siting (1.)
=1. for random siting
=2. for some selection in siting
=3. for good selection in siting
92. _____ Receiver antenna siting (1.)
=1. for random siting
=2. for some selection in siting
=3. for good selection in siting
93. _____ Climate (5.)
=1. for equatorial
=2. for continental subtropical
=3. for maritime subtropical
=4. for desert
=5. for continental temperate
=6. for maritime temperate overland
=7. for maritime temperate oversea

Figure B-11. Completed loss data sheet for Sample 2.

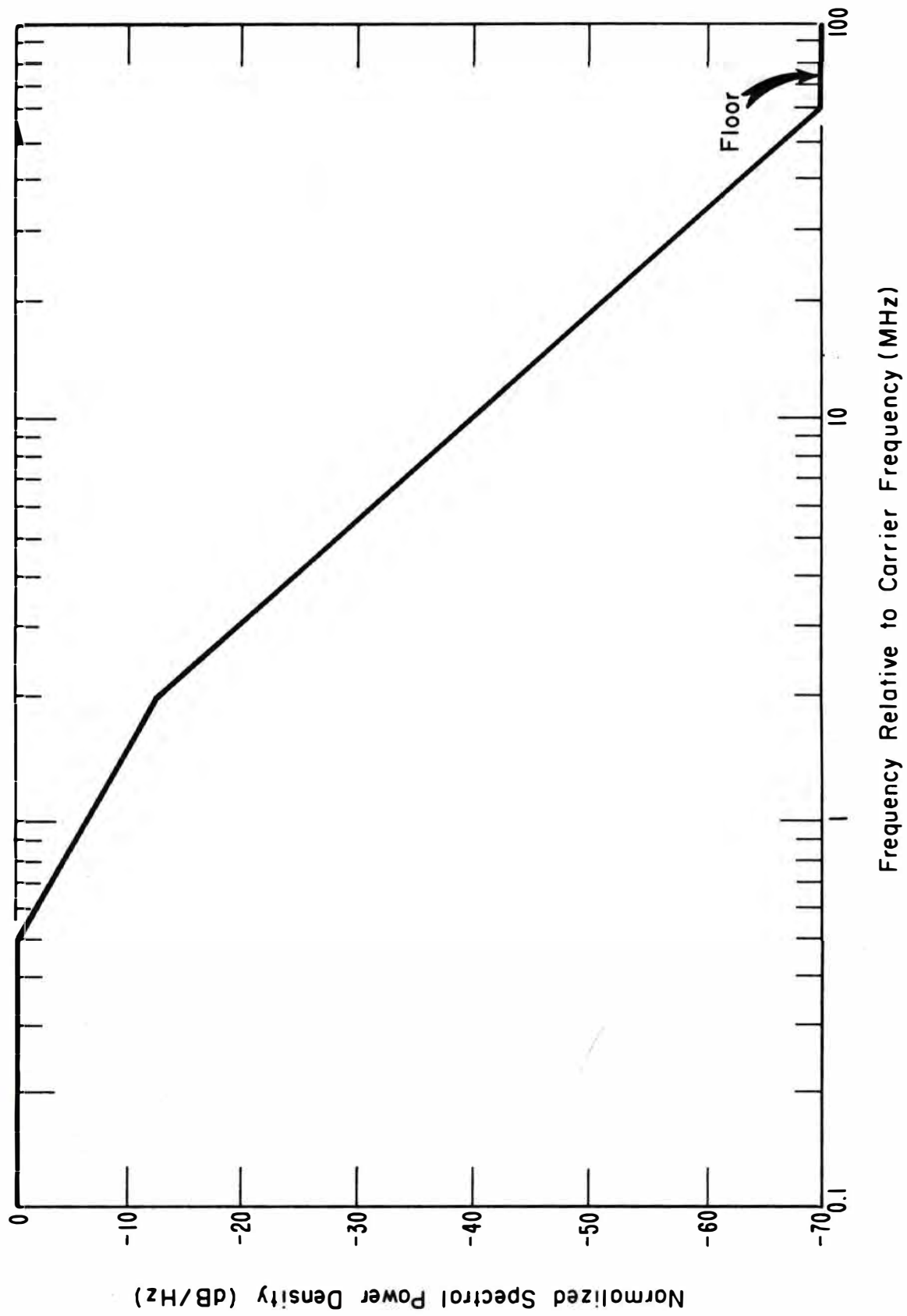


Figure B-12. Normalized spectral power density envelope for transmitter 3A for Sample 2.

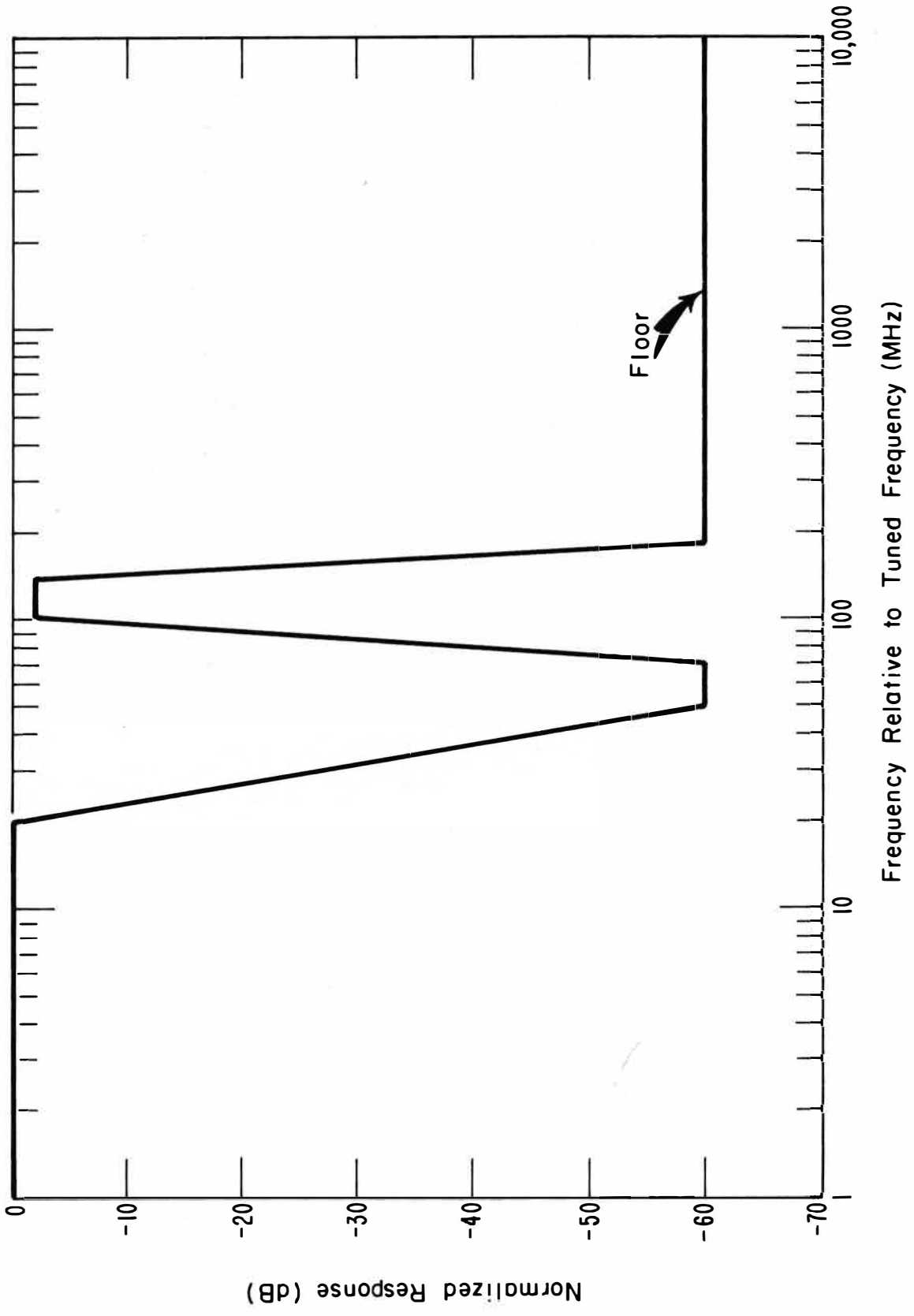


Figure B-13. Normalized selectivity curve for receiver 6A for Sample 2.

highest separation frequencies. (Experience with the F-D model on this problem showed the values could be -100 and 220 MHz.)

For this sample, as for sample No. 1, the INSPECT subroutine with point-amplitude specification was used to model the transmitter and receiver spectral characteristics (item 22 on figure B-9). The emission spectrum and receiver selectivity curve shown in figures B-12 and B-13 respectively are "bounding", straight-line segment plots. The point-amplitude data pairs on the INSPECT data sheet for emission spectrum and receiver response are the intersections of these straight-line segments.

Main beam-to-main beam antenna coupling was used for this sample (as for sample No. 1). The main-beam gain specified for the transmitter antenna is 0 dBi (item 42 on figure B-10). Reference to table D-3 (Appendix D) shows that a 1 dB standard deviation will be used (item 46). The main-beam gain specified for the receiving antenna is 20 dBi (item 52). A standard deviation of 2 dB (item 56) is associated with that gain (refer to table D-2, Appendix D). Notice that a minimum amount of user specified data for antenna statistics are used in this sample.

In this example, the ground-to-ground propagation loss model was used by specifying numeral 2 for item 61 on the loss data sheet, figure B-11. The transmitter antenna

height is specified (item 62) as 25 ft (7.62 m) and the receiver antenna height is specified (item 63) as 50 ft (15.24 m). Omitting specification for atmospheric constants, terrain characterization, and transmitter site elevation (items 64, 65 and 66) results in a smooth, $4/3$ earth effective radius being used in the calculations of propagation loss. The ground conductivity and dielectric constant values used are for "average" ground, by default.

Only the ground-to-ground loss model uses data defining antenna site selection and climate for the propagation region. The default values are used which give random site selection for both antennas (items 91 and 92) and propagation in a continental temperate climate (item 95).

Figure B-14 shows the statistical F-D curves generated for this example. These curves illustrate the dominant influence of the receiver response curve for this example with its image response. For distance separations of about 10 n mi (18.52 km) and less, the propagation is line-of-sight, then, at this point the diffraction mode begins. This change in propagation modes is shown by the discontinuity in the F-D curves at 10 n mi (18.52 km) and a larger spread between the 10%, 50%, and 90% curves.

STATISTICAL FREQUENCY-DISTANCE CURVES

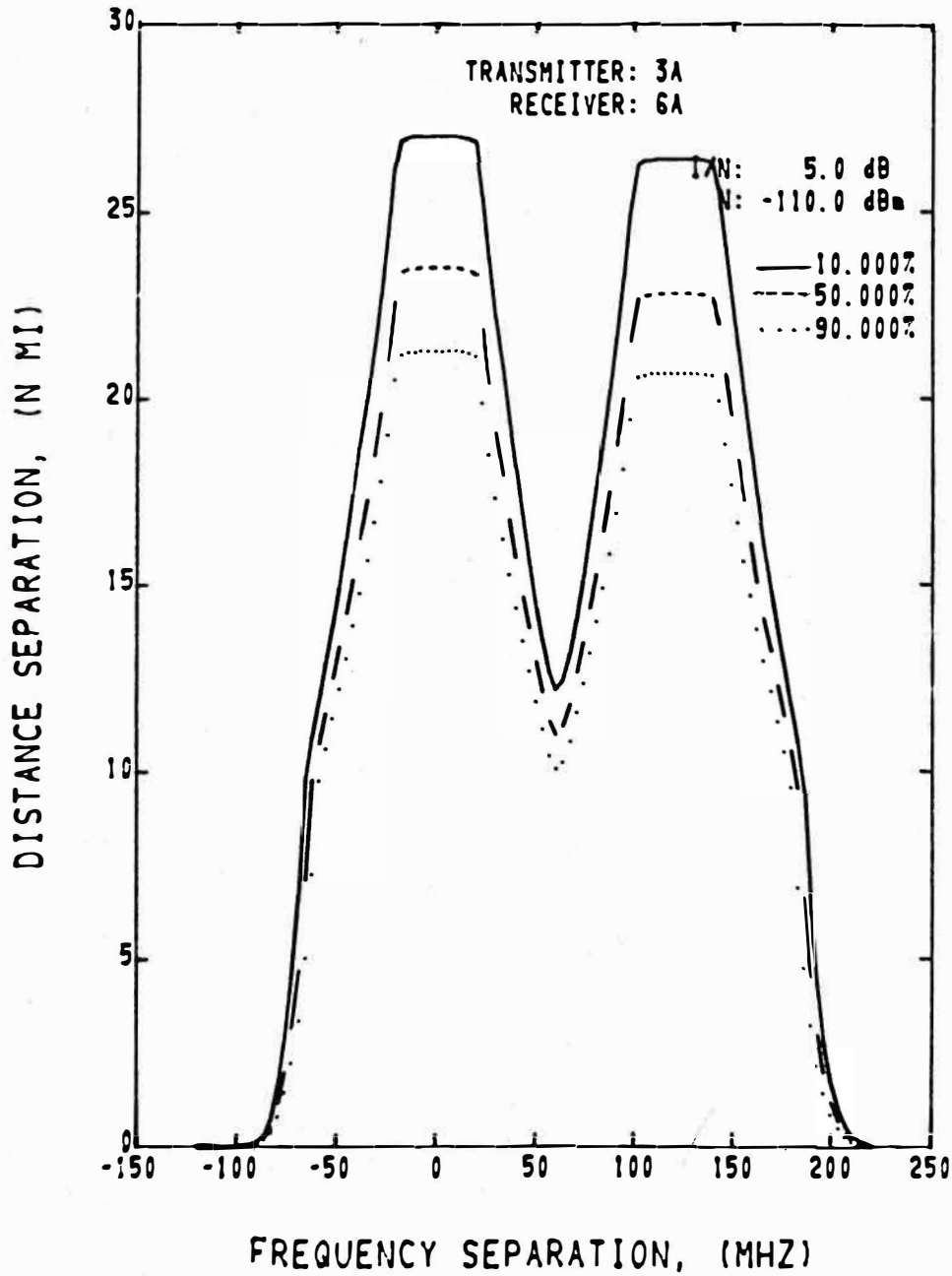


Figure B-14. Statistical frequency-distance curves for transmitter 3A-receiver 6A pair for Sample 2 using the ground-to-ground propagation loss model (1 n mi = 1.85 km).

B.3 Sample Number 3, Example of the Statistical F-D Model Using the Ground-to-Air Propagation Loss Model and Synthesized Spectrum and Receiver Response Characteristics.

The data forms as they were completed for this example are shown in figures B-15 through B-17. (Since a time domain pulse shape is used, data sheet 2 is not required. The loss data sheet also is not used, as explained later.) The item numbers referred to in the text are shown in these figures.

This third sample considers systems which operate at 1640 MHz. The transmitter is identified as NEWSPECT TEST, and the receiver is identified as TEST (21 PTS). This transmitter is a pulsed system with average output power of 23 dBm (items 2 and 3 on the general data sheet, figure B-15). The receiver noise power is -72 dBm (item 4). The interference criterion is that average interference power be 10 dB less than the receiver noise power ($I/N = -10$ dB shown in item 5).

As mentioned in the general introduction to this appendix, this sample uses the NEWSPEC subroutine to synthesize the emission spectrum and model the receiver filter. For this example, 21 frequency separations were used and entered in item 11, but fewer points could have been used with less smoothness in the generated statistical

DATA FORM
STATISTICAL FREQUENCY-DISTANCE CURVES MODEL

General Data

NEWSPECT TEST Transmitter identification (16 characters maximum)

TEST (21 PTS) Receiver identification (16 characters maximum)

1. 1640. *Carrier frequency, f_T , MHz
2. 23. *Output power, dBm
3. Type of output power (0.)
=0. if output power is average power, I_{AVG}
=1. if output power is peak power, I_{PK}
4. -72. *Receiver noise, N, dBm
5. -10. Interference-to-noise criterion, I/N, dB (0.)
6. Transmitter polarization (1.)
=1. for horizontal
=2. for vertical
11. 21. Number of frequency separations (101.)
12. Lowest frequency separation, MHz (0.)
13. 30. Highest frequency separation, MHz (100.)
14. Maximum distance separation to be plotted, n mi (0.)
=0. for model to calculate maximum
15. (10.)
16. (50.)
17. (90.)
18. Units for the distance (1.)
=1. for nautical miles (n mi)
=2. for statute miles (mi)
=3. for kilometers (km)
19. Type of output (1.)
=1. for statistical F-D and FDR curves
=2. for FDR curves only
21. Emission spectrum/receiver selectivity model (1.)
=1. for INSPECT, input 22
=2. for NEWSPEC, input 23 through 27

* Denotes required input data on each data sheet.

() Denotes values used if user does not specify.

Figure B-15. Completed general data sheet for Sample 3.

Subroutine NEWSPEC

- 23. 6.0 *Receiver (filter) bandwidth, MHz
- 24. .144 *Half amplitude pulse width, microseconds
- 25. .032 *10% - 90% rise time, microseconds
- 26. .040 *90% - 10% fall time, microseconds
- 27. 60,000 *Pulse repetition rate, pulses/second
- 28. _____ Type of filter (2.)
=1. for Chebyshev, input 27., 28., and 29.
=2. for Butterworth, input 27.
=3. for Elliptic, input 28., 29., 30., and 31.
- 29. _____ Number of poles or ripples (5.)
- 30. _____ Maximum Z-squared in pass band
- 31. _____ Minimum (allowable) Z-squared in pass band
- 32. _____ Maximum (allowable) Z-squared in stop band
- 33. _____ Beginning frequency of the stop band

Figure B-16. Completed data sheet for subroutine NEWSPEC for Sample 3.

Subroutine ANTSTAT (Antenna Statistics)
Transmitter

41. 6. Coupling (1.)
(Interference Notebook Tables)
=1. for main beam only, input 42.
=2. for side- and back-lobe only, input 42. and 44.
=3. for full pattern, input 42., 44., and 45.
(User-provided statistics)
=4. for main beam only, input 42. and 46.
=5. for side- and back-lobe only, input 47. and 48.
=6. for full pattern, input 42. and 45. through 48.
42. 10. *Median main-beam gain, G_{TM} , dBi
44. _____ Site condition (2.)
=1. for open
=2. for average
=3. for crowded
45. 90. 10 dB main-beam width, α_T , degrees
46. 1. Standard deviation, main-beam gain, σ_{TM} , dB
47. 0. Median side- and back-lobe gain, G_{TB} , dBi
48. 3. Standard deviation, side- and back-lobe gain, σ_{TB} , dB

Receiver

51. 6. Coupling (1.)
(Interference Notebook Tables)
=1. for main beam only, input 52. and 53.
=2. for side- and back-lobe only, input 52. and 54.
=3. for full pattern, input 52. through 55.
(User-provided statistics)
=4. for main beam only, input 52. and 56.
=5. for side- and back-lobe only, input 57. and 58.
=6. for full pattern, input 52. and 55. through 58.
52. 10. *Median main-beam gain, G_{RM} , dBi
53. _____ Polarization (1.)
=1. for horizontal
=2. for vertical
54. _____ Site condition (2.)
=1. for open
=2. for average
=3. for crowded
55. 90. 10 dB main-beam width, α_R , degrees
56. 1. Standard deviation, main-beam gain, σ_{RM} , dB
57. 0. Median side- and back-lobe gain, G_{RB} , dBi
58. 3. Standard deviation, side- and back-lobe gain, σ_{RB} , dB

Figure B-17. Completed data sheet for subroutine ANTSTAT for Sample 3.

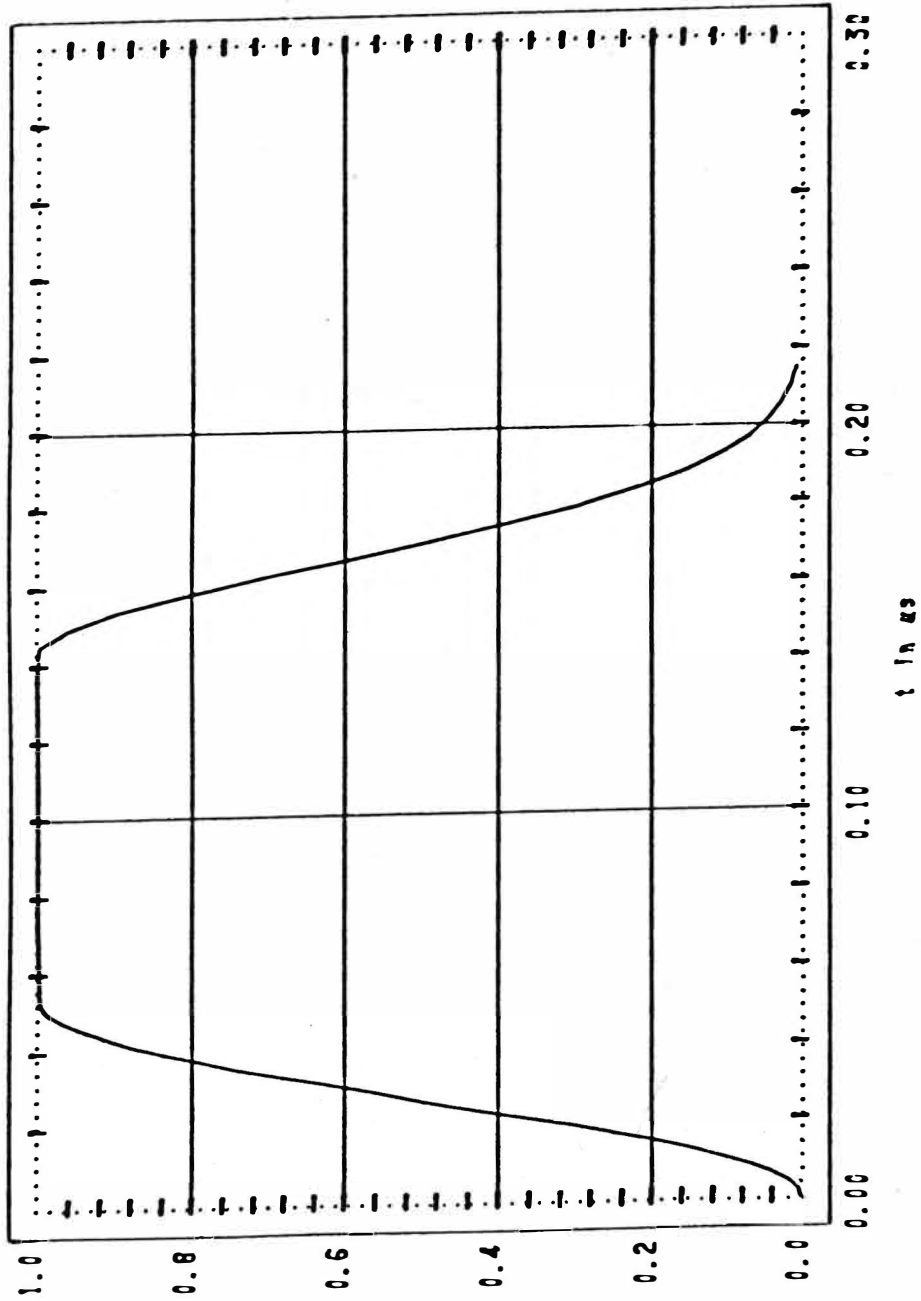
frequency-distance curves. More points could have been used, but to do so would have increased significantly the computer running time.

The highest frequency separation to be used in plotting the F-D curves is specified as 30 MHz in item 13. Using the default value of 0 MHz for the lowest frequency separation in item 12 is consistent with a symmetrical emission spectrum and receiver filter as have been synthesized by the NEWSPEC subroutine.

Only the required data are supplied in this example for the NEWSPEC subroutine. The receiver bandwidth is specified as 6 MHz in item 23. The pulse (time domain waveform of the transmitter) has half-amplitude width of 0.144 μ s, a rise time of 0.032 μ s (10% amplitude to 90% amplitude) and a fall time of 0.040 μ s (90% amplitude to 10% amplitude). The pulse repetition rate is 60,000 pps. These types of data usually are available.

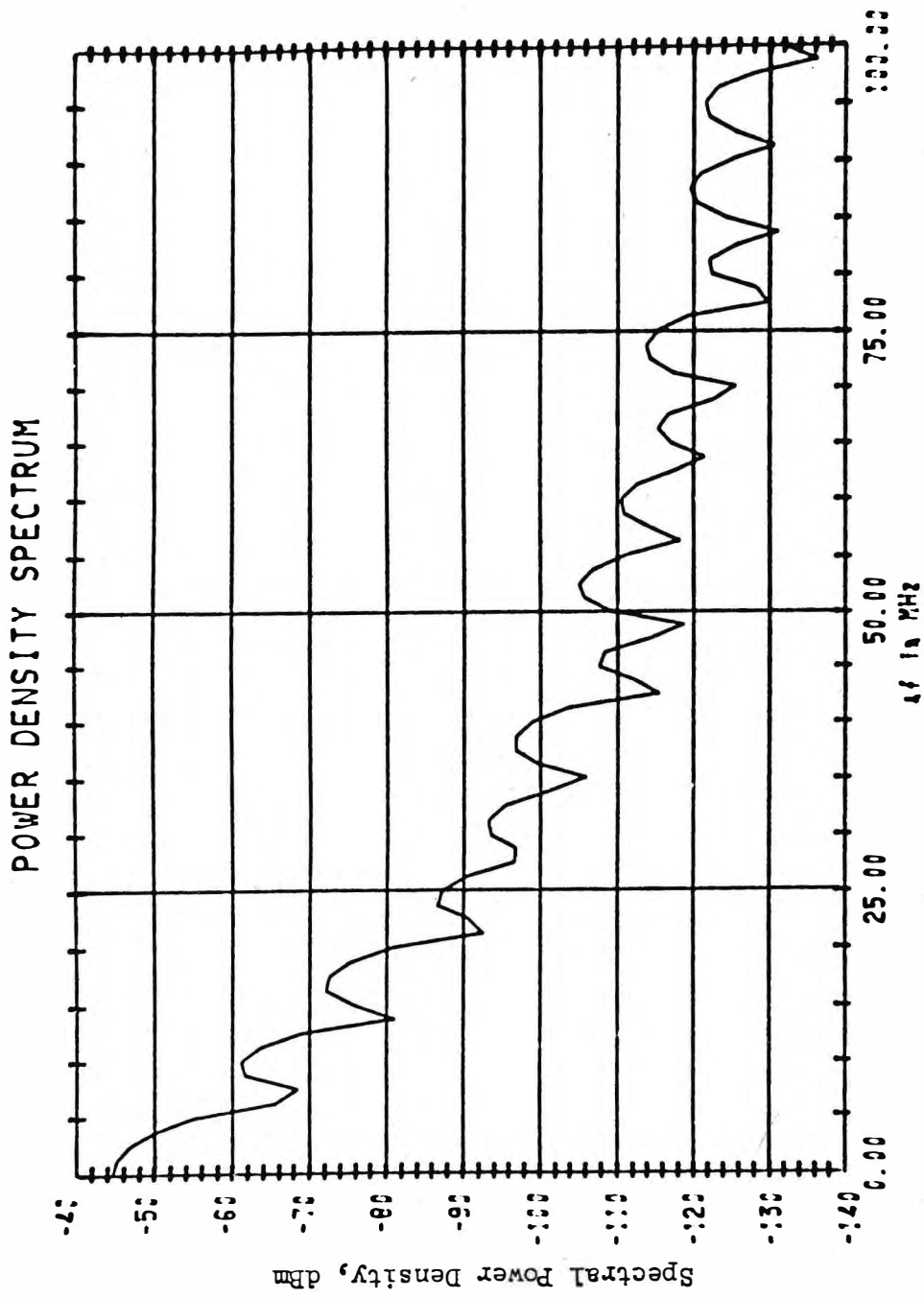
Figure B-18 shows the pulse shape (time-domain waveform) as synthesized by NEWSPEC from these data, and figure B-19 shows the synthesized emission spectrum. These plots are not a normal output when NEWSPEC is selected. They are included here only to help show how the NEWSPEC subroutine utilizes the same form of data as the INSPECT subroutine.

SHAPE FACTOR



$\tau_{AU} = 0.144$ $\tau_{AU_p} = 0.032$ $\tau_{AU_f} = 0.040$ $t = 0.000$ $P_{ave} = 23.300$

Figure B-18. Synthesized pulse (time domain waveform) for transmitter NEWSPECT TEST for Sample 3.



$\tau_{AU} = 0.146$ $\tau_{AU_f} = 0.032$ $\tau_{AU_f} = 0.040$ $\tau = 0.000$ $P_{ave} = 23.300$

Figure B-19. Synthesized spectral power density curve for transmitter NEWSPECT TEST for Sample 3.

Omitting specification of the filter type and the number of poles in items 28 and 29 results in the model choosing the receiver response curve of a 5-pole Butterworth filter. This normalized receiver response is shown in figure B-20. This receiver curve also is not normally output by the F-D model. Other items of the NEWSPEC data sheet, figure B-16, do not apply to this problem. (They are used when Chebyshev or elliptic filters are specified.)

In this example, considerable antenna coupling and statistical data have been used as model input. Default conditions were used only for items 44, 53, and 54, the transmitter site condition and the receiver polarization and site condition; all other items are specified. Most of the items were required inputs after the full-pattern antenna coupling was specified (option 6 in items 41 and 51).

The transmitter antenna was specified with median main-beam gain of 10 dBi in item 42 and associated standard deviation of 1 dB in item 46. The 10 dB main-beam width of the antenna has been specified as 90° in item 45. Side- and back-lobe gain for the transmitter antenna is specified with a median gain of 0 dBi in item 47 and associated standard deviation of 3 dB in item 48.

The receiving antenna data were the same as those data used for the transmitting antenna. They are shown in items

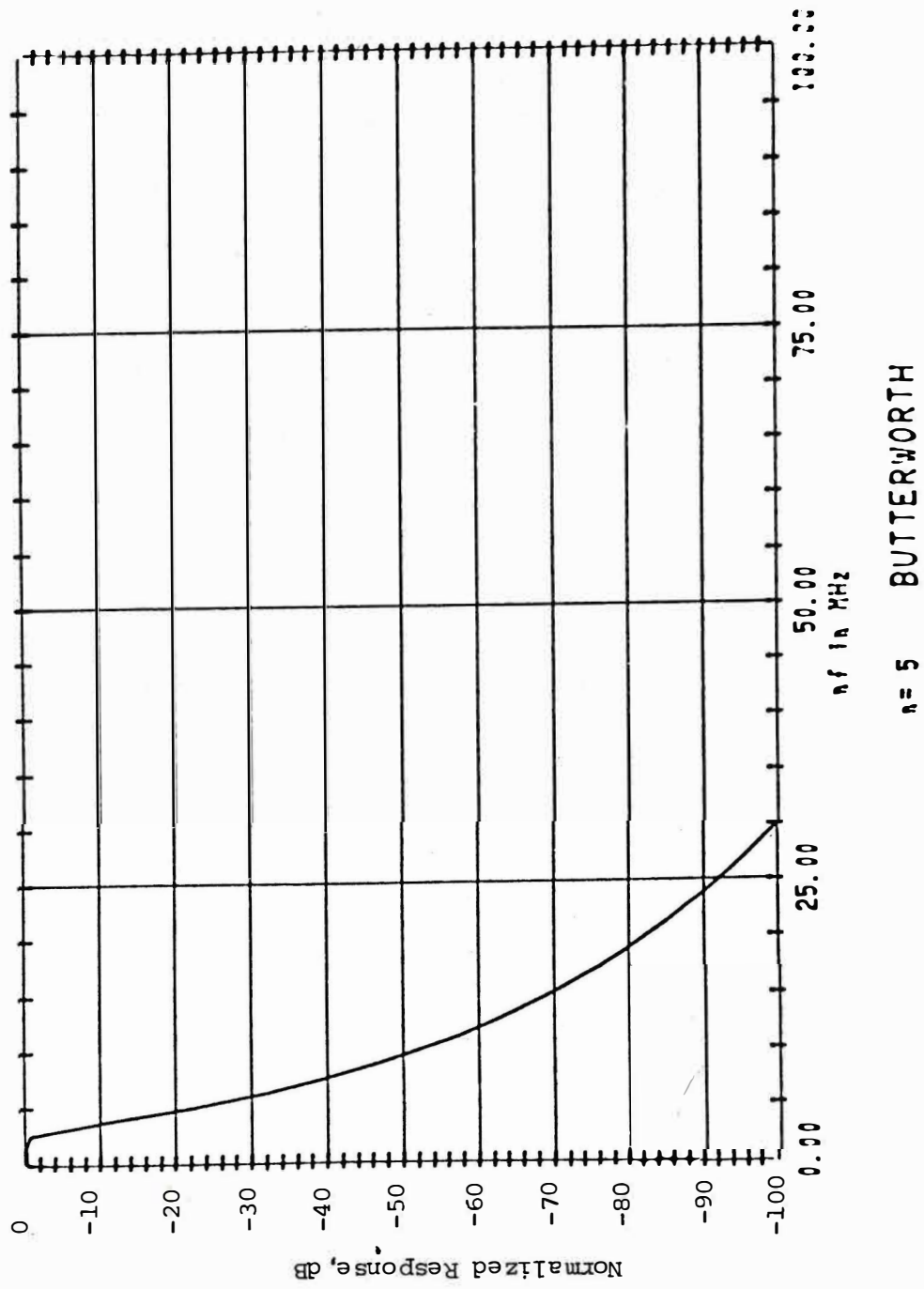


Figure B-20. Synthesized receiver selectivity curve for receiver TEST (21 PTS) for sample 3. This selectivity curve corresponds to a 5-pole Butterworth filter.

51 through 58 of figure B-17. The wide main-beam widths used are reasonable for aeronavigation antennas.

For propagation loss, this sample has used the ground-to-air model with all inputs conforming with the default values. Hence, no loss data sheet is included here.

The statistical F-D curves for this sample are shown in figure B-21. These curves are not as smooth as those of the previous samples because the number of data points were reduced to 21. The curves exhibit large variance at smaller values for Δf as shown by the large separation between the solid, dashed, and dotted curves. This is an influence of the propagation loss model. At about 10-12 MHz frequency separation, a slight "hump" occurs. This "humping" results from the receiver filter tending to trace out the shape of the emission spectrum, which occurs when the filter bandwidth is narrow with respect to the emission bandwidth.

STATISTICAL FREQUENCY-DISTANCE CURVES

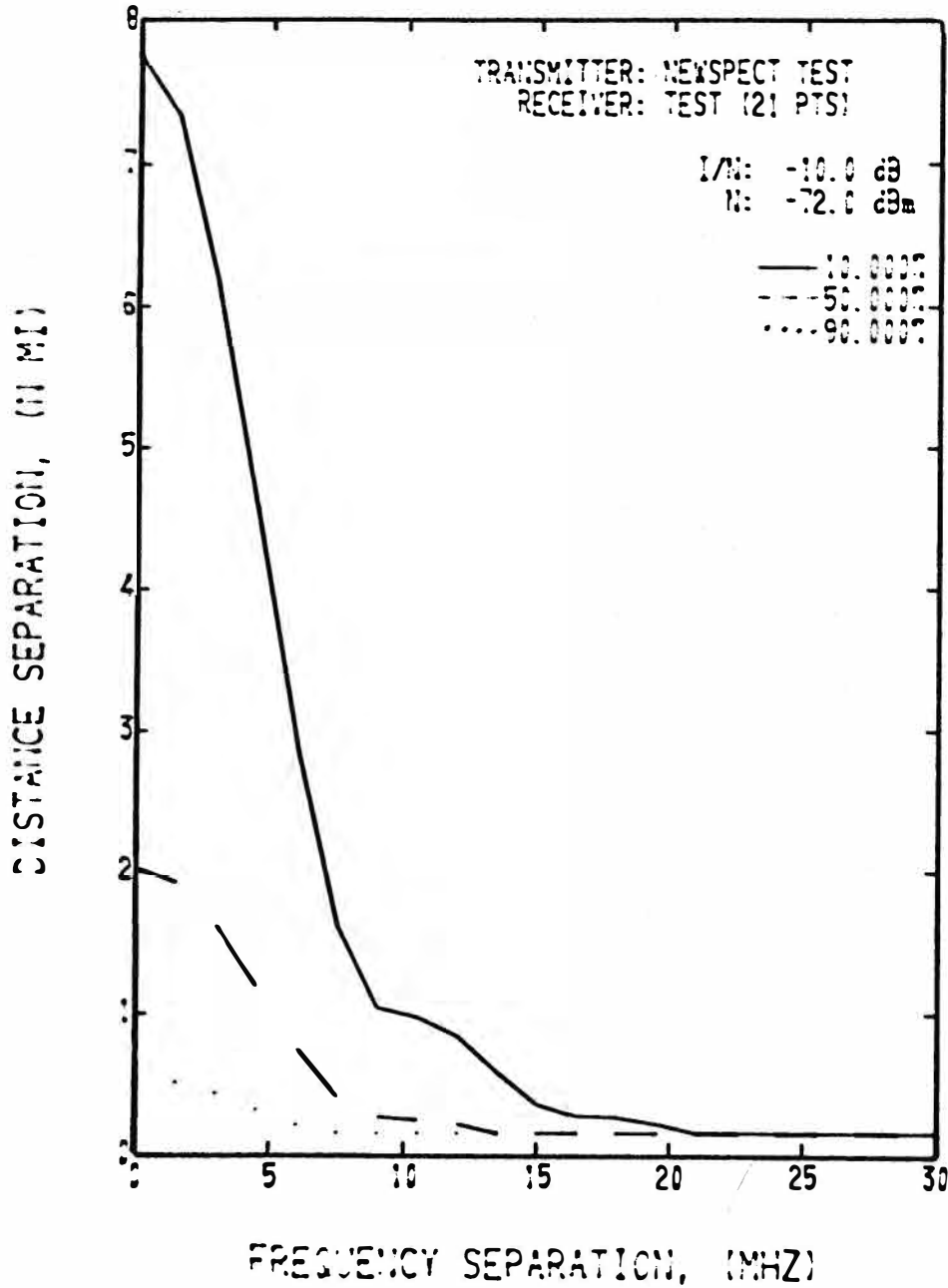


Figure B-21. Statistical frequency-distance curves for transmitter NEWSPECT TEST - receiver TEST (21 PTS) pair for Sample 3 using NEWSPEC subroutine and the ground-to-air propagation loss model (1 n mi = 1.85 km).

APPENDIX C. EMISSION SPECTRUM/RECEIVER SELECTIVITY MODELS

C.1 Subroutine INSPECT Theory and Application

The subroutine described in this appendix takes numerical descriptions of a transmitter emission spectrum and a receiver selectivity curve and then calculates their combined effects using numerical integration. The results are used with the user-supplied data for a maximum interference level to determine a loss value (interference protection) that is to be achieved by the distance separation between the systems.

In general, when the spectral power density from an interfering transmitter, $P(f)$, is multiplied with the power transfer function, $S(f)$, for a receiver, the power output from the receiver, p_r , is expressed as

$$p_r = \int_0 P(f)S(f)df, \quad (C.1-1)$$

assuming the interfering transmitter and victim receiver are tuned to the same frequency.

A measure of the extent to which the unwanted signal interferes at the receiver is obtained by specifying a maximum allowable power level, i , and defining a quantity called the interference protection, (ip) , as

$$(ip) = p_r/i = \frac{1}{i} \int_0 P(f)S(f)df. \quad (C.1-2)$$

Since specified performance levels are usually given in terms of required signal-to-noise ratios, the interference protection (in dB) may be written

$$\begin{aligned}
 &= 10 \log(p_r/N) - 10 \log(i/N) \\
 &= 10 \log \left[\int_0^{\infty} \frac{P(f) S(f)}{N} df \right] - (I/N)_{dB} \quad (C.1-3)
 \end{aligned}$$

where N is the noise power at the receiver output.

If the receiver is tuned at frequencies other than the carrier frequency of the transmitter, the power transfer function is dependent upon the frequency difference, Δf , as well as frequency, i.e., $S(f, \Delta f)$. The interference protection also becomes a function of Δf :

$$IP(\Delta f) = 10 \log \left[\int_0^{\infty} \frac{P(f) S(f, \Delta f)}{N} df \right] - (I/N)_{dB} \quad (C.1-4)$$

where Δf is a measure of the frequency offset between the interfering transmitter carrier frequency and the tuned frequency of the victim receiver.

In actual systems, of course, the interfering transmitter is not coupled directly to the receiver, and the spectral power density input is altered by the transmitting and receiving antennas plus the effects of the propagation path, i.e., the transmission loss associated with the system. The relationship between transmission loss, ℓ , and the interference protection as defined by (C.1-4) is derived as follows.

In general the undesired signal-to-noise ratio, (s_u/N) , at the output of the receiver can be expressed as

$$s_u/N = \int_0^{\infty} \left\{ \frac{P(f)}{\ell(f)} \right\} \left\{ \frac{S(f, \Delta f)}{N} \right\} df \sim \frac{1}{\ell} \int_{f_1}^{f_2} \frac{P(f) S(f, \Delta f)}{N} df, \quad (\text{C.1-5})$$

where $\{P(f)/\ell(f)\}$ represents the transmitter's spectral power density as reduced by the transmission loss over the link. We further assume that the loss is independent of frequency over the range of interest, f_1 to f_2 . Solving (C.1-5) for the loss and expressing the quantities in dB ($L \equiv 10 \log \ell$), we have

$$L \sim 10 \log \left[\int_0^{\infty} \frac{P(f) S(f, \Delta f)}{N} df \right] - 10 \log (s_u/N) \quad (\text{C.1-6})$$

It is apparent that for the particular value of the undesired signal-to-noise ratio, $(s_u/N) = (i/N)$, (C.1-6) provides an expression for the transmission loss in terms of the interference protection. In fact from (C.1-6) (with $s_u/N = i/N$) and (C.1-4), it follows that

$$L \sim 10 \log \left[\int_0^{\infty} \frac{P(f) S(f, \Delta f)}{N} df \right] - (I/N)_{\text{dB}} = IP(\Delta f). \quad (\text{C.1-7})$$

Going one step further we can find, by using a distance dependent transmission loss model, the distance separation required for a specified interference-to-noise ratio when the receiver is off-tuned from the interferer's carrier frequency by the frequency difference, Δf . Thus for loss

values, $L(d)$, equal to interference protection values, $IP(\Delta f)$, curves of distance versus Δf can be generated for given (I/N) .

In practical situations, it is usually the case that the receiver transfer function is given in terms of a normalized receiver response, $r(f)$, which is related to $S(f)$ by $S(f) = r_n r(f)$, where r_n is the value of S at the receiver tuned frequency, f_r . Although neither r_n nor N generally is known, it is possible to determine the input level (sensitivity), r_s , required to produce a given carrier power plus noise power to noise power level ratio, k . Thus, with N as the receiver noise power, we have

$$k = \frac{S(f_r) r_s + N}{N} = \frac{r_n r_s + N}{N}, \quad \frac{r_n}{N} = \frac{k-1}{r_s}. \quad (C.1-8)$$

The spectral power density may be given in either a normalized or non-normalized form and can be expressed as

$$P(f) = p_n p(f), \quad (C.1-9)$$

where $p(f)$ is the given form and p_n may or may not be known. Since the total transmitter power, p_T , is generally given, the factor p_n may be found from

$$p_n = \frac{\int_0^{\infty} P(f) df}{\int_0^{\infty} p(f) df} = p_T \frac{1}{\int_0^{\infty} p(f) df}. \quad (C.1-10)$$

With the use of (C.1-8) and (C.1-9), the expression for

interference protection as given by (C.1-4) becomes

$$IP(\Delta f) = 10 \log \left[\int_0^{\infty} p(f) r(f, \Delta f) df \right] + P_n + R_n - (I/N)_{dB}, \quad (C.1-11)$$

where

$$P_n = 10 \log \left[P_T / \int_0^{\infty} p(f) df \right], \quad R_n = 10 \log \left(\frac{k-1}{r_s} \right). \quad (C.1-12)$$

The integral in (C.1-11) must be evaluated numerically in the INSPECT program because the input functions, p and r , are entered in numerical form. The input arrays are

$$(\delta f_m, P_m), \quad m = 1, 2, \dots, M \quad \text{and} \quad (\delta f'_k, R_k), \quad k = 1, 2, \dots, K \quad (C.1-13)$$

where $P_m = 10 \log p_m$ is the decibel amplitude of the transmitter function, $R_k = 10 \log r_k$ is the decibel amplitude of the normalized receiver response, and $\delta f_m, \delta f'_k$ are the frequency differentials at which the P_m and R_k occur. New arrays then are formed corresponding to plots of P_m or R_k versus f_m or x_k , i.e., the arrays (f_m, P_m) and (x_k, R_k) , where $f_m = f_t + \delta f_m$, $x_k(\Delta f) = f_t + \delta f'_k + \Delta f$, and f_t is the transmitter carrier frequency.

It is assumed now that the transmitter and receiver functions are straight line segments with end points, P_m or

R_k , as plotted versus a $\log f$ or $\log x$ scale. Thus with $F = \log f$ and $X = \log x$, the functions (in dB) become

$$P(f) = P_m + \left(\frac{P_{m+1} - P_m}{F_{m+1} - F_m} \right) (F - F_m), \quad f_m \leq f \leq f_{m+1}, \quad (\text{C. 1-14a})$$

$$R(x) = R_k + \left(\frac{R_{k+1} - R_k}{X_{k+1} - X_k} \right) (X - X_k), \quad x_k \leq x = f \leq x_{k+1}. \quad (\text{C. 1-14b})$$

$$\text{or } p(f) = p_m \left(\frac{f}{f_m} \right)^{A_m}, \quad A_m = \frac{\log(p_{m+1}/p_m)}{\log(f_{m+1}/f_m)}, \quad f_m \leq f \leq f_{m+1}, \quad (\text{C. 1-15a})$$

$$r(x) = r_k \left(\frac{x}{x_k} \right)^{B_k}, \quad B_k = \frac{\log(r_{k+1}/r_k)}{\log(x_{k+1}/x_k)}, \quad x_k \leq x = f \leq x_{k+1}. \quad (\text{C. 1-15b})$$

Now the integral in (C.1-11) can be evaluated (remembering that x is a function of Δf) as

$$\begin{aligned} I(\Delta f) &= \int_0^{\infty} p(f) r(x) df = \sum_{i=1}^{I-1} \frac{p_m r_k}{f_m^{A_m} x_k^{B_k}} \int_{f_i}^{f_{i+1}} f^{A_m + B_k} df \\ &= \sum_{i=1}^{I-1} p_m r_k f_i \left(\frac{f_i}{f_m} \right)^{A_m} \left(\frac{f_i}{x_k} \right)^{B_k} \left\{ \frac{\left(\frac{f_{i+1}}{f_i} \right)^{A_m + B_k + 1} - 1}{A_m + B_k + 1} \right\}, \end{aligned}$$

$$A_m + B_k \neq -1, \quad (\text{C. 1-16a})$$

$$= \sum_{i=1}^{I-1} \left(\frac{P_m r_k}{f_m^{A_m} x_k^{B_k}} \right) \ln \left(f_{i+1}/f_i \right), \quad A_m + B_k = -1, \quad (\text{C. 1-16b})$$

where

$$A_m = \frac{\log(p_{m+1}/p_m)}{\log(f_{m+1}/f_m)}, \quad f_m \leq f_i < f_{m+1}, \quad (\text{C. 1-17a})$$

$$B_k = \frac{\log(r_{k+1}/r_k)}{\log(x_{k+1}/x_k)}, \quad x_k \leq f_i < x_{k+1}, \quad (\text{C. 1-17b})$$

and the f_i 's are formed by ordering f_m and x_k in increasing order, i.e.,

$$f_i = \text{ORD}(f_m, x_k), \quad f_1 = \text{Max}(f_1, x_1), \quad f_I = \text{Min}(f_M, x_K). \quad (\text{C. 1-18})$$

The integration in (C.1-10) is accomplished in the same manner as above, the final result being

$$P_n = P_T - 10 \log I_p, \quad I_p = \int_0^{\infty} p(f) df = \sum_{m=1}^{M-1} T(f_m), \quad (\text{C. 1-19})$$

$$T(f_m) = \begin{cases} p_m f_m \left[\frac{(f_{m+1}/f_m)^{A_m+1} - 1}{A_m + 1} \right], & A_m \neq -1, & (\text{C. 1-20a}) \\ \left(p_m / f_m^{A_m} \right) \ln \left(f_{m+1}/f_m \right), & A_m = -1, & (\text{C. 1-20b}) \end{cases}$$

where A_m is defined the same as in (C.1-17a) and P_T is the total transmitter power in dBm.

With the substitution of (C.1-16) into (C.1-11), the interference protection for a chosen Δf becomes

$$PI(\Delta f) = 10 \log I(\Delta f) + P_n + R_n - (I/N)_{dB}, \quad (C.1-21)$$

with P_n given by (C.1-19) and R_n given by (C.1-12).

An optional form of the input functions, p and r , in INSPECT is to give their slopes at the frequency differentials, δf_m and $\delta f'_k$. The program then takes the slope information to form arrays, (f_m, P_m) and (x_k, P_k) , equivalent to the input arrays entered in the preceding discussion and calculates $I(\Delta f)$ by the method already outlined.

C.2 Subroutine NEWSPEC Theory and Application

The following is a description of the pulsed emission and receiver selectivity synthesis subroutine that is used as part of the frequency-distance model. The purpose of NEWSPEC is to provide power density spectra from analytic descriptions of actual pulse shapes, and filter responses from analytic filter characterizations.

Many times, in pulse system analyses, the given input information is the half-amplitude pulse width (denoted here by τ), the pulse rise-time of the leading edge between the 10% and 90% amplitude values (τ_r), the fall-time between the 90% and 10% amplitude values (τ_f), and the average power associated with the pulse. The pulse shape then is approximated as a trapezoid and the analysis performed.

Because of the discontinuities or sharp edges of the trapezoidal form, the resulting power density spectrum can be misleading, especially at frequencies well away from the carrier frequency. In the present model, an expression has been derived for a "smooth" pulse shape (again using τ , τ_r , and τ_f as the input information) with the added condition that the integration giving the power density spectrum is expressible in closed form. The latter condition is introduced in order to avoid the frustrating and time-consuming problems connected with the numerical integration

of complex functions.

After a number of forms were studied--each having various advantages and disadvantages--the following was chosen for the general pulse shape:

$$F(t) = e^{i\omega_0 t} K \hat{F}(t) , \quad (C.2-1)$$

where $\omega_0 = 2\pi f_0$ is the angular carrier frequency, K is an amplitude factor, and $\hat{F}(t)$ is the (normalized) shape function,

$$\hat{F}(t) = \begin{cases} e^{\beta_1^2 (t-t_0)^2} e^{-\beta_1^2 (t-t_0)^2} , & t_0 \leq t \leq t_1 \\ 1 & , t_1 \leq t \leq t_2 \\ e^{-\beta_2^2 (t-t_2)^2} & , t \geq t_2 \end{cases} \quad (C.2-2)$$

with

$$\beta_1 = 0.584460/\tau_r , \beta_2 = 1.192834/\tau_f ,$$

$$t_1 = 1.170982\tau_r + t_0 , \quad (C.2-3)$$

$$t_2 = \tau + 0.824049\tau_r - 0.697963\tau_f + t_0 .$$

The time-shift term, t_0 , is introduced merely to allow a possible shift in time from whatever origin is chosen; normally it is set equal to zero.

The shape function, $\hat{F}(t)$, rises from zero at $t=t_0$ to a value of unity at $t=t_1$; it has constant amplitude until $t = t_2$, at which point it falls again to zero for large t . Note that a restriction on the shape is that t_2 must be greater than or equal to t_1 , or in terms of the pulse width and rise and fall times:

$$\tau \geq 0.886933\tau_r + 0.697963\tau_f \quad . \quad (C.2-4)$$

Examples of (C.2-2) for various values of the τ 's are shown in figures C.2-1 to C.2-6 for the following radar altimeters: AN/APN-133 (two modes), AN/APN-159 (two modes), In-Flight Devices GAR, and Bonzer TRN-70.

The frequency spectrum of the pulse now is given by the Fourier transform of (C.2-1):

$$G(w) = K \int_{-\infty}^{+\infty} \hat{F}(t)e^{-iwt} dt = K G_1(w) + G_2(w) + G_3(w) \quad , \quad (C.2-5)$$

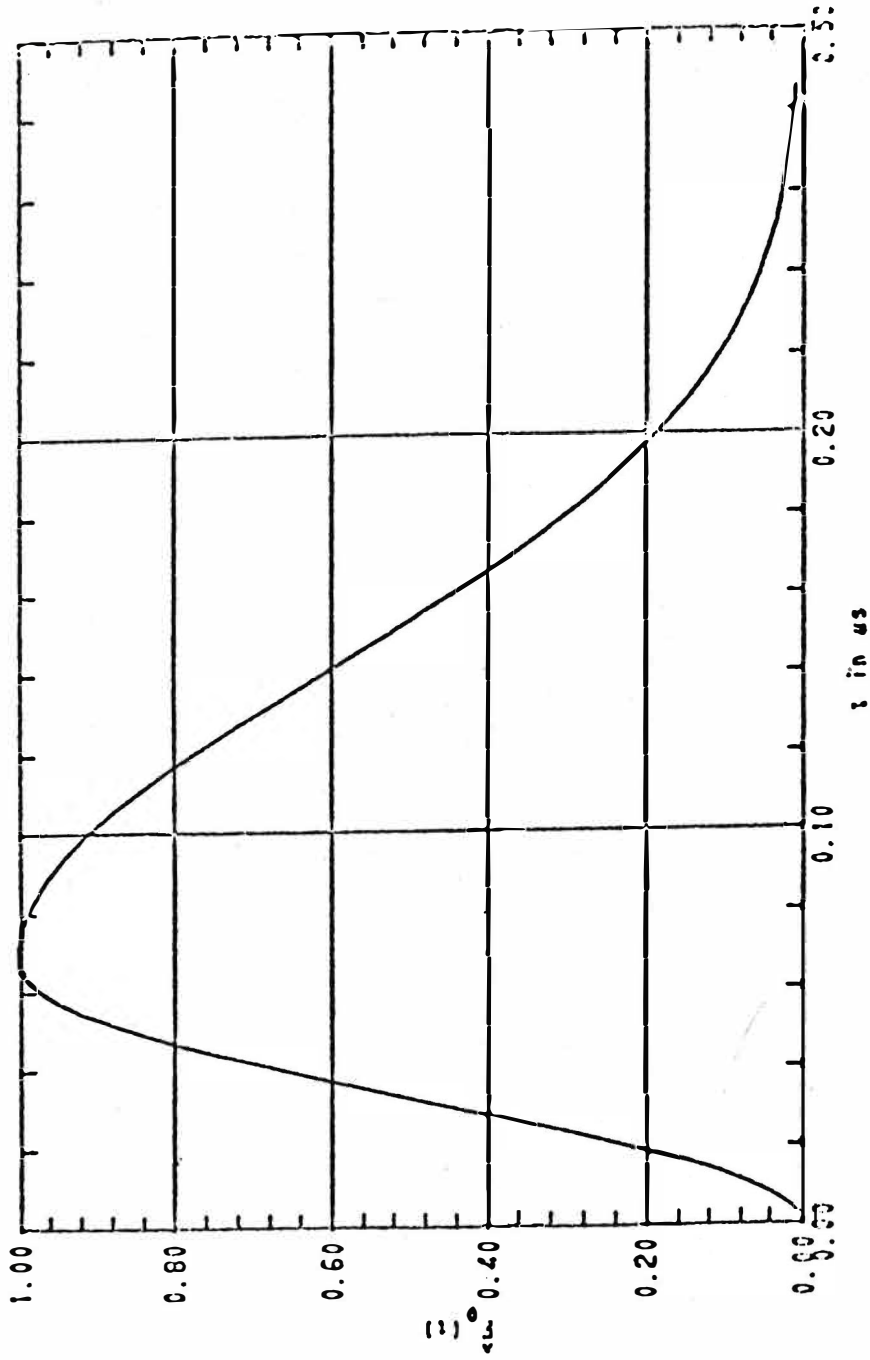
where

$$w \equiv \omega - \omega_0 = 2\pi(f - f_0) = 2\pi\Delta f,$$

$$G_1(w) = e^{-iwt_0} \left(\frac{eT_1}{2} \right) \left[\left(\frac{z_0-1}{e} \right) e^{-2z_0} - z_0 + \sqrt{\pi} \left(z_0^2 + \frac{1}{2} \right) e^{z_0^2} \{ \operatorname{erfc}(z_0) - \operatorname{erfc}(z_1) \} \right] \quad , \quad (C.2-6)$$

$$G_2(w) = \frac{e^{-iwt_1} - e^{-iwt_2}}{iw}, \quad G_3(w) = e^{-iwt_2} \left(\frac{\sqrt{\pi}T_2}{2} \right) e^{z_2^2} \operatorname{erfc}(z_2),$$

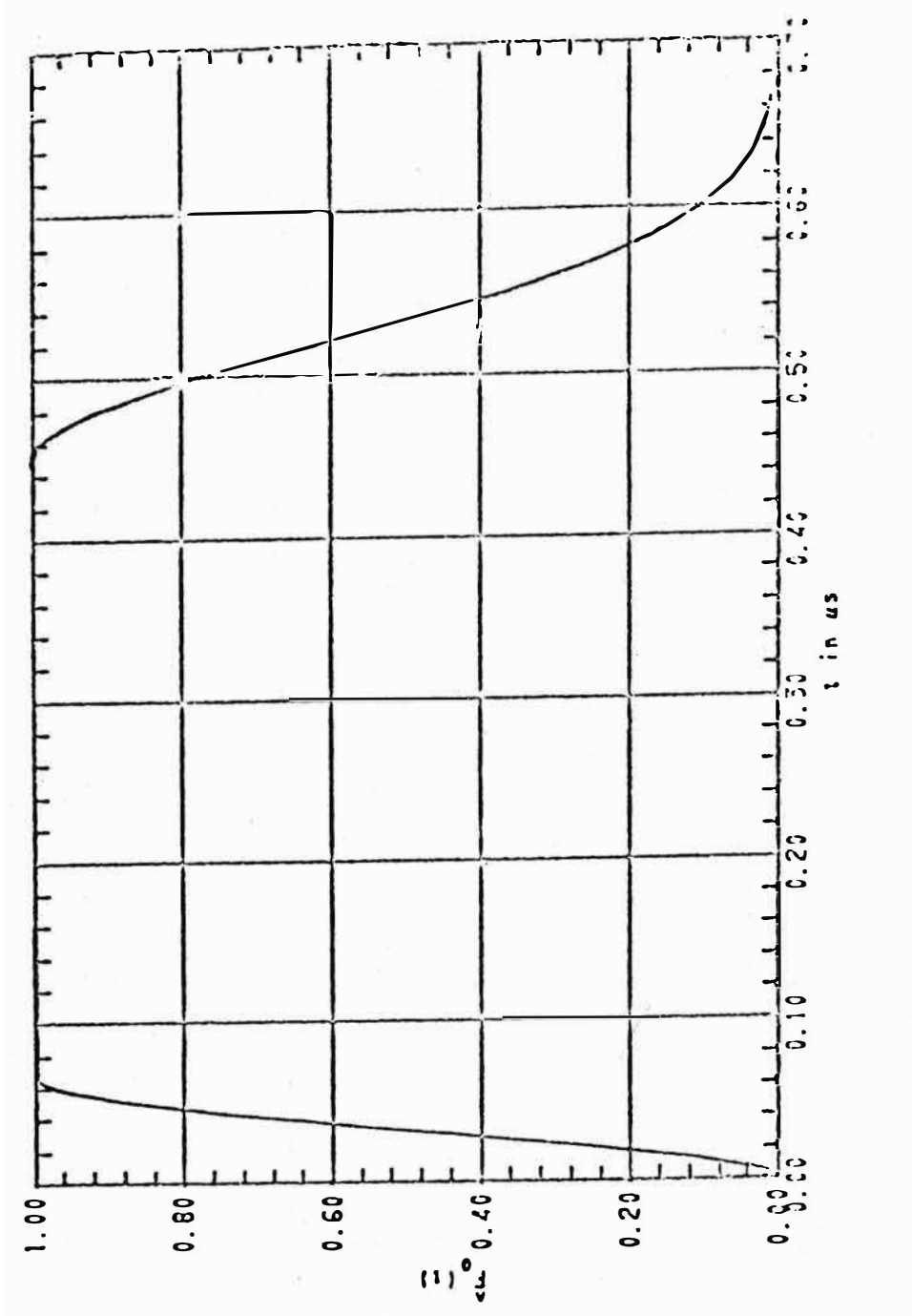
SHAPE FACTOR



TAU = 0.120 TAU_p = 0.040 TAU_r = 0.120 τ₀ = 0.000

Figure C.2-1. Synthesized pulse shape for the AN/APN-133 radar altimeter operating in the low altitude mode.

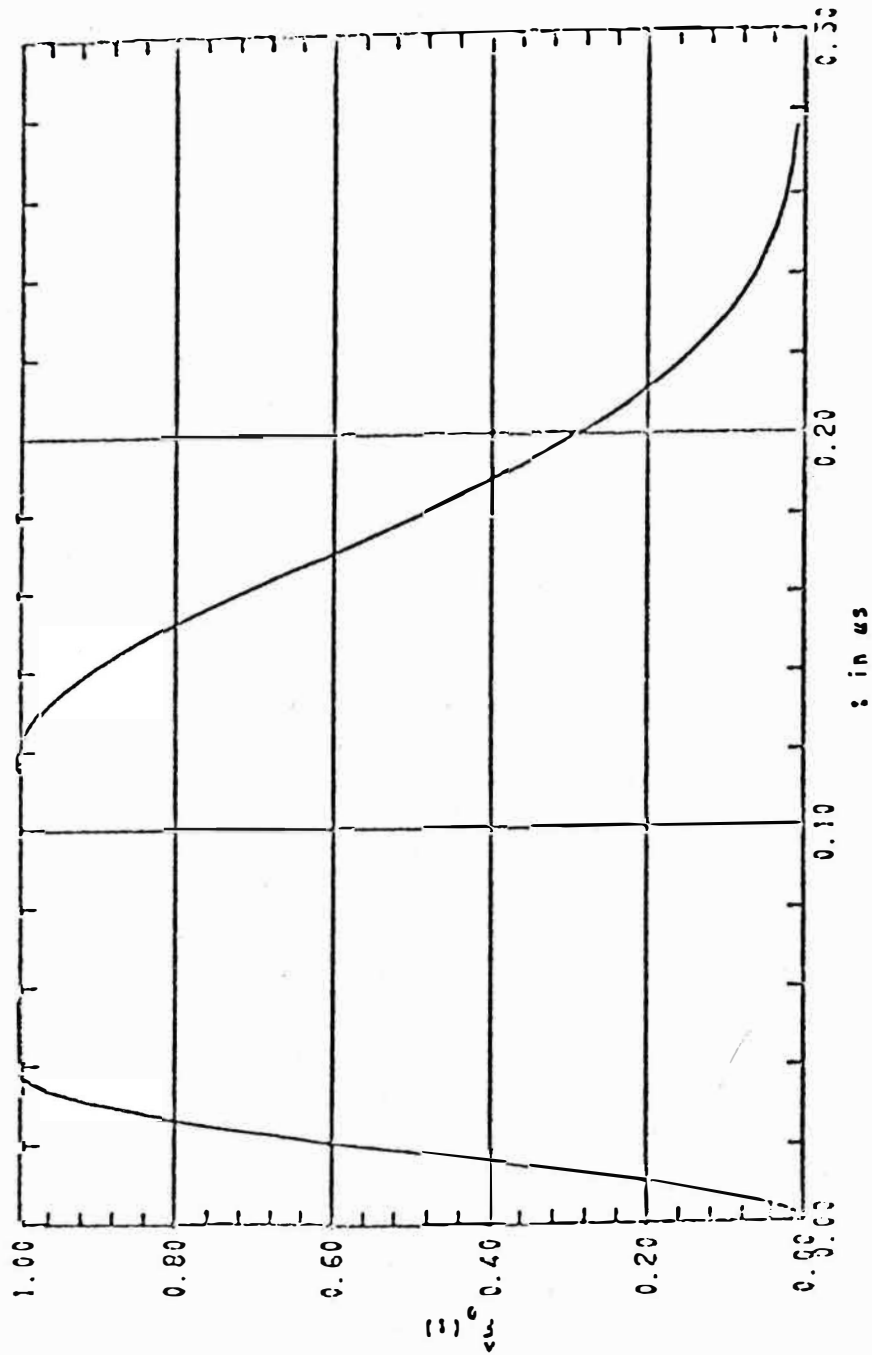
SHAPE FACTOR



TAU = 0.500 TAU_r = 0.040 TAU_f = 0.120 t_c = 0.000

Figure C.2-2. Synthesized pulse shape for the AN/APN-133 radar altimeter operating in the high altitude mode.

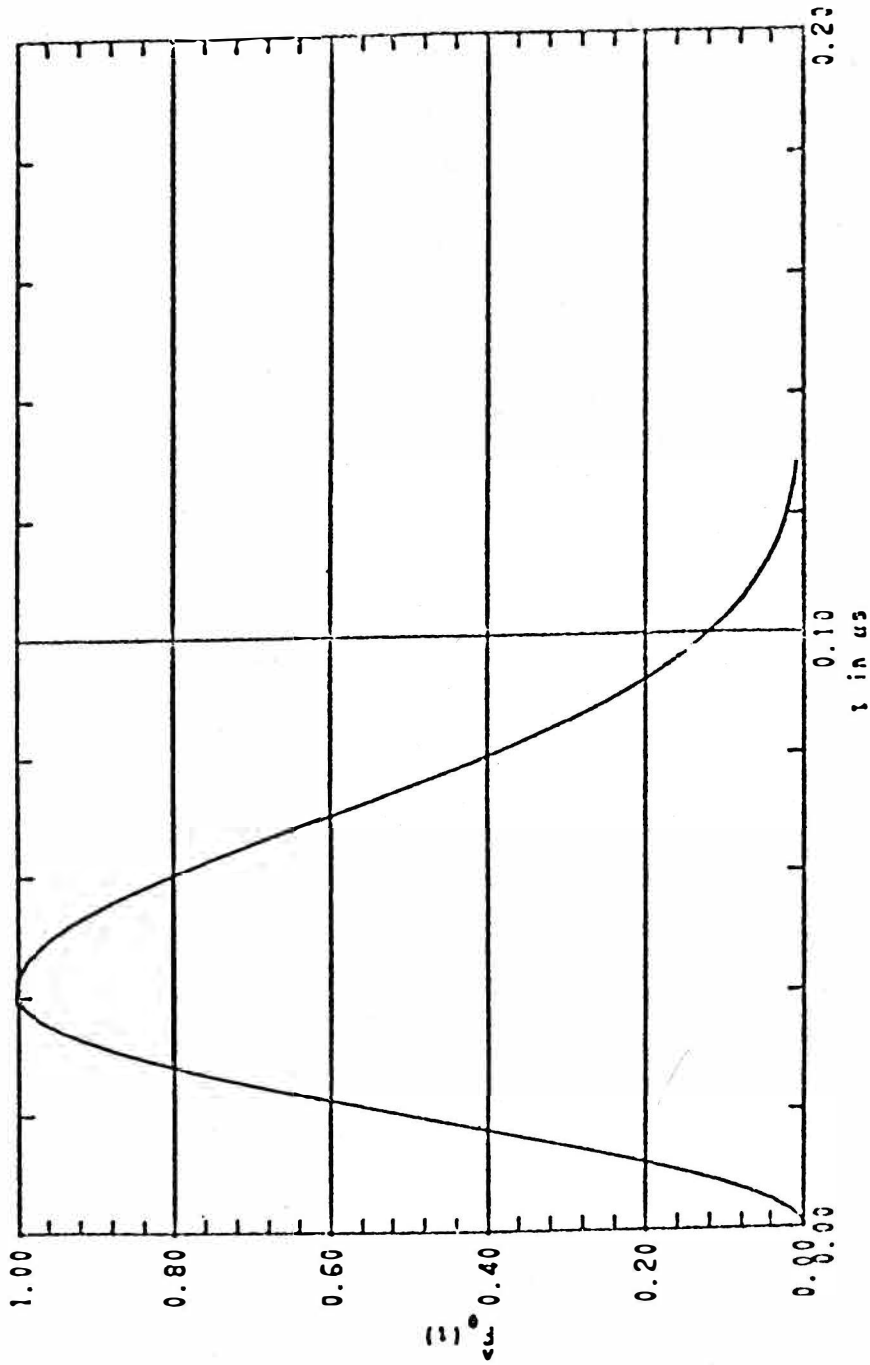
SHAPE FACTOR



$\tau = 0.160$ $\tau_r = 0.023$ $\tau_f = 0.038$ $t_0 = 0.000$

Figure C.2-3. Synthesized pulse shape for the AN/APN-159 radar altimeter operating in the high altitude mode.

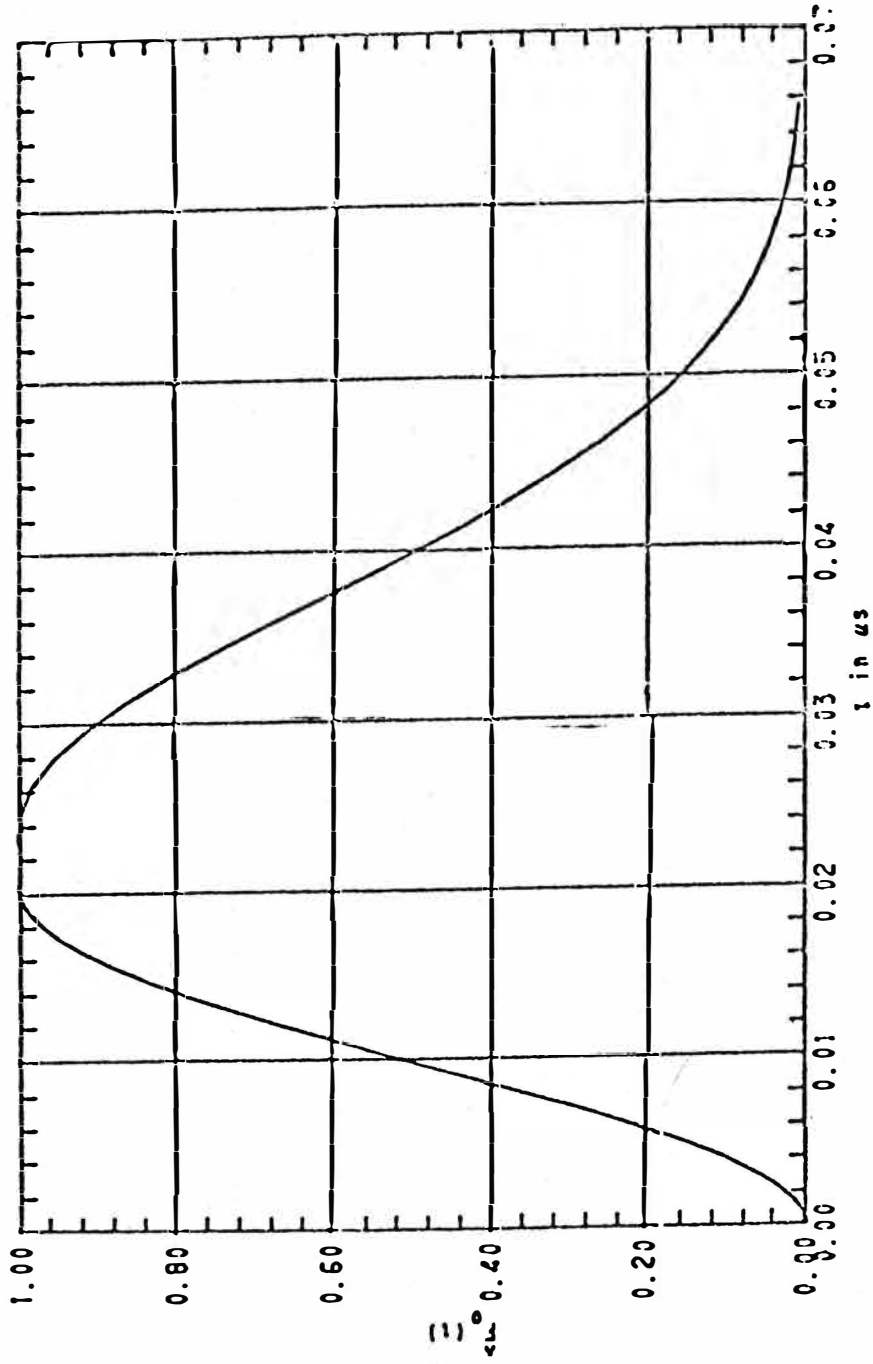
SHAPE FACTOR



TAU = 0.055 TAU_r = 0.024 TAU_f = 0.048 τ₀ = 0.000

Figure C.2-4. Synthesized pulse shape for the AN/APN-159 radar altimeter operating in the low altitude mode.

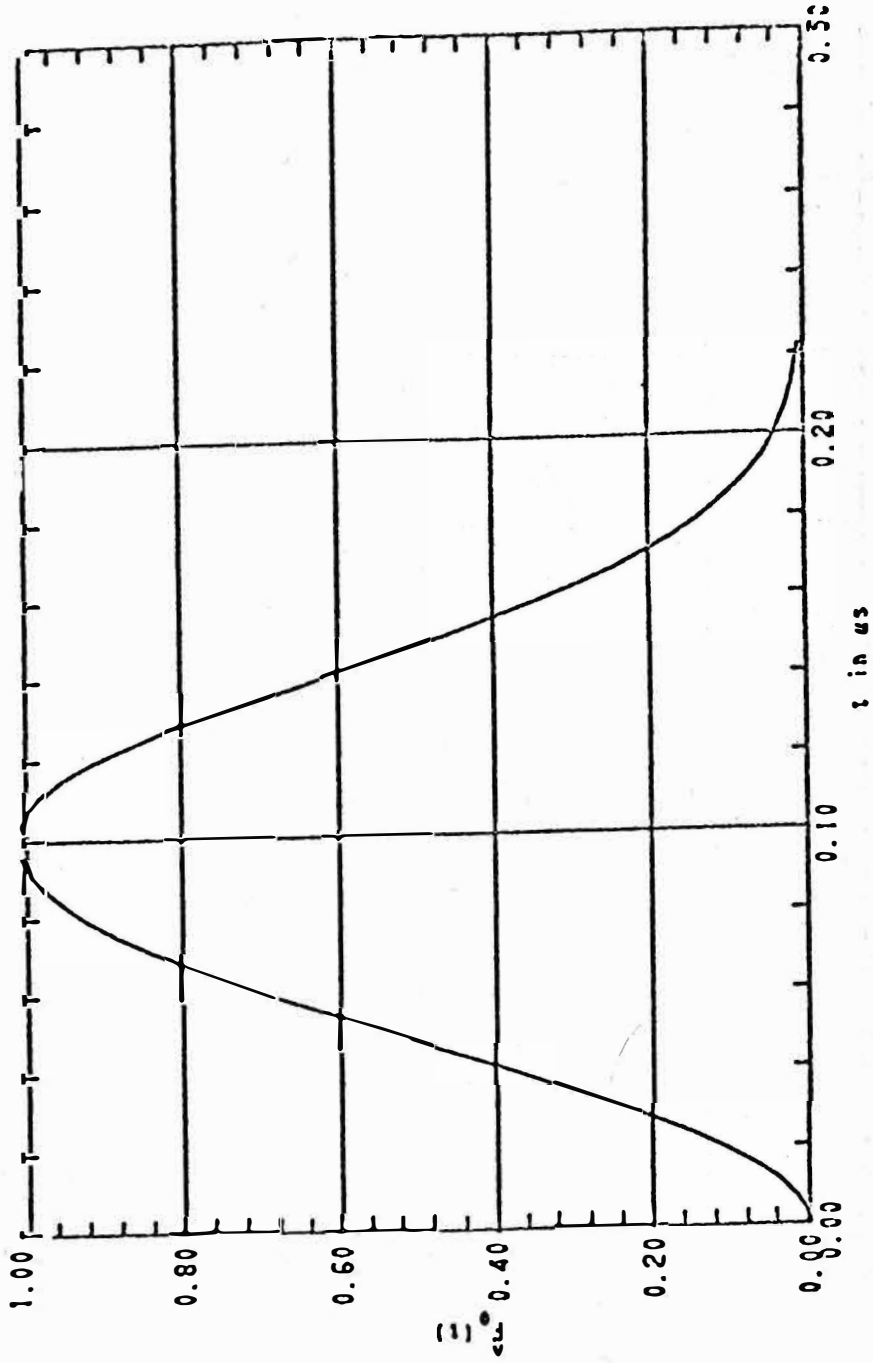
SHAPE FACTOR



TAU = 0.030 TAU_r = 0.012 TAU_f = 0.023 t₀ = 0.000

Figure C.2-5. Synthesized pulse shape for the In-Flight Devices ground avoidance radar.

SHAPE FACTOR



TAU = 0.100 TAU_r = 0.058 TAU_f = 0.064 t₀ = 0.000

Figure C.2-6. Synthesized pulse shape for the Bonzer TRN-70 radar altimeter.

and

$$T_1 = 1.710982\tau_r, \quad T_2 = 0.838339\tau_f,$$

$$z_0 = iwT_1/2, \quad z_1 = 1+z_0, \quad z_2 = iwT_2/2;$$

$\operatorname{erfc}(z)$ denotes the complementary error function (Abramowitz and Stegun, 1964).

The limiting forms of (C.2-5) for small ($w \ll 0.1$) and large ($w \gg 10$) values of w are

$$G(0) = K(\tau_r - 0.005711\tau_r + 0.044996\tau_f), \quad (\text{C.2-7a})$$

$$G(w) \sim ie^{-iwt_0} \left\{ \frac{2KT_1}{(wT_1)^3} \right\} \left[e+2e^{-iwT_1} - \left(\frac{T_1}{T_2} \right)^2 e^{-iw(t_2-t_0)} \right]. \quad (\text{C.2-7b})$$

Note that $G(w)$ falls off as w^{-3} for large w ; the corresponding decrease for a trapezoidal pulse is w^{-2} .

In order to obtain the average power density spectrum, $P(w)$, in terms of the total average power, P_{avg} , the factor K in (C.2-5) must be determined. Since the total energy, E is given by

$$E = \int_{-\infty}^{+\infty} |G(w)|^2 df = \int_{-\infty}^{+\infty} |F(t)|^2 dt = K^2 \hat{E}, \quad (\text{C.2-8})$$

we have the relationship

$$K^2 \hat{E} = T_p P_{\text{avg}}, \quad (\text{C.2-9})$$

where T_p is the reciprocal of the pulse repetition frequency

and

$$\hat{E} = \int_{-\infty}^{+\infty} \hat{F}^2(t) dt = \tau - 0.217601\tau_r - 0.172612\tau_f. \quad (C.2-10)$$

Denoting the quantity in the square brackets of (C.2-5) by

$G_o(w)$, the power density spectrum is then

$$P(w) = \frac{K^2 |G_2(w)|^2}{T_p} = \frac{P_{avg} |G_2(w)|^2}{\hat{E}}, \quad w = 2\pi\Delta f. \quad (C.2-11)$$

In units of dBm/Hz, (C.2-11) may now be written as

$$P(\Delta f) = P_{avg} \text{ dBm} - 10 \log \hat{E} + 10 \log |G_o(w)|^2 - 60, \quad \text{dBm/Hz} \quad (C.2-12)$$

where frequencies are in MHz and time is in microseconds.

Power density spectra, using (C.2-12), for the pulses of figures C.2-1 to C.2-6 are shown in figures C.2-7 to C.2-12.

The filters chosen for inclusion in this model are the Chebyshev, Butterworth, and elliptic function filters (Weinberg, 1962). The Chebyshev filter is defined as

$$|Z|^2 = \frac{1}{1 + \epsilon^2 T_n^2(x)}, \quad T_n(x) = \begin{cases} \cos(ncos^{-1}x), & 0 \leq |x| \leq 1 \\ \cosh(ncosh^{-1}x), & |x| \geq 1 \end{cases} \quad (C.2-13)$$

where ϵ is a parameter determining the depth of the ripples in the band, and x depends on the bandwidth under consideration. As the value of n increases, the wings of

POWER DENSITY SPECTRUM

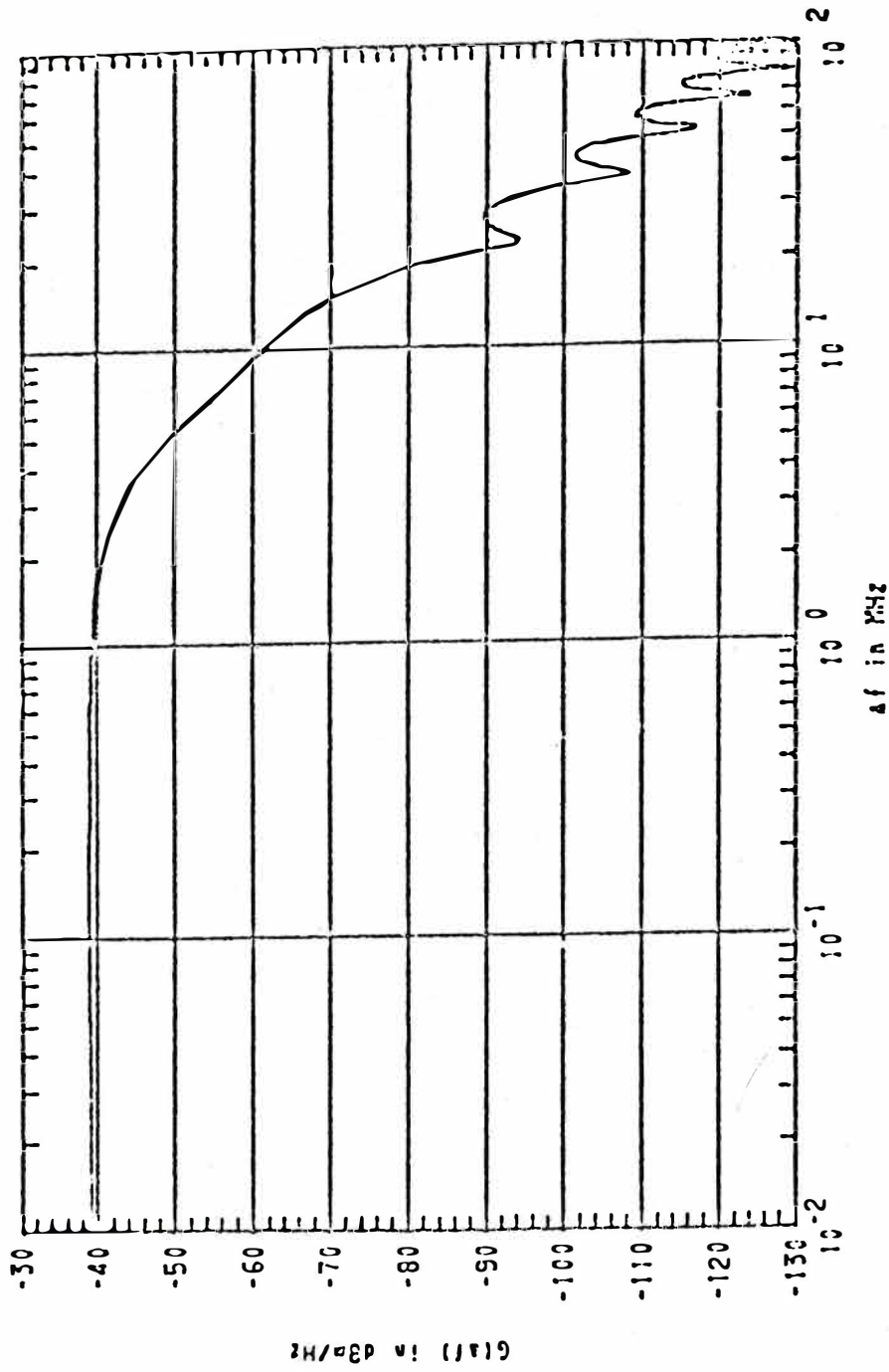
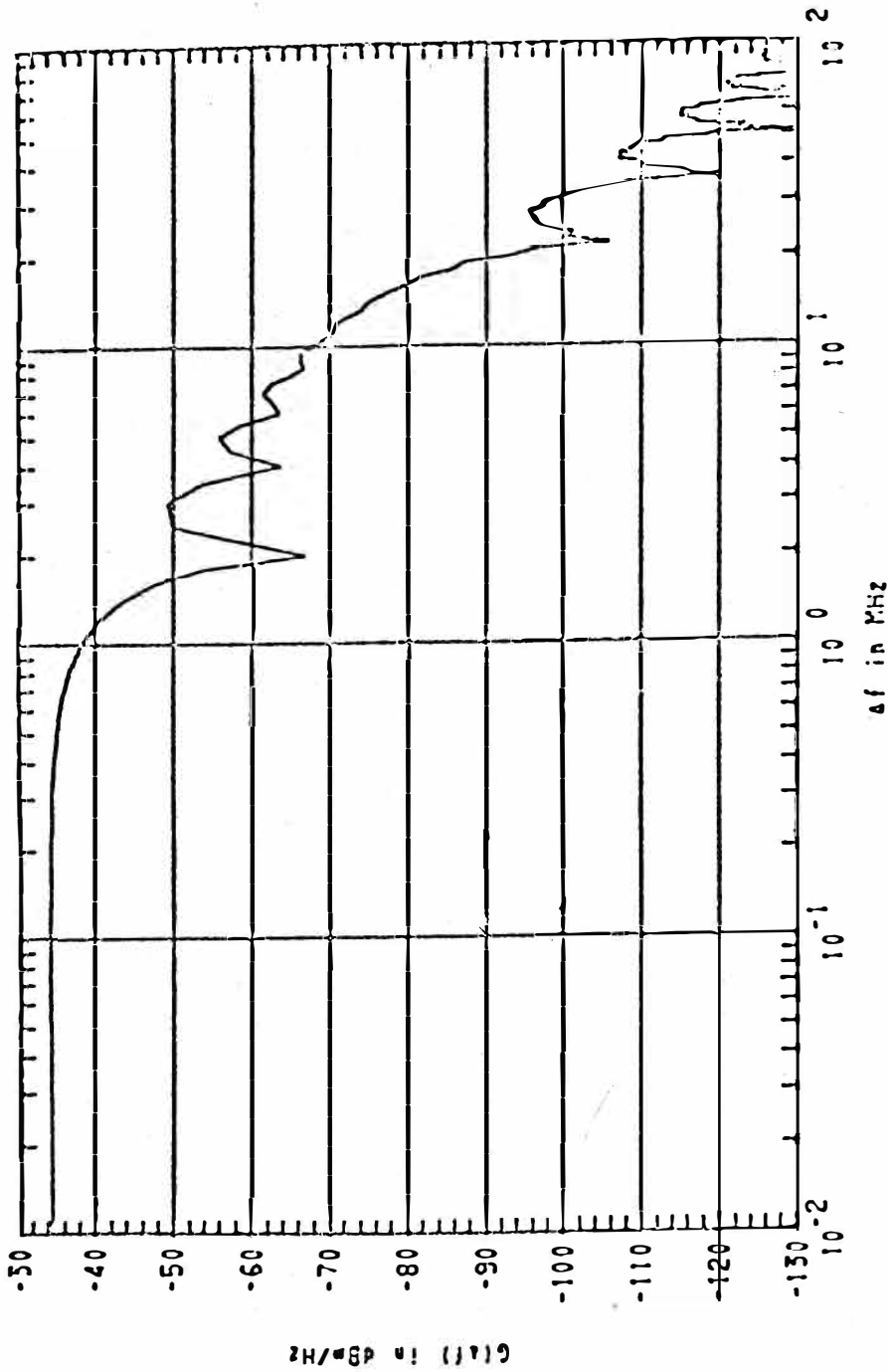


Figure C.2-7. Synthesized power density spectrum for the AN/APN-133 radar altimeter operating in the low altitude mode.

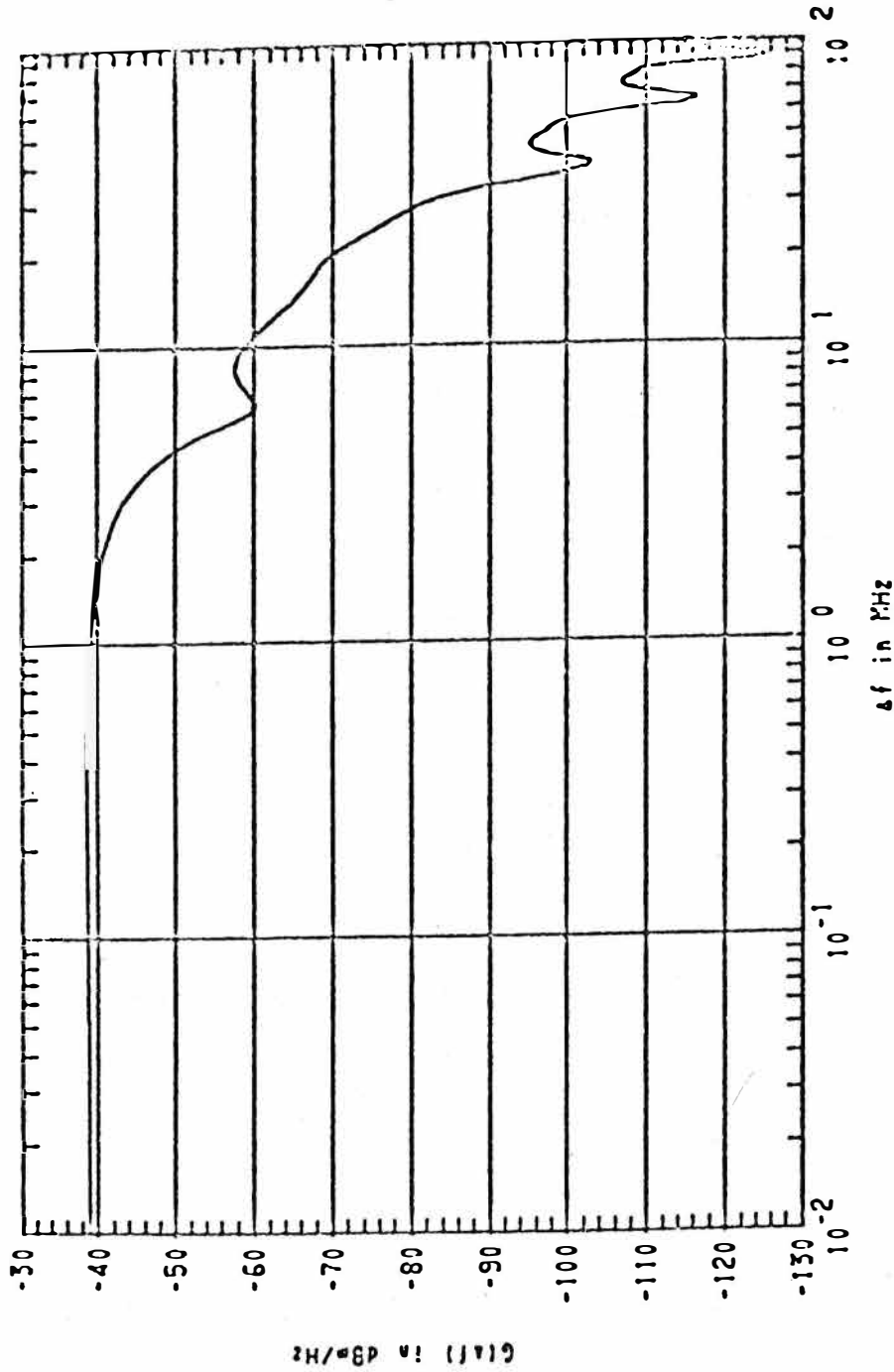
POWER DENSITY SPECTRUM



TAU = 0.500 TAU_r = 0.040 TAU_f = 0.120 τ_φ = 0.000 P_{avg} = 20.700

Figure C.2-8. Synthesized power density spectrum for the AN/APN-133 radar altimeter operating in the high altitude mode.

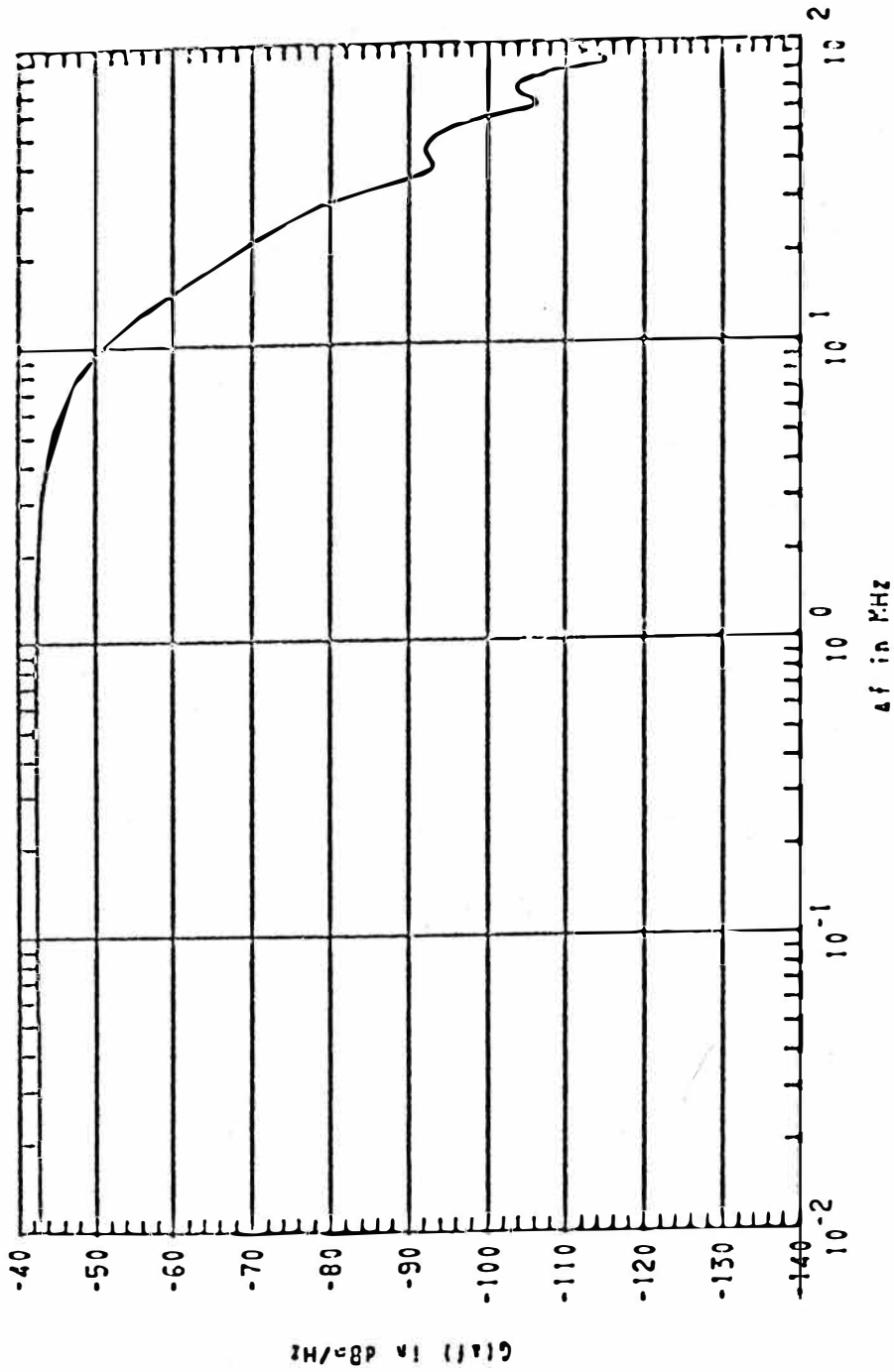
POWER DENSITY SPECTRUM



TAU = 0.160 TAU_r = 0.023 TAU_f = 0.088 τ₀ = 0.000 P_{avg} = 29.700

Figure C.2-9. Synthesized power density spectrum for the AN/APN-159 radar altimeter operating in the high altitude mode.

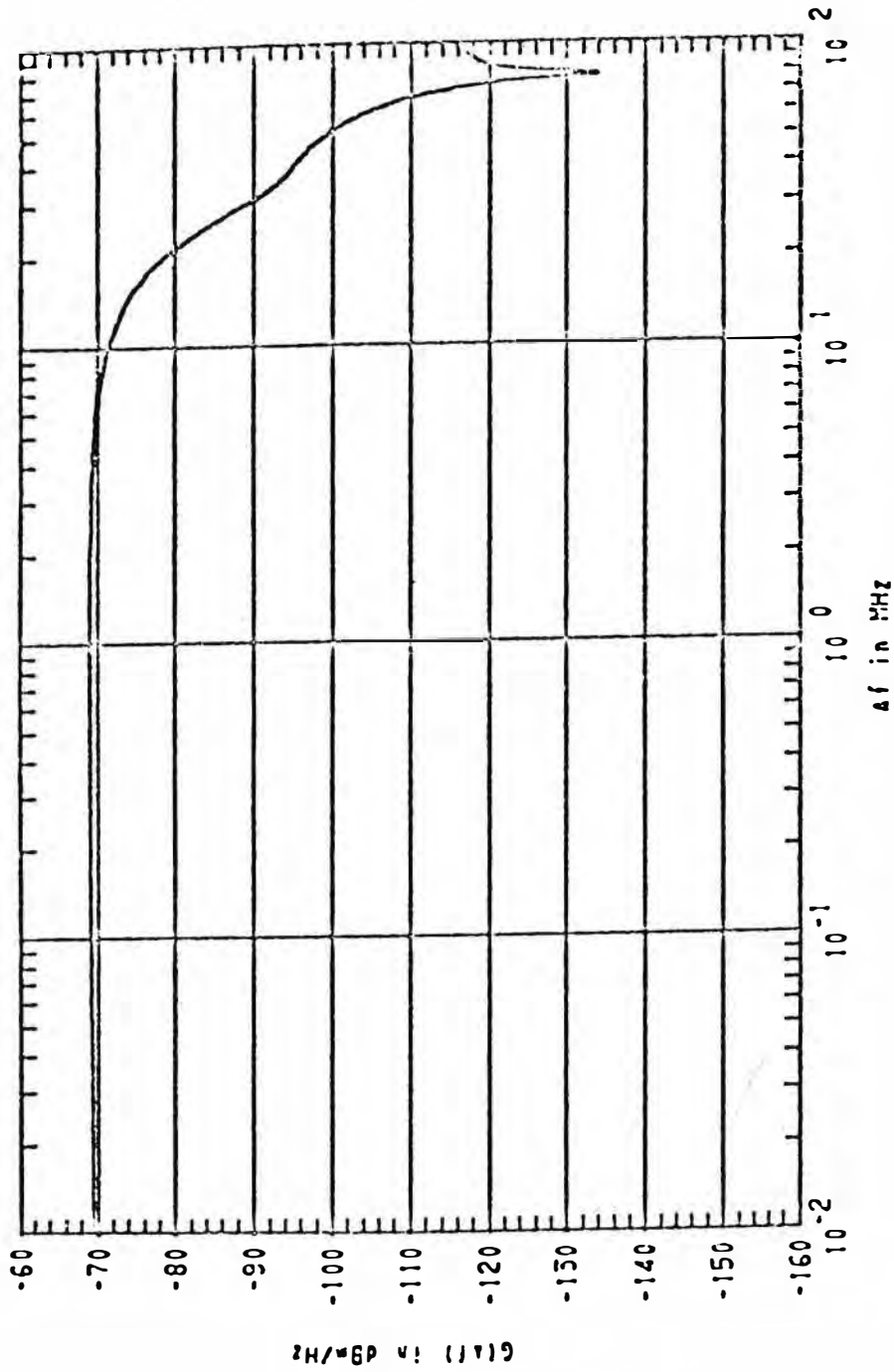
POWER DENSITY SPECTRUM



TAU = 0.055 TAU_r = 0.024 TAU_f = 0.048 τ₀ = 0.000 P_{avg} = 28.700

Figure C.2-10. Synthesized power density spectrum for the AN/APN-159 radar altimeter operating in the low altitude mode.

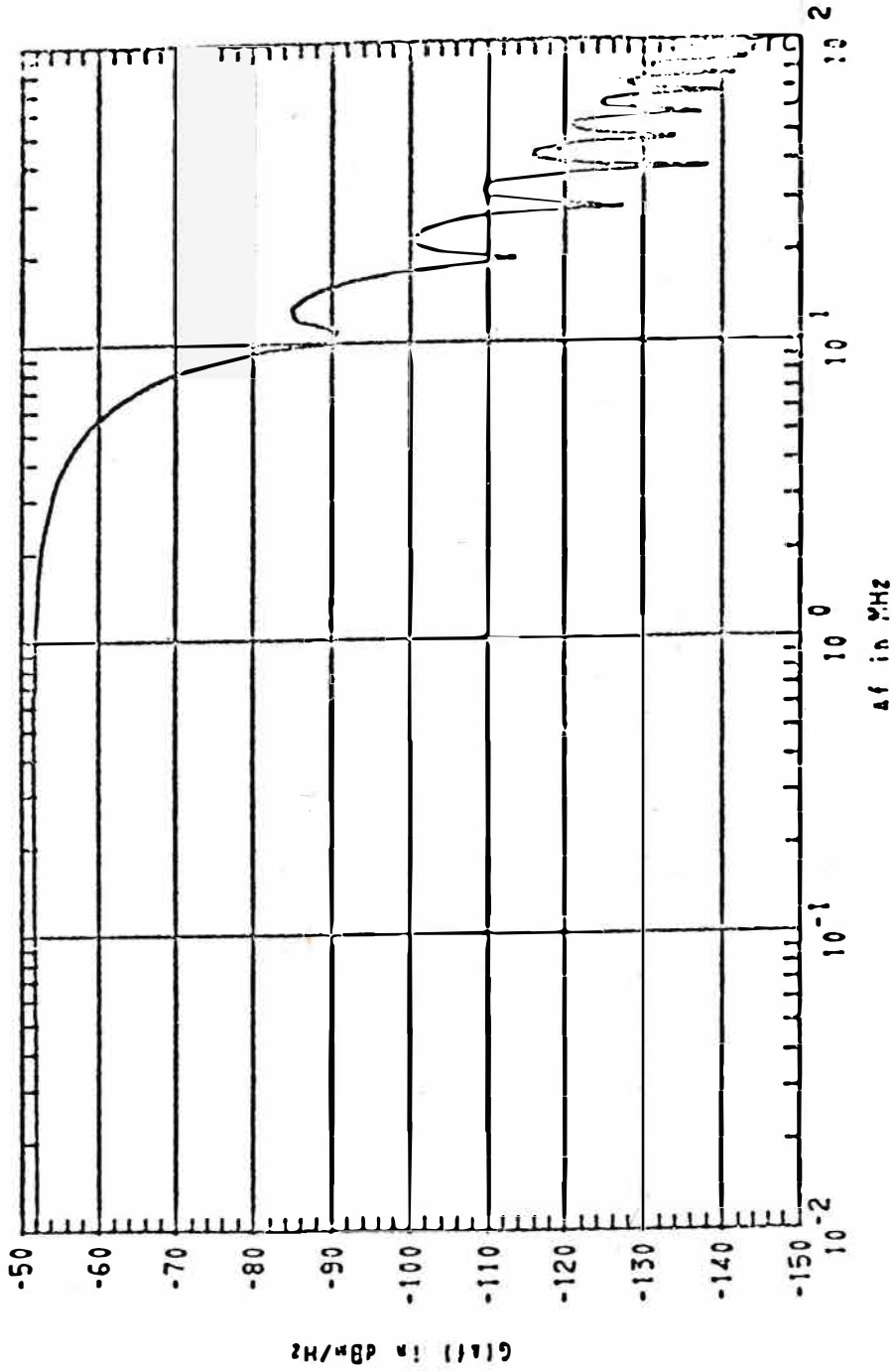
POWER DENSITY SPECTRUM



TAU = 0.030 TAU_r = 0.012 TAU_f = 0.023 t₀ = 0.000 P_{avg} = 4.9:0

Figure C.2-11. Synthesized power density spectrum for the In-Flight Devices ground avoidance radar.

POWER DENSITY SPECTRUM



TAU = 0.100 TAU_r = 0.058 TAU_f = 0.064 τ_0 = 0.000 P_{avg} = 17.000

Figure C. 2-12. Synthesized power density spectrum for the Bonzer TRN-70 radar altimeter.

the response fall off more sharply. Examples of (C.2-13) for $n=3$ and 5 are shown in figures C.2-13 and C.2-14.

The Butterworth filter is defined as

$$|Z|^2 = \frac{1}{1 + x^{2n}} \quad , \quad (C.2-14)$$

where, again, n determines the slope of the wings.

The elliptic function filter can provide a "sharper" filter by allowing one to choose the frequency at which the stop-band is to begin. Given the following input parameters:

A_o = maximum $|Z|^2$ in the pass-band

A_p = minimum (allowable) $|Z|^2$ in the pass-band

A_s = maximum (allowable) $|Z|^2$ in the stop-band

f_1 = center frequency of the pass-band

f_2 = end frequency of the pass-band

f_3 = beginning frequency of the stop-band ($f_3 > f_2 > f_1$)

Z = magnitude of the normalized transfer impedance,

the mathematical expression for the elliptic function filter is

$$|Z|^2 = \frac{A_o}{1 + \epsilon^2 R_n^2(x)} \quad , \quad \epsilon^2 = (A_o/A_p) - 1. \quad (C.2-15)$$

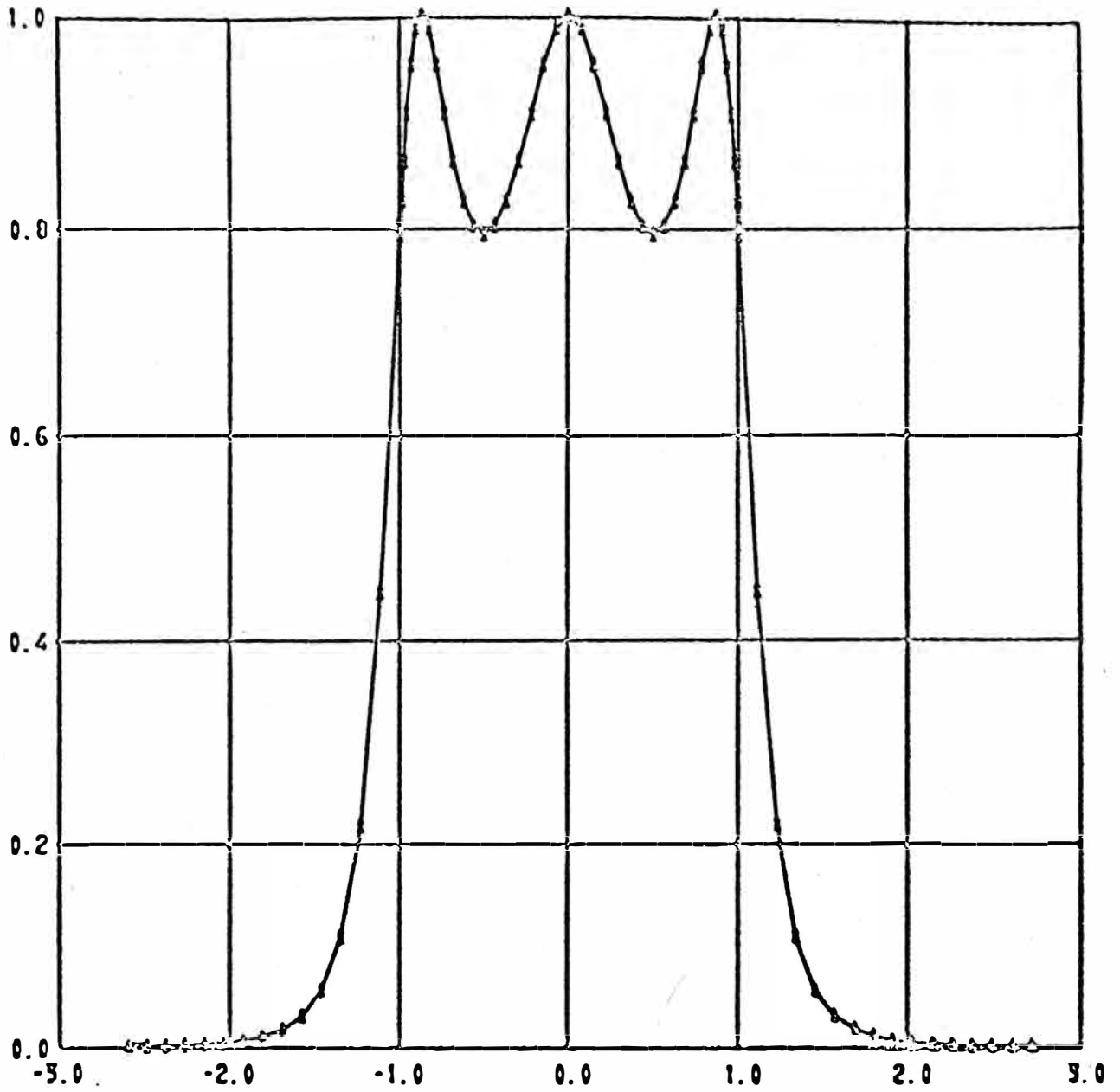


Figure C.2-13. Chebyshev filter with 1 dB ripple in the passband ($\epsilon^2=0.259$) and $N=3$ controlling the slope of the wings.

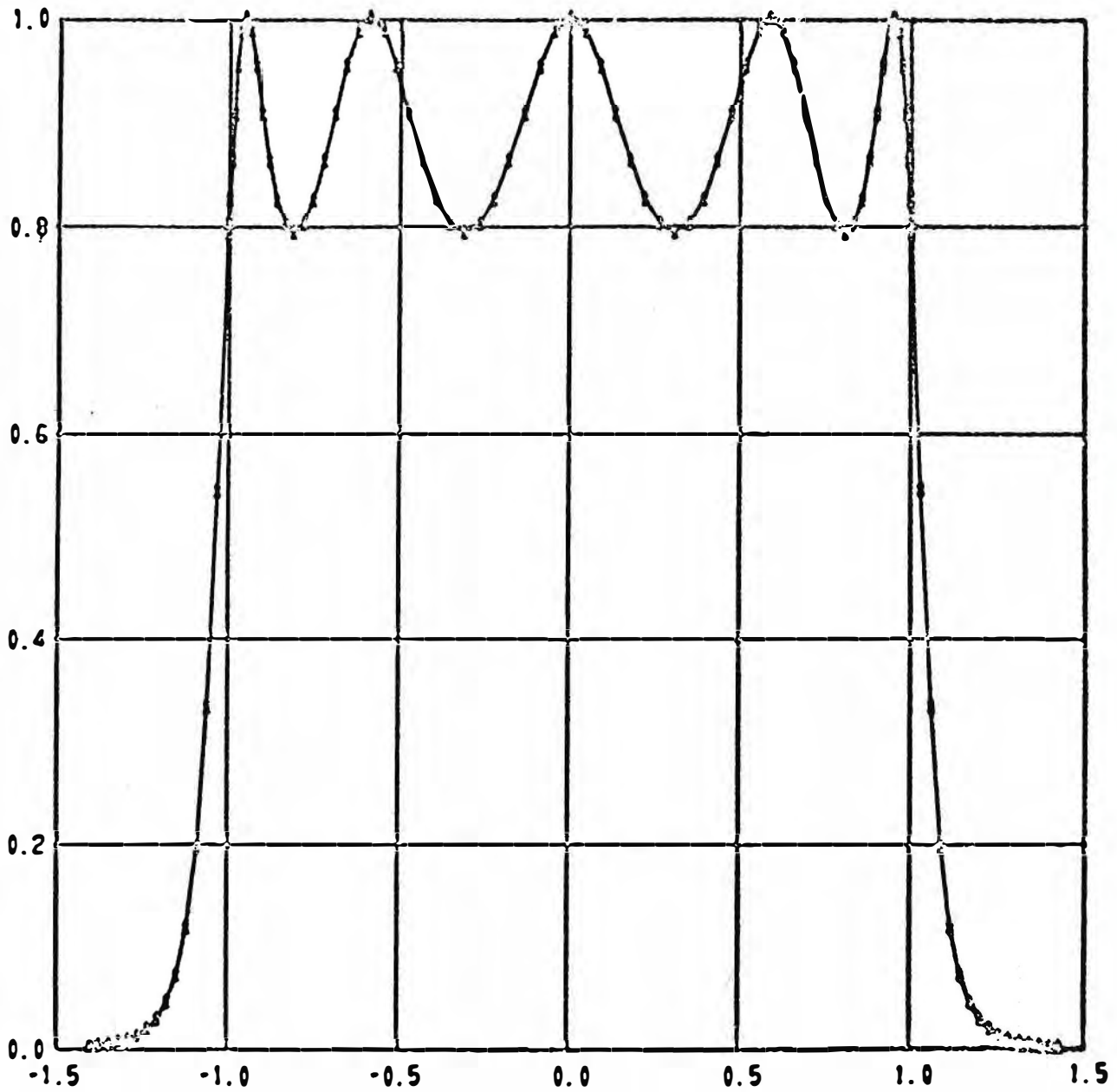


Figure C.2-14. Chebyshev filter with 1 dB ripple in the passband ($\epsilon^2=0.259$) and $N=5$ controlling the slope of the wings.

The definition of $R_n(x)$ in (C.2-15) depends on whether the integer n is even or odd, where

$$n \equiv [\nu] \text{ (the symbol } [\nu] \text{ denotes the smallest integer } \geq \nu \text{)} \quad (\text{C.2-16a})$$

and

$$\nu = \frac{K(k)}{K'(k)} \cdot \frac{K_1'(k_1)}{K_1(k_1)}, \quad k = \frac{f_2 - f_1}{f_3 - f_1}, \quad k_1 = \sqrt{\frac{(A_o/A_p)-1}{(A_o/A_s)-1}}; \quad (\text{C.2-16b})$$

$K(k)$ and $K_1(k_1)$ in (C.2-16b) are the complete elliptic integrals of moduli k and k_1 , respectively. A prime refers to the complete elliptic integral of comodulus of the argument, e.g., $K'(k) = K(\sqrt{1-k^2})$.

For n even ($n=2m$), $R_n(x)$ is given by

$$R_n^2(x) = N^2 \left[\frac{(x^2 - x_1^2) \dots (x^2 - x_m^2)}{(1 - k^2 x_1^2 x^2) \dots (1 - k^2 x_m^2 x^2)} \right]^2, \quad (n=2m), \quad (\text{C.2-17a})$$

and for n odd ($n = 2m+1$), $R(x)$ becomes

$$R_n^2(x) = N^2 \left[\frac{x(x^2 - x_1^2) \dots (x^2 - x_m^2)}{(1 - k^2 x_1^2 x^2) \dots (1 - k^2 x_m^2 x^2)} \right]^2, \quad (n=2m+1), \quad (\text{C.2-17b})$$

$$\text{where } N = \left[\frac{(1-k^2 x_1^2) \dots (1-k^2 x_m^2)}{(1-x_1^2) \dots (1-x_m^2)} \right], \quad (\text{C.2-18})$$

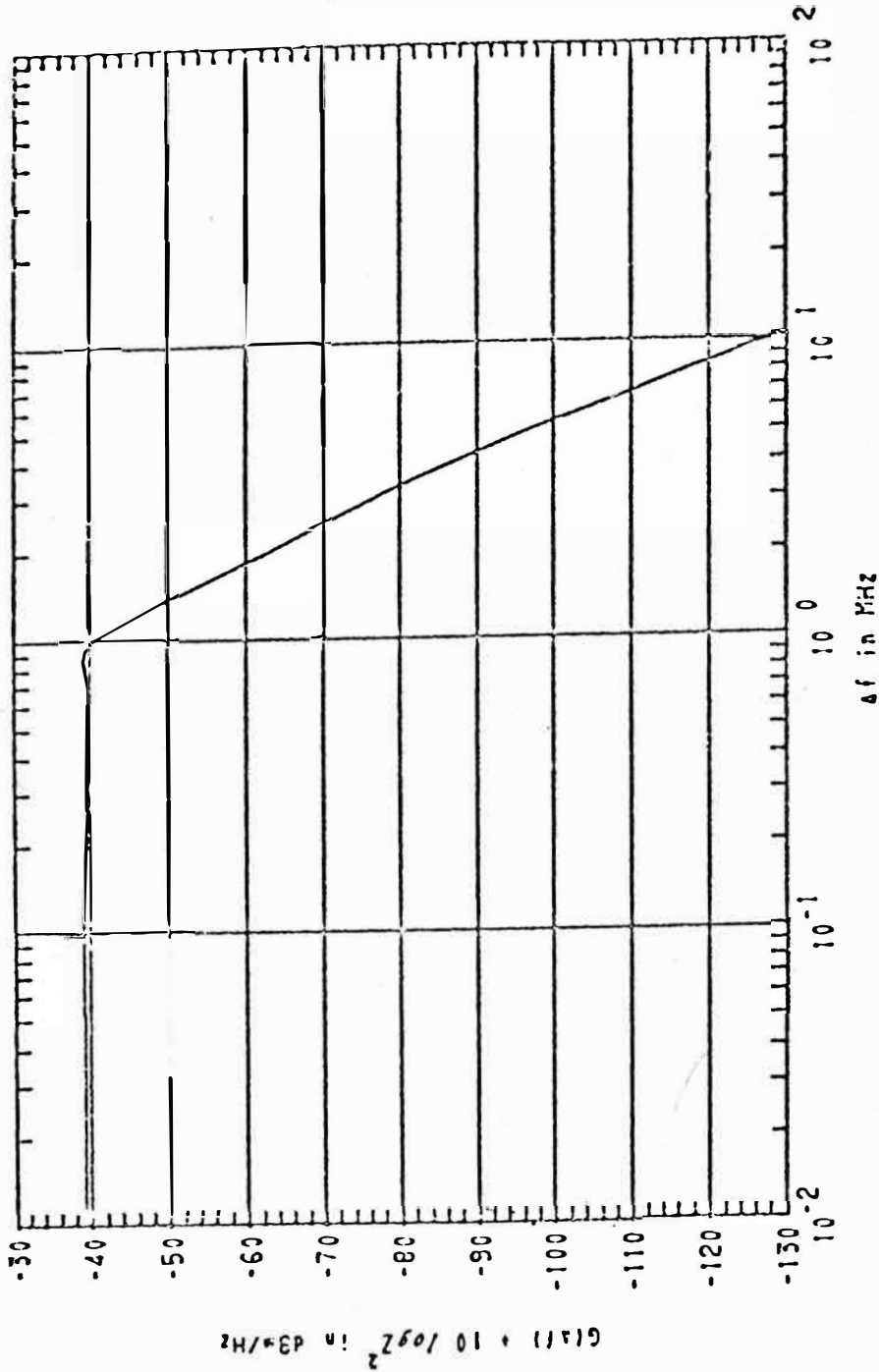
$$x_\ell = \begin{cases} \text{sn} \left\{ \frac{(2\ell-1)K}{n}, k \right\} & (\text{n even} = 2m) \\ \text{sn} \left\{ \frac{2\ell K}{n}, k \right\} & (\text{n odd} = 2m+1) \end{cases} \quad \ell = 1, 2, \dots, m. \quad (\text{C.2-19})$$

The symbol $\text{sn}(z, k)$ denotes the elliptic sine of z with modulus k .

The filters can be applied to the power spectra in at least two ways. As "emission" filters, with bandwidth centered at the carrier frequency of the interfering pulse, the resulting power density in the pass-band region will be comparable to the original power density; beyond this, the power will be reduced at a rate dependent on the slope of the filter wing. Thus, interference due to the pulse may be restricted.

If the filter is considered a part of the receiver, with bandwidth centered some distance from the carrier frequency of the interfering pulse, the application of the filter to (C.2-12) will give an estimate of the amount of interfering power allowed to reach the receiver detector.

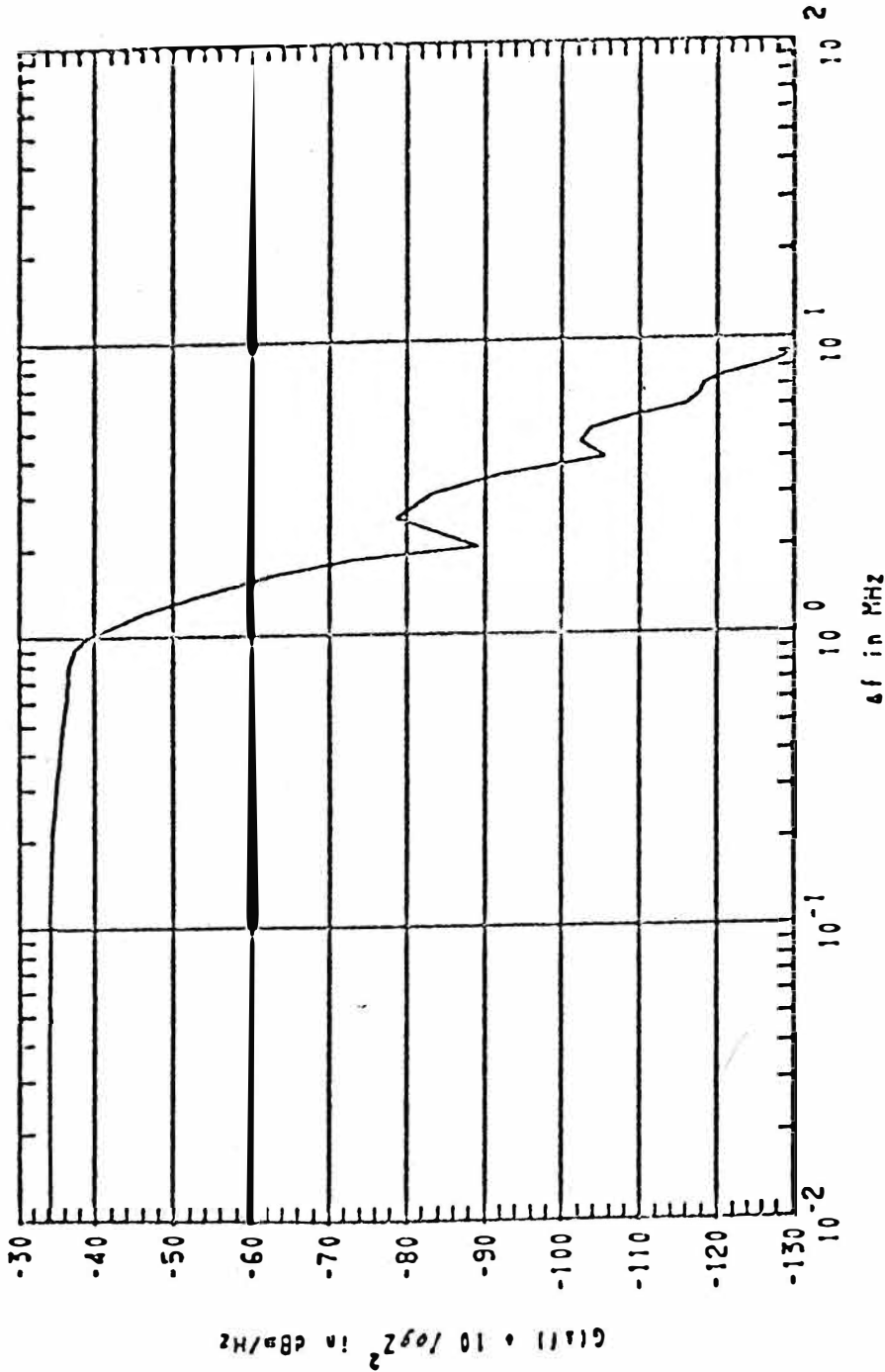
POWER SPECTRUM WITH FILTER



$N = 3$ $\epsilon^2 = 0.258925$
 $\tau_{AU} = 0.120$ $\tau_{AU_f} = 0.040$ $\tau_{AU_f} = 0.120$ $\tau_0 = 0.000$ $P_{avg} = 28.700$

Figure C.2-15. Synthesized spectral power density for the AM/APN-133 radar altimeter in the low altitude mode after additional filtering using a 3-pole Chebyshev filter with 1 dB ripple in the passband.

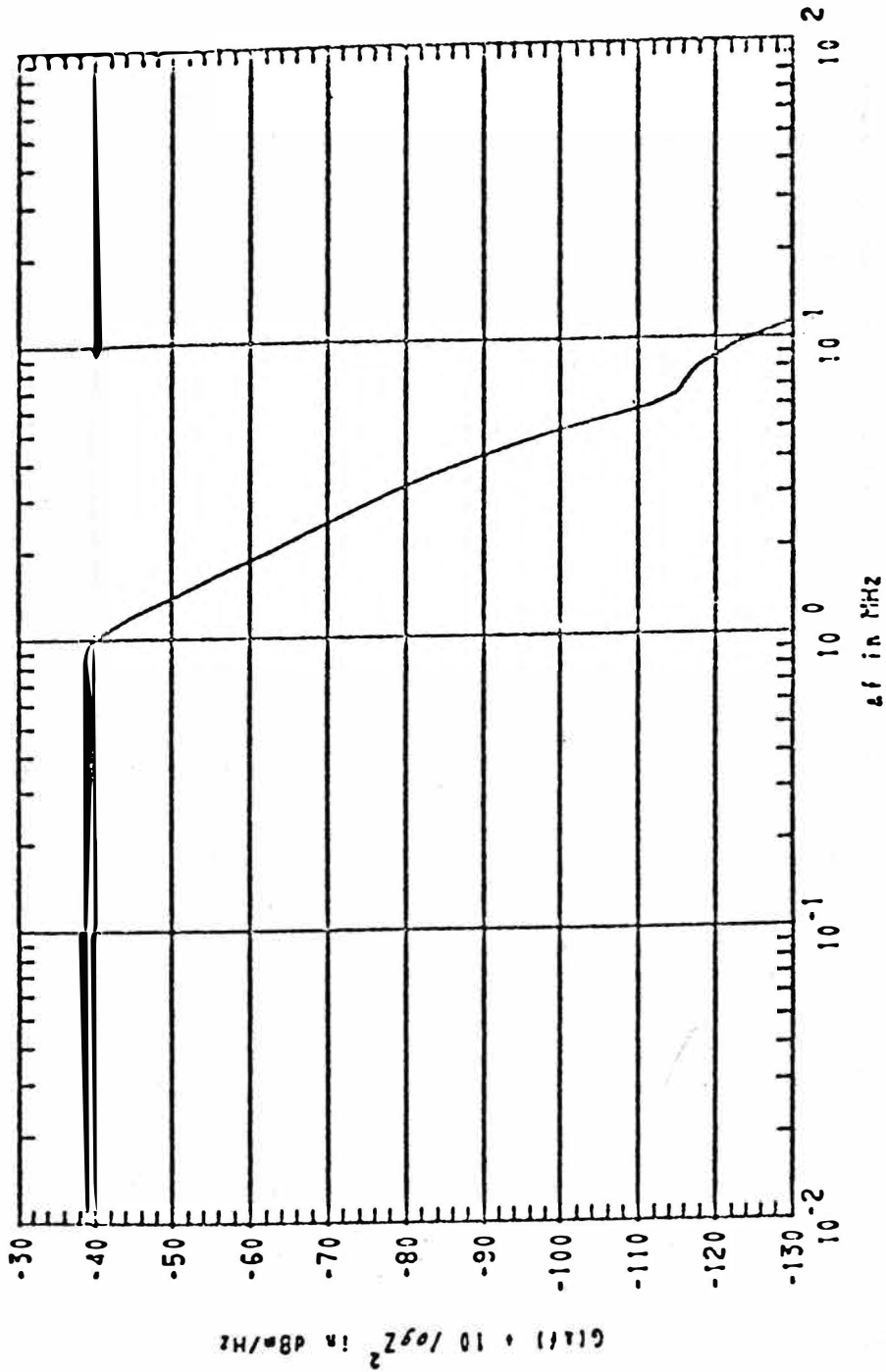
POWER SPECTRUM WITH FILTER



$N = 3$ $\epsilon^2 = 0.258925$
 $\tau_{AU} = 0.500$ $\tau_{AU_f} = 0.040$ $\tau_{AU_f} = 0.120$ $\tau_0 = 0.000$ $P_{avg} = 28.700$

Figure C.2-16. Synthesized spectral power density for the AN/APN-133 radar altimeter in the high altitude mode after additional filtering using a 3-pole Chebyshev filter with 1 dB ripple in the passband.

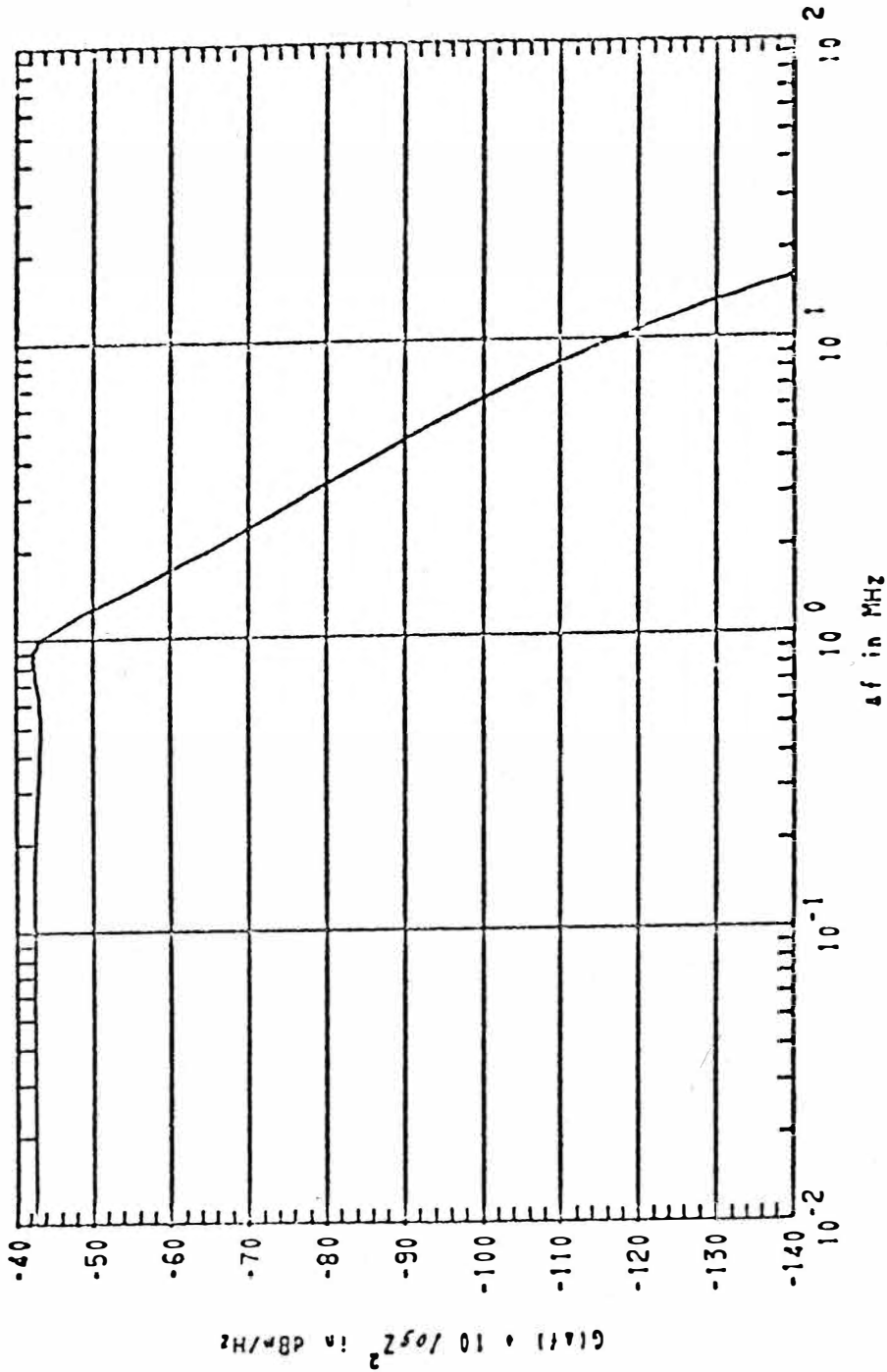
POWER SPECTRUM WITH FILTER



$N = 3$ $\epsilon^2 = 0.258925$
 $\tau_{AU} = 0.160$ $\tau_{AU_f} = 0.023$ $\tau_{AU_f} = 0.080$ $\tau_0 = 0.000$ $P_{avg} = 20.700$

Figure C.2-17. Synthesized spectral power density for the AN/APN-159 radar altimeter in the high altitude mode after additional filtering using a 3-pole Chebyshev filter with 1 dB ripple in the passband.

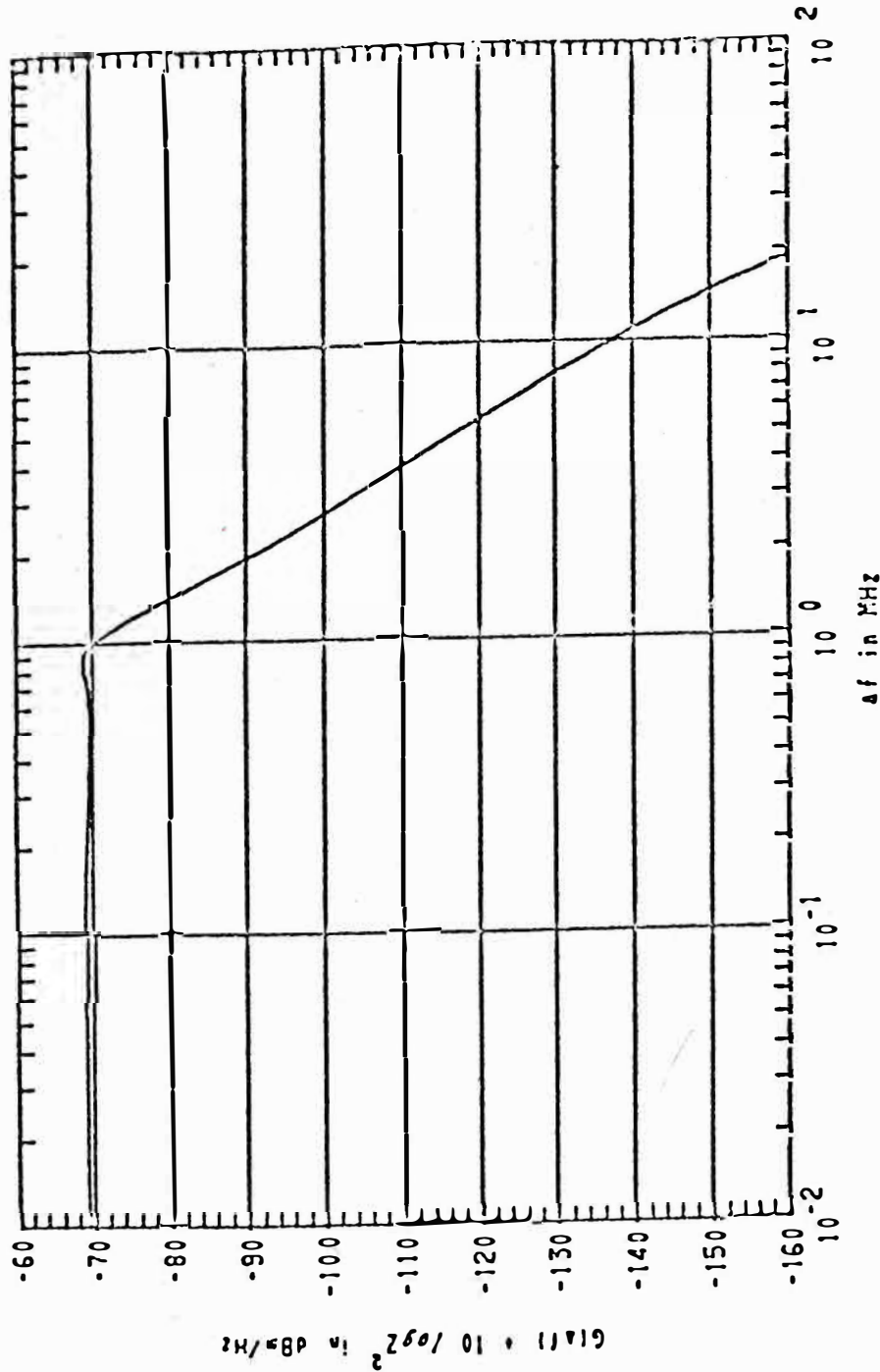
POWER SPECTRUM WITH FILTER



$N = 3$ $\epsilon^2 = 0.258925$
 $\tau_{AU} = 0.055$ $\tau_{AU_f} = 0.024$ $\tau_{AU_f} = 0.048$ $\gamma_0 = 0.000$ $P_{avg} = 28.700$

Figure C.2-18. Synthesized spectral power density for the AN/APN-159 radar altimeter in the low altitude mode after additional filtering using a 3-pole Chebyshev filter with 1 dB ripple in the passband.

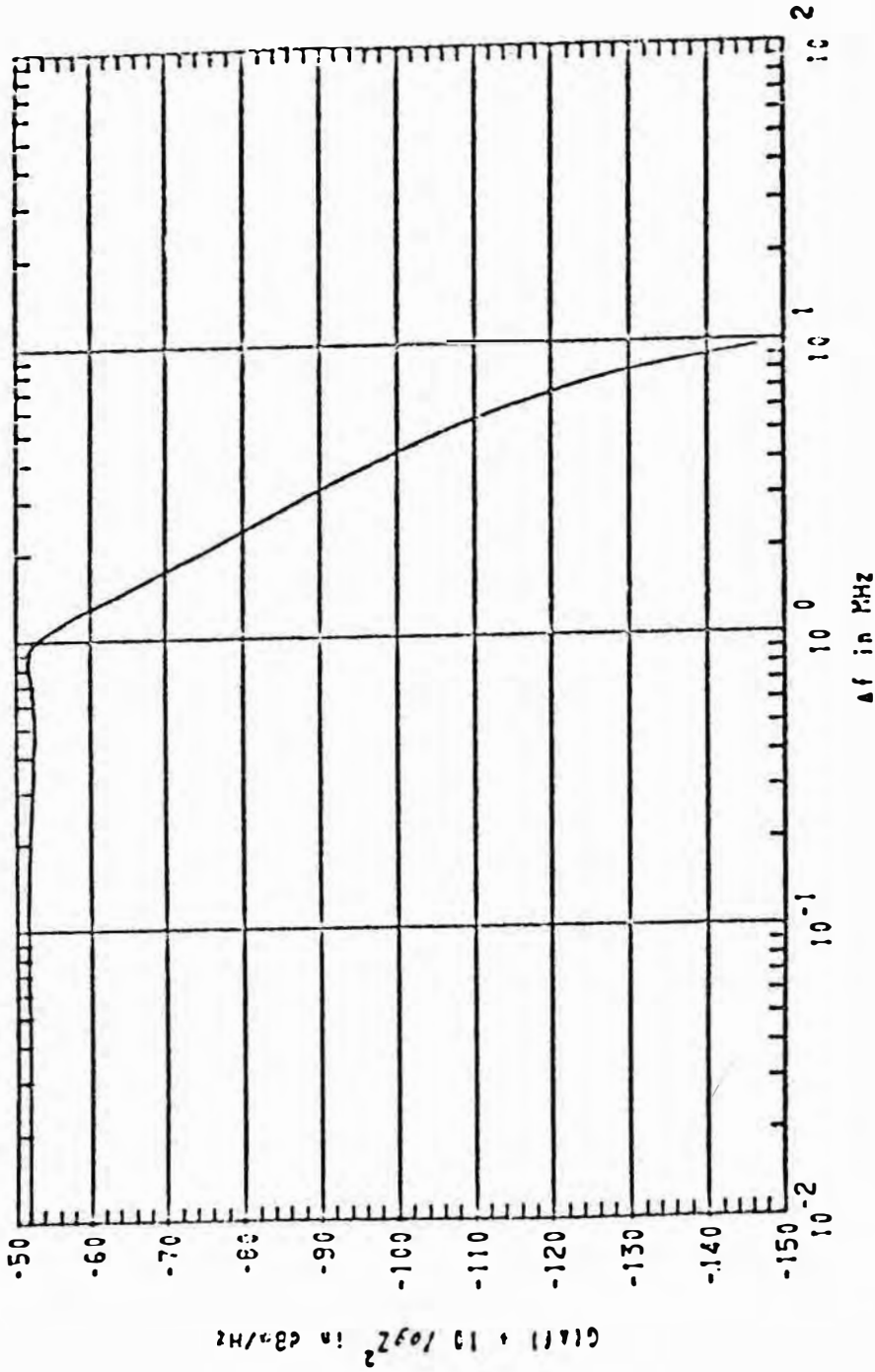
POWER SPECTRUM WITH FILTER



$N = 3$ $\epsilon^2 = 0.258925$
 $\tau_{AU} = 0.030$ $\tau_{AU_f} = 0.012$ $\tau_{AU_f} = 0.023$ $\tau_0 = 0.000$ $P_{avg} = 4.500$

Figure C.2-19. Synthesized spectral power density for the In-Flight Devices ground avoidance radar after additional filtering using a 3-pole Chebyshev filter with 1 dB ripple in the passband.

POWER SPECTRUM WITH FILTER



$N = 3 \quad \epsilon^2 = 0.258925$

$\tau_{AU} = 0.100 \quad \tau_{AU_f} = 0.058 \quad \tau_{AU_f} = 0.064 \quad \tau_0 = 0.000 \quad P_{avg} = 17.000$

Figure C.2-20. Synthesized spectral power density for the Bonzer TRN-70 radar altimeter after additional filtering using a 3-pole Chebyshev filter with 1 dB ripple in the passband.

For given receiver thresholds, predictions then may be made regarding the compatibility of different systems.

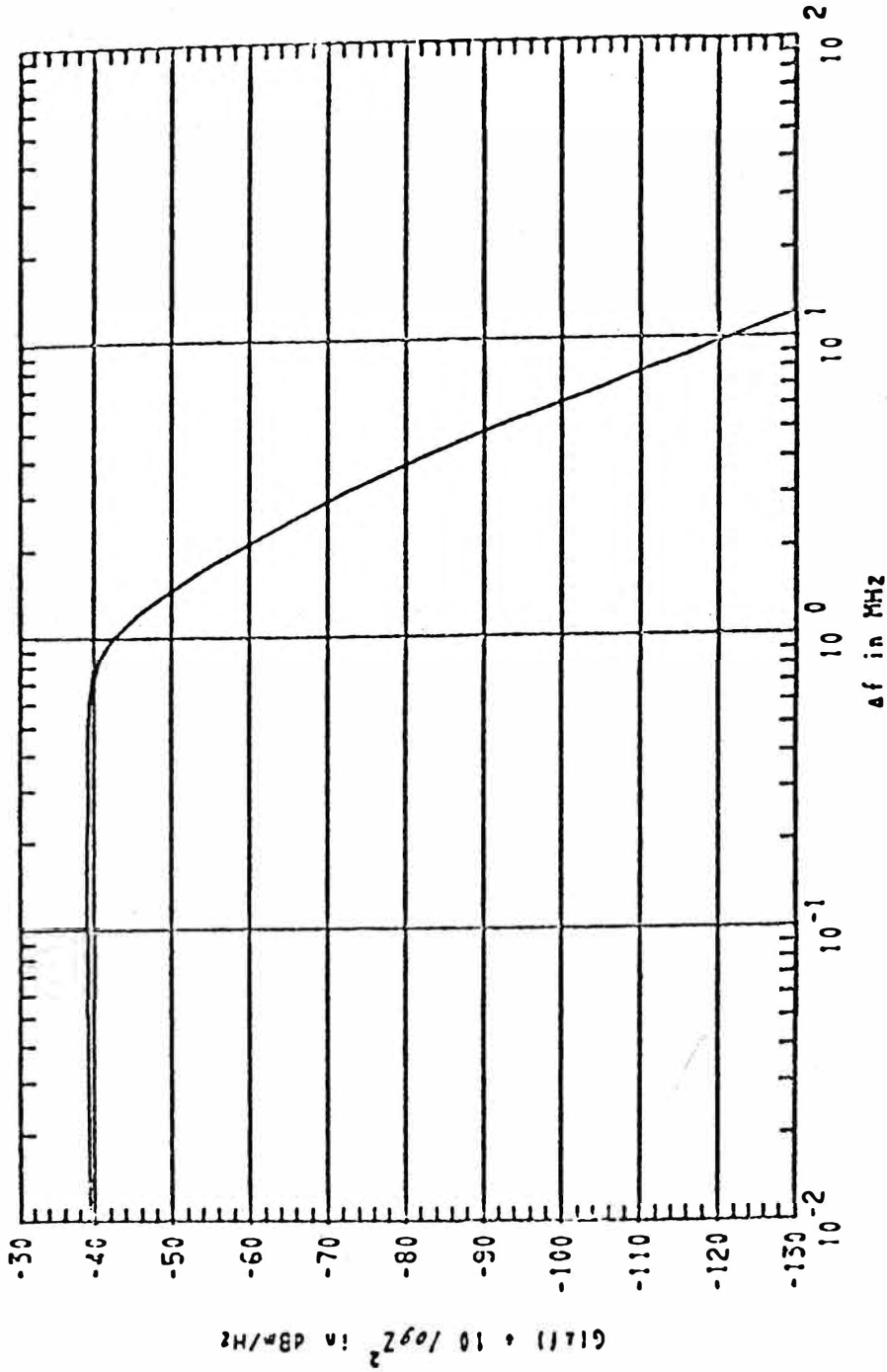
Figures C.2-7 to C.2-12 show spectral power density without emission filtering; figures C.2-15 to C.2-20 show spectral power density combined with a 3-pole emission (Chebyshev) filter. The relationship between the filter variable, x , in (C.2-13) and (C.2-14) and the frequency difference, Δf , in the power spectrum is

$$x = \frac{\Delta f - (f_1 - f_0)}{(f_2 - f_1)} \quad (\text{C.2-20})$$

where f_1 denotes the center frequency of the filter, and f_2 ($f_2 > f_1$) is the frequency at the wing of the filter determined by the desired filter bandwidth. For the examples shown, it has been assumed that $f_1 = f_0$ and $(f_2 - f_1) = 1$ MHz.

A comparison of figures C.2-7 to C.2-12 with figures C.2-15 to C.2-20, respectively shows the effectiveness of the example filter in limiting the power output beyond 1 MHz from the carrier frequency. For instance in the system designated AN/APN-133 (low altitude) (Figures C.2-7 and C.2-15), the power density spectrum without filtering gives a value of -60 dBm/Hz at $\Delta f = 10$ MHz; with filtering added, the value becomes -130 dBm/Hz.

POWER SPECTRUM WITH BUTTERWORTH FILTER

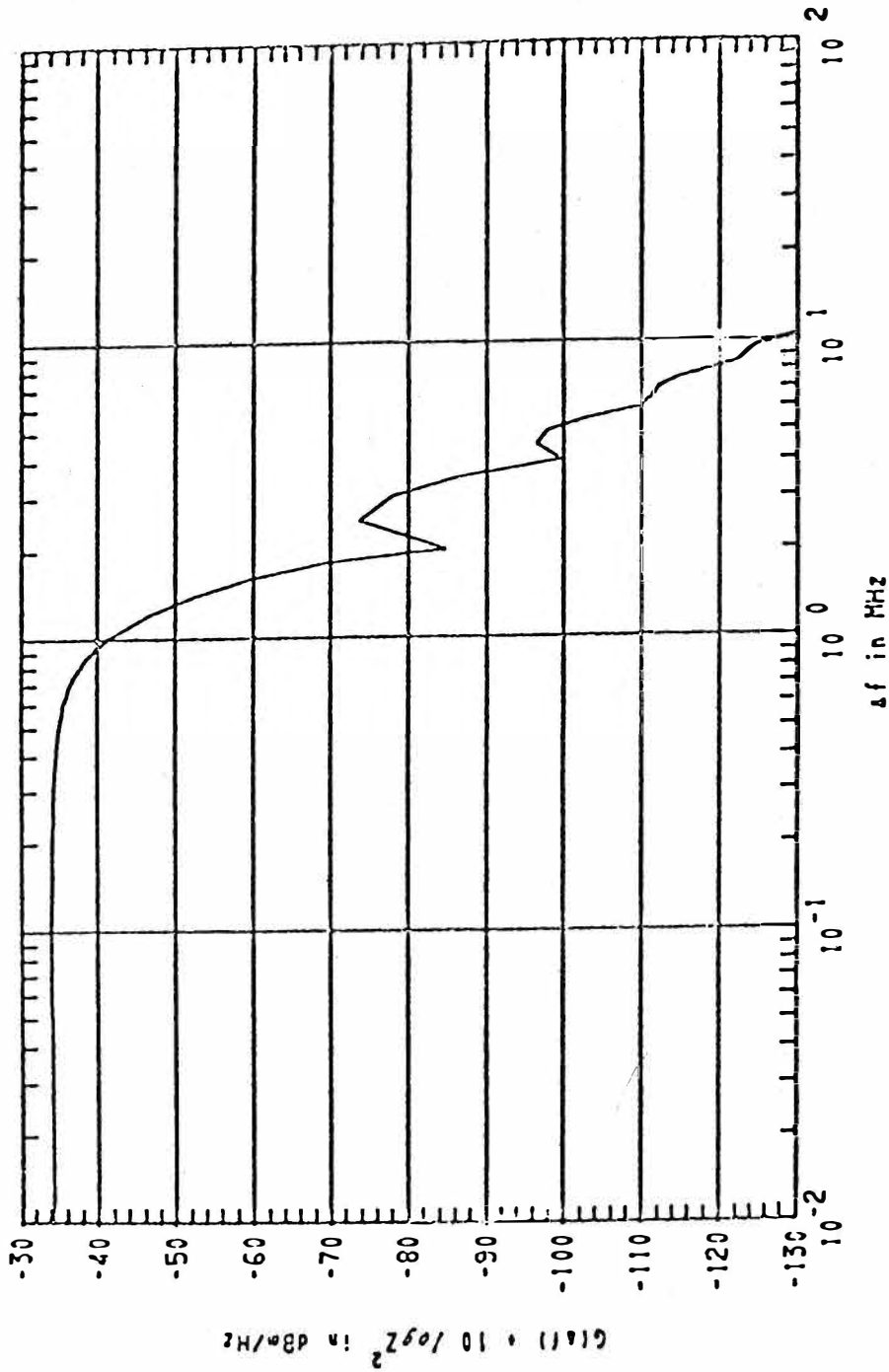


N = 3

TAU = 0.120 TAU_f = 0.040 TAU_f = 0.120 t₀ = 0.000 P_{avg} = 28.700

Figure C.2-21. Synthesized spectral power density for the AN/APN-133 radar altimeter in the low altitude mode after additional filtering using a 3-pole Butterworth filter.

POWER SPECTRUM WITH BUTTERWORTH FILTER

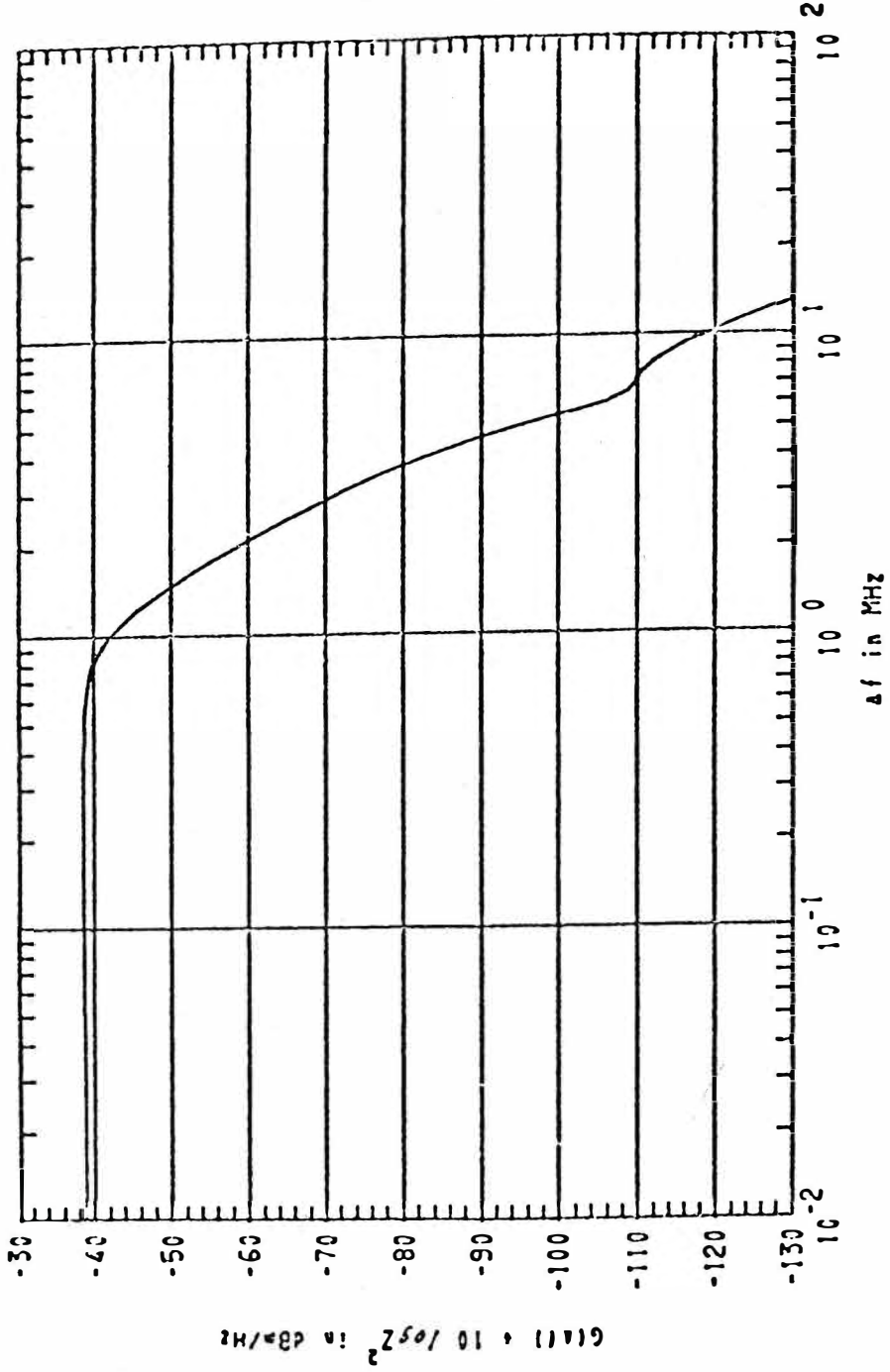


$N = 3$

$\tau_{AU} = 0.500$ $\tau_{AU_f} = 0.040$ $\tau_{AU_f} = 0.120$ $\tau_0 = 0.000$ $P_{avg} = 28.700$

Figure C.2-22. Synthesized spectral power density for the AN/APN-133 radar altimeter in the high altitude mode after additional filtering using a 3-pole Butterworth filter.

POWER SPECTRUM WITH BUTTERWORTH FILTER

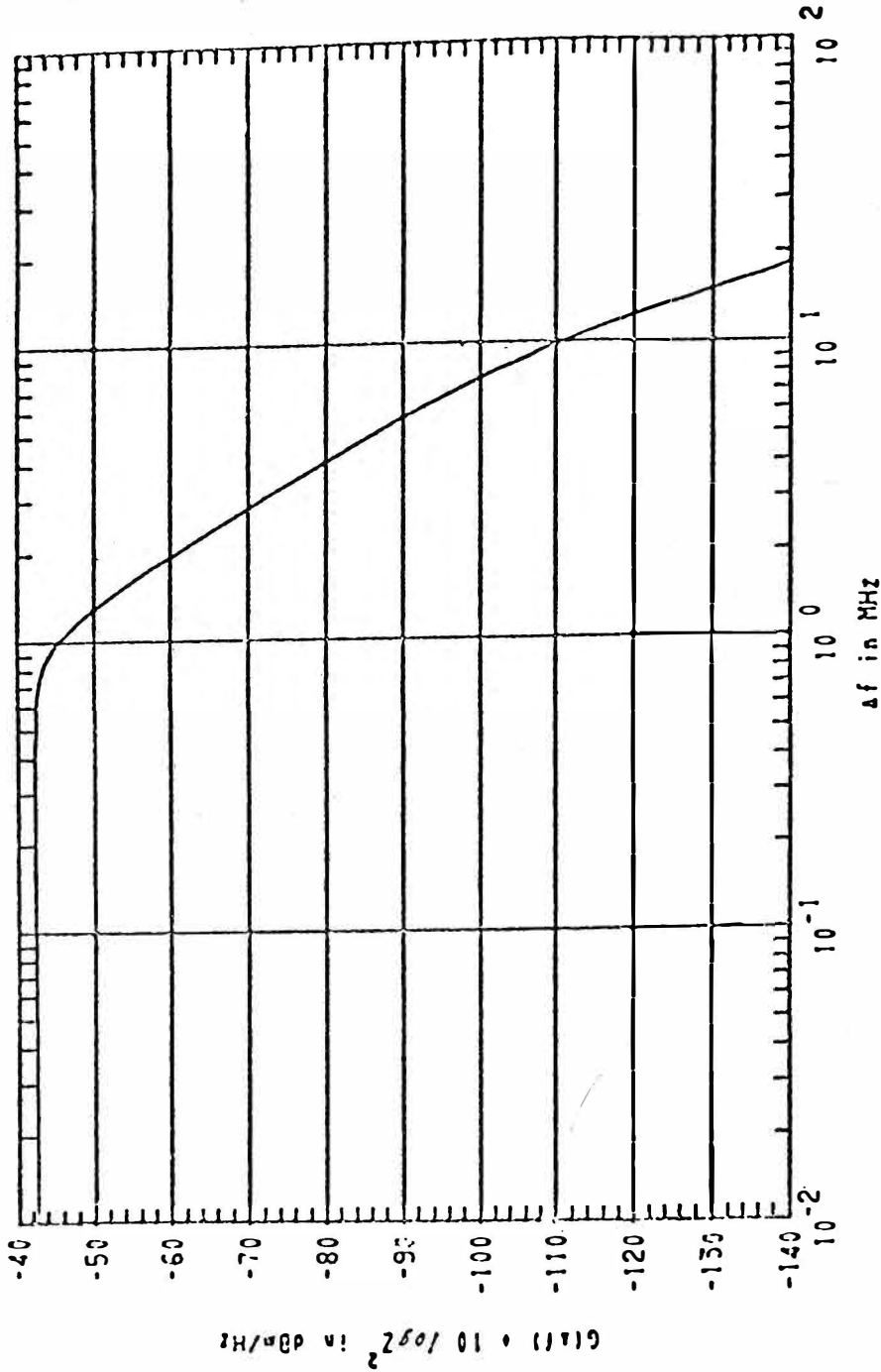


N = 3

TAU = 0.160 TAU_f = 0.023 TAU_r = 0.088 τ₀ = 0.000 P_{avg} = 28.700

Figure C.2-23. Synthesized spectral power density for the AN/APN-159 radar altimeter in the high altitude mode after additional filtering using a 3-pole Butterworth filter.

POWER SPECTRUM WITH BUTTERWORTH FILTER

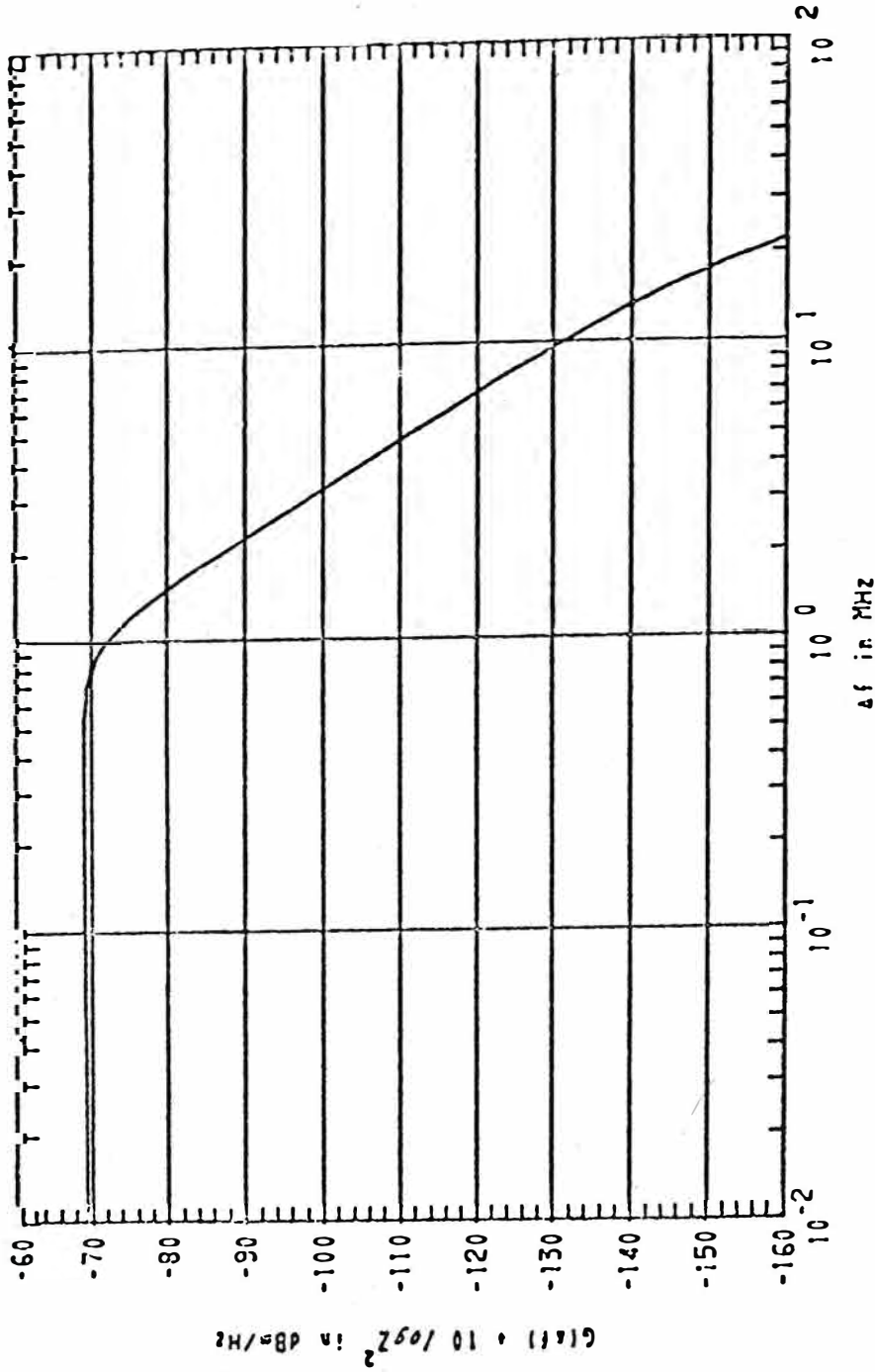


N = 3

TAU = 0.055 TAU_r = 0.024 TAU_f = 0.048 τ₀ = 0.000 P_{avg} = 28.700

Figure C.2-24. Synthesized spectral power density for the AN/APN-159 radar altimeter in the low altitude mode after additional filtering using a 3-pole Butterworth filter.

POWER SPECTRUM WITH BUTTERWORTH FILTER

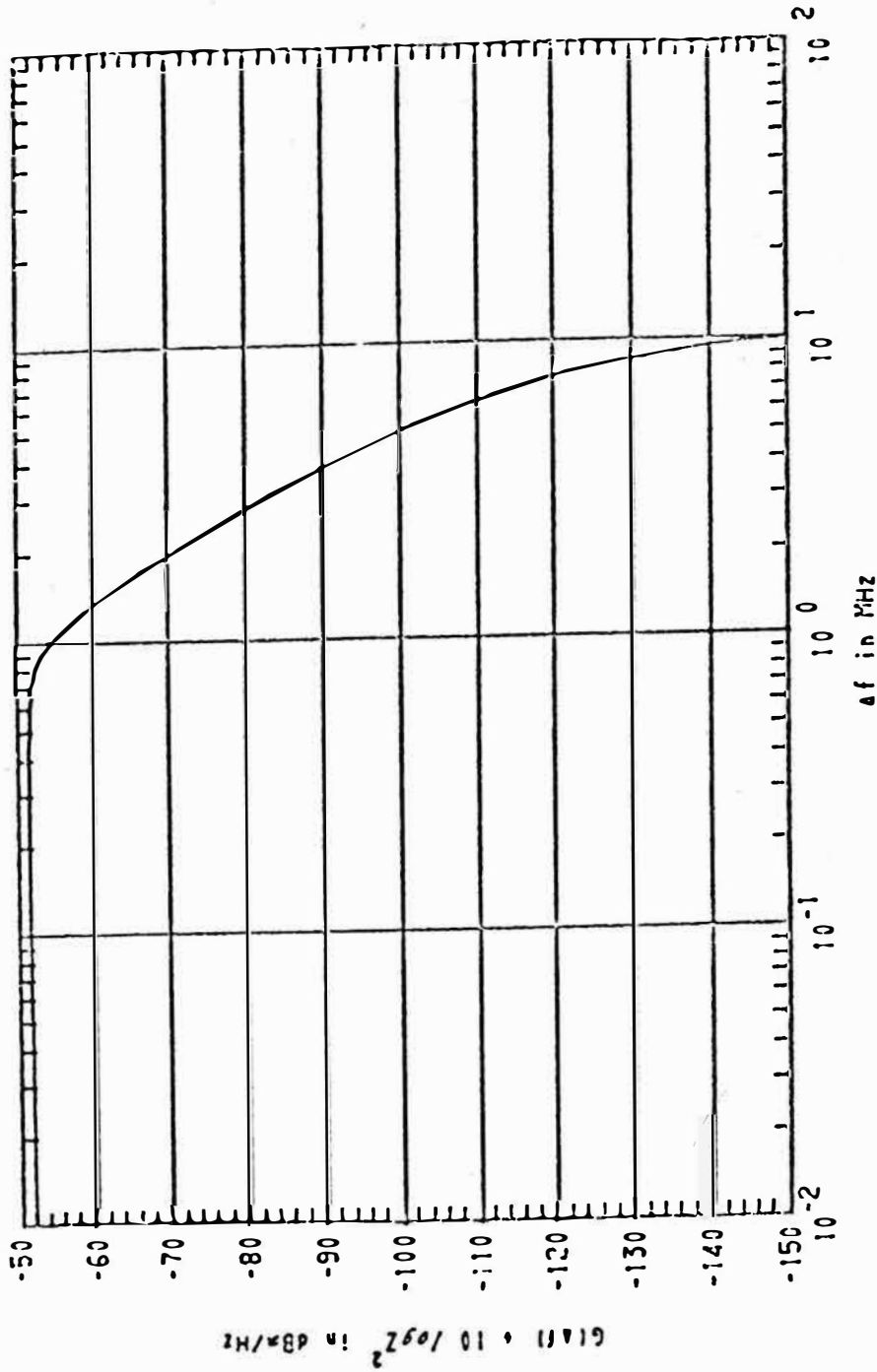


N = 3

TAU = 0.030 TAU_r = 0.012 TAU_f = 0.023 τ₀ = 0.000 P_{avg} = 4.900

Figure C.2-25. Synthesized spectral power density for the In-Flight Devices ground avoidance radar after additional filtering using a 3-pole Butterworth filter.

POWER SPECTRUM WITH BUTTERWORTH FILTER



N = 3

TAU = 0.100 TAU_f = 0.058 TAU_r = 0.064 t₀ = 0.000 P_{avg} = 17.000

Figure C.2-26. Synthesized spectral power density for the Bonzer TRN-70 radar altimeter after additional filtering using a 3-pole Butterworth filter.

Figures C.2-21 to C.2-26 show the effects of combining a Butterworth filter (eq (C.2-14) with $n=3$) with the power density spectra of figures C.2-7 to C.2-12. The decrease in power density beyond the filter passband is somewhat less than for the Chebyshev filter; however, the change is small.

The effect of the filter will depend, of course, not only on the choice of n , but also on the filter passband that is used. The equations presented in this appendix, together with the computer program based on these equations, have been generalized so that a wide variety of situations can be investigated.

APPENDIX D. ANTENNA POWER GAIN STATISTICS

Antenna radiation patterns are not easily determinable in field installations. The patterns may have been measured on a test range or calculated from theory, but when an antenna is installed in a system, the pattern is affected by the surrounding structures such as the towers, buildings, other antennas, etc.

The effect on the pattern of the antenna is most pronounced on the side lobe magnitudes and their angular positions. It is in this region of the antenna pattern that most of the interference radiation and/or reception takes place. Consequently, in order to characterize the antenna in the overall EMC problem, some statistical range of values for the magnitude of the power radiated or received through the antenna is desired.

The Rome Air Development Center has developed a method (RADC, 1966) to determine the statistical characteristics of the antenna radiation patterns. That method is based on an extensive amount of empirical data. They have shown that for their data the side-lobe gain values expressed in decibels relative to an isotrope (dBi) are normally distributed. Gain values for the main-beam region also are distributed according to another normal distribution. These facts allow a single class of antennas to be represented by their mean gain and standard deviation values for each region. The

RADC Interference Notebook establishes three antenna classifications. These classifications are high-gain antennas (greater than 25 dBi gain), medium-gain antennas (10-25 dBi gain), and low-gain antennas (less than 10 dBi gain). Statistical quantities for each classification of antennas are shown in tables D-1 through D-3. For each antenna classification, statistical quantities are shown for the mainbeam and side- and back-lobe regions considering polarization and site conditions.

The following definitions are required to understand the data contained in tables D-1, D-2, and D-3:

G_M : median gain value in dBi for the mainbeam region.

σ_M : standard deviation in dB for the mainbeam region.

G_B : median gain value in dBi for the side- and back-lobe region.

σ_B : standard deviation in dB for the side- and back-lobe region.

α_M : beamwidth in degrees of mainbeam region.

G_O : maximum gain value in dBi at design frequency and polarization.

α_O : beamwidth in degrees of mainbeam region at which gain is $10 \text{ dB} < G_O$.

Table D-1. Statistics for Typical High-Gain Antennas ($G > 25\text{dBi}$)

Operational Conditions		Side and Back Lobe Region		Main Beam Region		
Polarization	Site	G_B	σ_B	α_M	G_M	σ_M
		dB/Iso	dB	deg	dB/Iso	dB
Design	Open	-15	8			
	Average	-10	6	α_o	G_o	2
	Crowded	- 5	4			
Orthogonal to Design	Open	-15	8			
	Average	-10	6	$7\alpha_o$	$G_o -15$	3
	Crowded	- 5	4			

Table D-2. Statistics for Typical Medium-Gain Antennas (10 dBi \leq G \leq 25 dBi)

Operational Conditions		Side and Back Lobe Region		Main Beam Region		
		G_B	σ_B	α_M	G_M	σ_M
Polarization Design	Site					
		dB/Iso	dB	deg	dB/Iso	dB
	Open	-10	6			
	Average	- 8	5	α_O	G_O	2
	Crowded	- 5	4			
Orthogonal to Design	Open	-10	6			
	Average	- 8	5	$3\alpha_O$	$G_O - 10$	3
	Crowded	- 5	4			

Table D-3. Statistics for Typical Low-Gain Antennas ($G < 10\text{dBi}$)

Operational Conditions		Extraneous Lobe Region		Major Lobe Region		
Polarization	Site	G_B	σ_B	α_M	G_M	σ_M
		dB/Iso	dB	deg	dB/Iso	dB
Design	Open	-7	4		G_O	1
	Average	-5	3	α_O		
	Crowded	-3	2			
Orthogonal to Design	Open	-7	4			
	Average	-5	3	$1.4\alpha_O$	$(G_O - 3)$	2
	Crowded	-3	2			

These tabular data have been incorporated into a computer subroutine called ANTSTAT for use in the statistical F-D curves model. This subroutine does a table look-up based on user-supplied information as described earlier in Appendix A of this report. The appropriate values for median gain and standard deviation then are used according to the specification of option 1 or 2 in items 41 and 51 of the user-supplied input data. Options 3 and 6 under items 41 and 51 in the input data forms are designated by the term "full pattern." In this case, the statistical distribution describing the gain of the antenna is a combination of both the main-beam and side- and back-lobe regions. If α_M is the main-beam width in degrees, then a randomly located receiving point has a probability of $\alpha_M/360$ of being in the main-beam; the probability of being in the side- and back-lobe region is, thus, $1-(\alpha_M/360)$. The gain distributions in the main-beam and side- and back-lobe regions are assumed to be normal with medians, G_M and G_B , and standard deviations, σ_M and σ_B , respectively. The "full pattern" distribution of gain for the antenna is now given by

$$P(G) = (\alpha_M/360^\circ) \Pr(G \leq G_M + \sigma_M t) + [1 - (\alpha_M/360^\circ)] \Pr(G \leq G_B + \sigma_B t), \quad (D-1)$$

where t is the standard normal deviate.

With narrow-beam antennas, the above formula gives more weight to the side- and back-lobe region, and the "full-pattern" distribution is usually very similar to that for the side- and back-lobe region. However, a large variance in the main-beam region could cause a more noticeable difference.

The logic of the interference situation (e.g. cross-polarized coupling between the side- and back-lobe regions of each antenna) defines the gain distribution for each antenna to be used in the convolution, described in Appendix G, performed to obtain the mutual antenna power gain distribution.

APPENDIX E. OFF-FREQUENCY REJECTION CALCULATION

The concept of off-frequency rejection (OFR) has been developed and reported by others such as Fleck (1967). The output of OFR data is very straight-forward for a model such as the statistical frequency distance curves model. Therefore, a brief discussion of the calculations providing OFR as a function of frequency difference between transmitter and receiver tuned frequency (Δf) is presented in this appendix.

Transmitter output power as a function of frequency may be expressed as $P(f)$ and the total output power as $\int_0^{\infty} P(f)df$. The receiver selectivity (or power transfer characteristic) as a function of frequency and frequency difference between transmitter and receiver may be represented as $S(f,\Delta f)$. Then the total received power, at the receiver detector, is called spectrum dependency and denoted by SD in this report. It is the convolution of $P(f)$ and $S(f,\Delta f)$. That is,

$$SD_{\Delta f} = \int_0^{\infty} P(f)S(f,\Delta f)df. \quad (E-1)$$

The spectrum dependency which results when the receiver and transmitter of interest are tuned to the same frequency ($\Delta f=0$) follows as

$$SD_{f=0} = \int_0^{\infty} P(f)S(f,0)df. \quad (E-2)$$

Off-frequency rejection now can be expressed as

$$\text{OFR} = \frac{\int_0^{\infty} P(f) S(f, \Delta f) df}{\int_0^{\infty} P(f) S(f, 0) df} = \frac{SD_{\Delta f}}{SD_{\Delta f=0}} \quad (\text{E-3})$$

It follows directly that $\text{OFR}_{\Delta f=0} = 1$ and that $\text{OFR}_{\Delta f \neq 0} \leq 1$. Similarly, expressed in decibels, $\text{OFR}_{\Delta f=0} \text{ (dB)} = 0$ and $\text{OFR}_{\Delta f \neq 0} \text{ (dB)}$ is a negative quantity portraying the rejection of interference power which occurs as the transmitter and receiver are separated in tuned frequency.

However, many engineers and analysts concerned with electromagnetic compatibility evaluations use the term "off-frequency rejection" when referring to the overall rejection of energy incident on a receiver. This overall rejection results from two causes. First, reduction of energy to the receiver occurs due to difference in tuned frequency between the interfering transmitter and the victim receiver. This reduction is the actual off-frequency rejection which has been defined. A second cause of reduced energy reaching the receiver defector is important when the emission spectrum of the transmitter is broader than the receiving bandwidth. Even when the transmitter and receiver are tuned to the same frequency ($\Delta f=0$), only a fraction of the incident energy is accepted, although off-frequency rejection is zero ($\text{OFR} \equiv 0_{\Delta f=0}$).

The total rejection that results both from difference between tuned frequency for the transmitter and receiver and

from the receiver bandwidth being less than the emission spectrum width is termed frequency-dependent rejection (FDR). As noted earlier, when the total output power of the transmitter is $\int_0^{\infty} P(f) df$ and the total received power is given by equation (E-1). then frequency-dependent rejection is

$$FDR = \frac{\int_0^{\infty} P(f) S(f, \Delta f) df}{\int_0^{\infty} P(f) df} = \frac{SD_{\Delta f}}{\int_0^{\infty} P(f) df}. \quad (E-4)$$

Just as the definition of OFR led to conclusions about the range of values for OFR, likewise it follows that $FDR < 1$, regardless of frequency separation, whenever the receiving bandwidth is less than the emission spectrum width.

Expressed in decibels, FDR (dB) is a negative quantity portraying the overall rejection of interference power that is realized due to tuned frequency separation and bandwidth difference.

It is evident that FDR is a more useful conceptual quantity than OFR to the engineer or analyst. Tabular data for both OFR and FDR are provided by the model. A selectable option discussed in Appendix A, allows the model user to ask for a plot of FDR only.

APPENDIX F. PROPAGATION LOSS MODELS

The two models that are used in this report differ primarily in their intended application. The ground-to-ground propagation model is briefly described in section F.1 of this appendix. Details are given in a report by Longley and Rice (1968). The ground-to-air propagation loss model is briefly described in section F.2 of this appendix. The details are given in a report by Gierhart and Johnson (1973).

F.1 Ground-to-Ground Propagation Model

This program predicts long-term median radio transmission loss over irregular terrain. The method is based on well-established propagation theory and has been tested against a large number of propagation measurements. It is applicable for radio frequencies above 20 MHz and uses statistical estimates of terrain irregularity representative of the terrain characteristics for a given area. Estimates of terrain characteristics are based on a large number of terrain profiles for several types of terrain, including plains, desert, rolling hills, foothills, and rugged mountains.

Given radio frequency, antenna heights, and an estimate of terrain irregularity, median reference values of attenuation relative to the transmission loss in free space are calculated as a function of distance. For radio line-

of-sight paths, the calculated reference is based on two-ray theory and an extrapolated value of diffraction attenuation. For trans-horizon paths, the reference value is either diffraction attenuation or forward scatter attenuation, whichever is smaller.

This prediction method was developed for use with a digital computer and has been made sufficiently general to provide estimates of transmission loss expected over a wide range of frequencies, path lengths, and antenna height combinations, over smooth to highly rugged terrain, and for both vertical and horizontal polarization.

Predictions have been tested against data for wide ranges of frequency, antenna height and distance, and for all types of terrain from very smooth plains to extremely rugged mountains. The data base includes more than 500 long-term recordings throughout the world in the frequency range 40 to 10,000 MHz, and several thousand mobile recordings in the United States at frequencies from 20 to 1,000 MHz. The method is intended for use within the following ranges:

<u>Parameter</u>	<u>Range</u>
Frequency	20 to 40,000 MHz
Antenna heights	0.5 to 3,000 m
Distance	1 to 2,000 km
Surface refractivity	250 to 400 N-units

F.2 Ground-to-Air Propagation Model

The propagation model used in the ground-to-air program is applicable to telecommunications links operating at radio frequencies from about 0.1 to 20 GHz with aircraft altitudes less than 300,000 ft (91,440 m). Ground-station antenna heights must be (1) greater than 1.5 ft (0.5 m), (2) less than 9,000 ft (2,743 m), and (3) at an altitude below the aircraft. In addition, the elevation of the radio horizon must be less than the aircraft altitude.

Conceptually the model is very similar to the Longley-Rice (1968) propagation model for propagation over irregular terrain; i.e., attenuation versus distance curves calculated for the (a) line-of-sight (b) diffraction, and (c) scatter regions are blended together to obtain values in transition regions. In addition, the Longley-Rice relationships involving the terrain parameter, Δh , are used to estimate radio horizon parameters when such information is not available. The model includes allowance for (a) average ray bending (b) horizon effects, (c) long-term power fading, (e) surface reflection multipath, (f) tropospheric multipath, and (g) atmospheric absorption. However, special allowances

are not included for (a) ducting, (b) rain attenuation, (c) rain scatter, or (d) ionospheric scintillations.

APPENDIX G. CONVOLUTION SUBROUTINE

The technique used in combining the antenna power gain and propagation loss statistics is described in this appendix. The technique is generally applicable to any random variables such as the x and y illustrated, so that the results are not restricted to propagation loss and antenna gains.

The convolution subroutine used in generating the statistical portions of the frequency/distance calculations uses as input the cumulative distributions of the statistical variables for the propagation loss and antenna gains. If x and y are two independent variables with probability density functions, $p_1(x)$ and $p_2(y)$, and cumulative distributions

$$P_1(X) = \int_{-\infty}^x p_1(x)dx, \quad P_2(Y) = \int_{-\infty}^Y p_2(y)dy, \quad (G-1)$$

then the probability that their sum or difference is less than or equal to some value, Z , is

$$\Pr(y+x \leq Z) = \int_{-\infty}^{+\infty} \left[\int_{-\infty}^{Z-y} p_1(x)dx \right] p_2(y)dy = \int_{-\infty}^Z P_1(Z-y)dP_2(y), \quad (G-2a)$$

$$\begin{aligned} \Pr(y-x \leq Z) &= \int_{-\infty}^{\infty} \left[\int_{y-Z}^{\infty} p_1(x)dx \right] p_2(y)dy \\ &= 1 - \int_{-\infty}^Z P_1(y-Z) d P_2(y), \end{aligned} \quad (G-2b)$$

where use is made of the relationship, $p_2(y)dy=dP_2(y)$.

Since only numerical values of each cumulative distribution and its associated variable, P , are used (rather than analytic expressions), the integrals in (G-2) are numerically evaluated. Thus, the input to the convolution subroutine consist of: (1) the arrays $P_1(X_{\min})$ to $P_1(X_{\max})$ and $P_2(Y_{\min})$ to $P_2(Y_{\max})$; (2) N , the number of integration points desired; and (3) M the total number of desired output levels, Z , (together with their associated probabilities).

It is assumed in the numerical integrations that $P_1(X < X_{\min})$ and $P_2(Y < Y_{\min})$ are always zero, and that $P_1(X > X_{\max})$ and $P_2(Y > Y_{\max})$ are always unity.

The differential, $dP_2(y)$, is approximated by the difference

$$\Delta(Y_n) = P_2(Y_n + \delta) - P_2(Y_n - \delta), \quad (G-3)$$

where

$$Y_n = Y_{\min} + (2n-1)\delta, \quad \delta = \frac{Y_{\max} - Y_{\min}}{2N} \quad (G-4)$$

and n is an integer running from 0 to $N+1$. Values of P_2 for Y 's not in the given array are obtained by interpolation.

To ensure that the output levels, Z_m associated with the desired probabilities, encompass the total range of given X 's and Y 's the levels are defined as

$$Z_m = Y_{\min} - \delta + \left\{ m + [X_{\min}/2\delta] \right\} 2\delta \quad (G-5)$$

for use in the "sum" convolution (G-2a), and

$$Z_m = Y_{\min} - \delta + \{m - [X_{\max}/2\delta]\} 2\delta \quad (G-6)$$

for use in the "difference" convolution (G-2b), where m is an integer specifying a particular output level Z . The symbol $[u]$ denotes the integer part of u .

A set of X 's is now formed using the relationship

$$X_j = \{[X_{\min}/2\delta] - (N+1) + j\} 2\delta, \quad j = 0, 1, 2, \dots, J, \quad (G-7)$$

where

$$J = -[X_{\min}/2\delta] + [X_{\max}/2\delta] + 2(N+1) \quad (G-8)$$

and, by interpolation in the given $P_1(X)$ array, an array of $P_1(X_j)$ is generated.

The numerical evaluation of (G-2) now may be accomplished with the use of (G-3) and the appropriate portion of the $P_1(X_j)$ array as follows:

$$P_r(Y+X \leq Z_m) \sim \sum_{n=0}^{N+1} P_1(X_{N+1+m-n}) \Delta(Y_n) \equiv P_3^+(Z_m), \quad (G-9a)$$

$$P_r(Y-X \leq Z_m) \sim 1 - \sum_{n=0}^{N+1} P_1(X_{1-m+n}) \Delta(Y_n) \equiv P_3^-(Z_m), \quad (G-9b)$$

with the Z_m given by either (G-5) or (G-6). Since the number of elements in the output cumulative distribution

array, $P_3(Z)$, is M (a given input), the integer m is made to vary as

$$m = [I/M]k, \quad k = 1, 2, \dots, M, \quad (G-10)$$

where
$$I = -[X_{\min}/2\delta] + [X_{\max}/2\delta] + (N+1). \quad (G-11)$$

The probabilities $P_3^\pm(Z_0)$ and $P_3^\pm(Z_1)$ are essentially zero and unity, respectively. The superscript $+$ or $-$ of the P_3 corresponds to the $+$ or $-$ in $\Pr(Y \pm X \leq Z_m)$.

In combining the statistics for the transmitting and receiving antennas, use is made of (G-9a) to compute the combined cumulative distribution P of antenna gain. The X 's could correspond to the random transmitting antenna gain data, and the Y 's could correspond to the random receiving antenna gain data. This resultant antenna distribution then is combined with the propagation loss distribution by using (G-9b). The loss variable in this case would correspond to the Y variable, and the antenna distribution would correspond to the X variable. The result is an array of M levels of the combined propagation loss and antenna gain statistical distribution functions. Then, when a specific probability of occurrence level is requested (e.g., 90%, 80%, 50%, 1%, etc.), the computer interpolates between the appropriate prior calculated levels for the level corresponding to the requested probability.

BIBLIOGRAPHIC DATA SHEET

1. PUBLICATION OR REPORT NO. OTR 76-84		2. Gov't Accession No.	3. Recipient's Accession No.
4. TITLE AND SUBTITLE Statistical Frequency-Distance Curves, Initial Model		5. Publication Date April 1976	
		6. Performing Organization Code OT/ITS, Division 1	
7. AUTHOR(S) R. D. Jennings, L. E. Vogler, and J. J. Stephenson		9. Project/Task/Work Unit No. 9106523	
8. PERFORMING ORGANIZATION NAME AND ADDRESS U. S. Department of Commerce Office of Telecommunications Institute for Telecommunication Sciences Boulder, Colorado 80302		10. Contract/Grant No.	
		12. Type of Report and Period Covered OT Technical Report	
11. Sponsoring Organization Name and Address U. S. Department of Commerce Office of Telecommunications Office of Telecommunication Policy Washington, D. C. 20005		13.	
14. SUPPLEMENTARY NOTES			
15. ABSTRACT (A 200-word or less factual summary of most significant information. If document includes a significant bibliography of literature survey, mention it here.) This report describes an initial computer program that produces statistical frequency-distance curves. The computer program has been developed as a tool for use by the frequency managers' community of OTP/IRAC. The statistical frequency-distance curves estimate the minimum distance separation that is required between a victim receiver and an interferer as a function of the frequency offset between them. The curves are parametric in the probability or percent of time that interference is permissible. The model uses statistical variations in antenna gain and propagation loss to compute the probability of interference. Appendices of the report describe the propagation loss and antenna gain models and the method used to combine them to produce the statistical frequency-distance curves. Operating instructions and several sample applications also are included as appendices.			
16. Key words (Alphabetical order, separated by semicolons) Compatibility; computer model; distance seapration; electromagnetic compatibility; emission spectrum; frequency-distance curve; frequency management; frequency separation; interference; off-frequency rejection; propagation loss; receiver selectivity; statistics.			
17. AVAILABILITY STATEMENT <input checked="" type="checkbox"/> UNLIMITED. <input type="checkbox"/> FOR OFFICIAL DISTRIBUTION.		18. Security Class (This report) UNCLASSIFIED	20. Number of pages 202
		19. Security Class (This page) UNCLASSIFIED	21. Price: